

ECE 538: 2D Material Electronics and Photonics

Chapter 2: Transition Metal Dichalcogenides

Wenjuan Zhu

Associate Professor

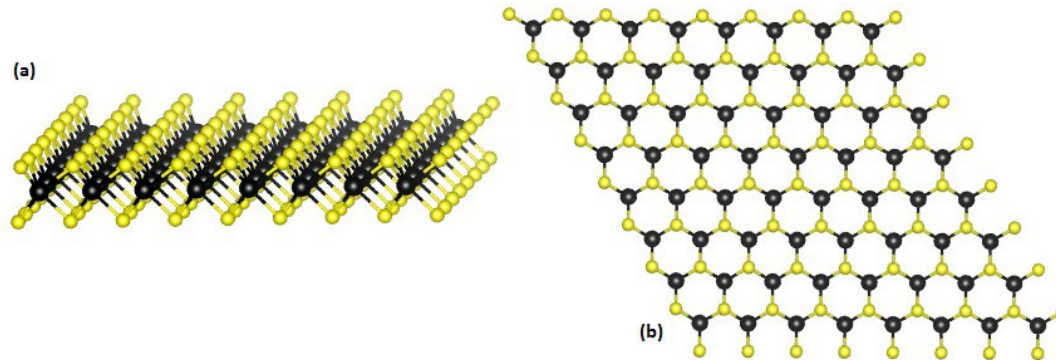
Department of Electrical and Computer Engineering
Office: MNTL 3258, Email: wjzhu@Illinois.edu

Outline

- 
- Introduction of transition metal dichalcogenides (TMDs)
 - Synthesis of TMDs
 - Current transport and electronic devices
 - Optical properties and photonic devices

Transition metal dichalcogenides (TMD): MX_2

H	Chalcogens X																		He
Li	Be																		
Na	Mg																		
K	Ca	Sc	Ti	V	Cr	Mn	Fe	Co	Ni	Cu	Zn	Ga	Ge	As	Se	Br	Kr		
Rb	Sr	Y	Zr	Nb	Mo	Tc	Ru	Rh	Pd	Ag	Cd	In	Sn	Sb	Te	I	Xe		
Cs	Ba	La - Lu	Hf	Ta	W	Re	Os	Ir	Pt	Au	Hg	Tl	Pb	Bi	Po	At	Rn		
Fr	Ra	Ac - Lr	Rf	Db	Sg	Bh	Hs	Mt	Ds	Rg	Cn	Uut	Fl	Uup	Lv	Uus	Uuo		



One layer of transition metal atoms is sandwiched between two layers of chalcogen atoms.

M. Chhowalla et al, Nature Chemistry (2013)
 K.S. Novoselov, et al, Proc. Nat. Acad. Science (2005)
 J.N. Coleman, et al, Science (2011)

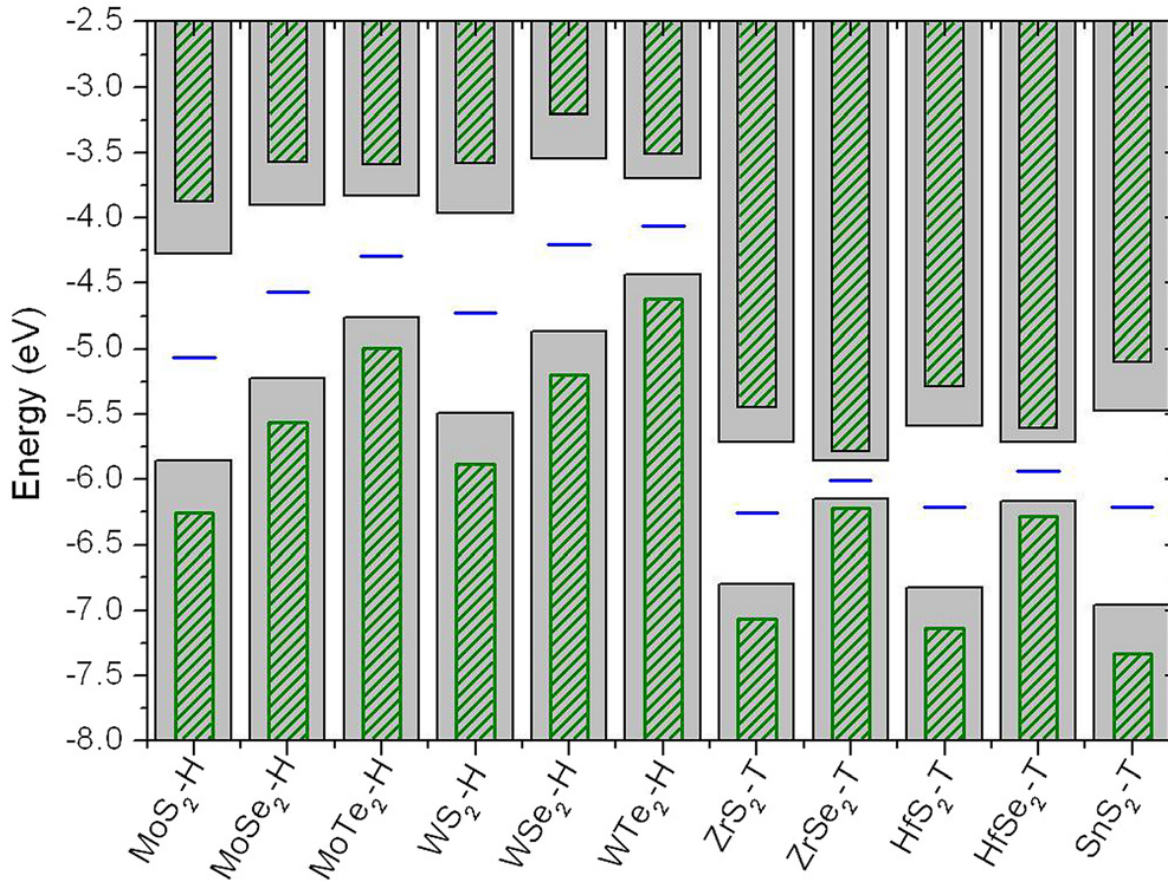
Diverse properties of TMDs

Group	M	X	Properties
4	Ti, Hf, Zr	S, Se, Te	Semiconducting ($E_g = 0.2\text{--}2\text{ eV}$). Diamagnetic.
5	V, Nb, Ta	S, Se, Te	Narrow band metals ($\rho \sim 10^{-4} \Omega\text{ cm}$) or semimetals. Superconducting. Charge density wave (CDW). Paramagnetic, antiferromagnetic, or diamagnetic.
6	Mo, W	S, Se, Te	Sulfides and selenides are semiconducting ($E_g \sim 1\text{ eV}$). Tellurides are semimetallic ($\rho \sim 10^{-3} \Omega\text{ cm}$). Diamagnetic.
7	Tc, Re	S, Se, Te	Small-gap semiconductors. Diamagnetic.
10	Pd, Pt	S, Se, Te	Sulfides and selenides are semiconducting ($E_g = 0.4\text{ eV}$) and diamagnetic. Tellurides are metallic and paramagnetic. PdTe_2 is superconducting.

When the orbitals are partially filled, as in the case of 2H-NbSe₂ and 1T-ReS₂, TMDs exhibit metallic conductivity. When the orbitals are fully occupied, such as in 1T-HfS₂, 2H-MoS₂ and 1T-PtS₂, the materials are semiconductors.

M. Chhowalla et al, Nature Chemistry (2013)

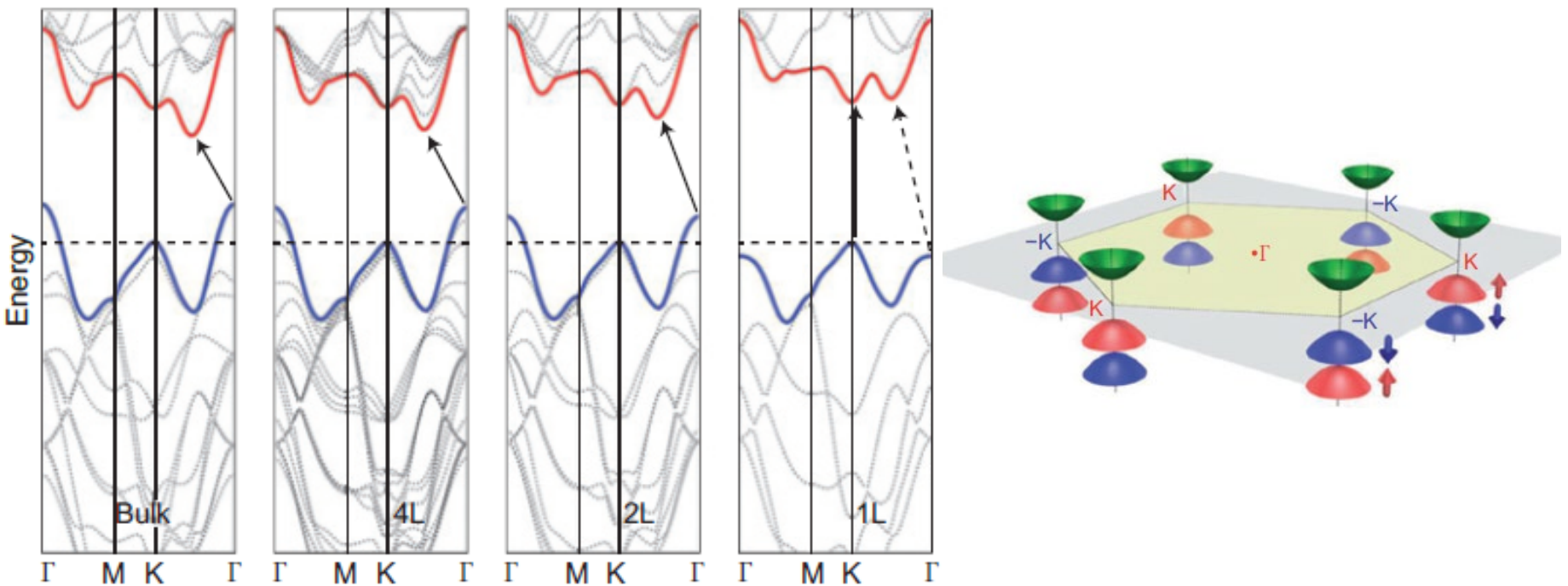
Band alignment of TMDs



As the atomic indices of chalcogen species increase from S to Te, the valence band edge undergoes a conspicuous energy increase, associated with a relatively smaller energy increase of conduction band edge, resulting in a decreasing energy gap.

Cheng Gong, Kyeongjae Cho, et.al., Applied Physics Letters, 103, 053513, 2015

Band gap of MoS₂

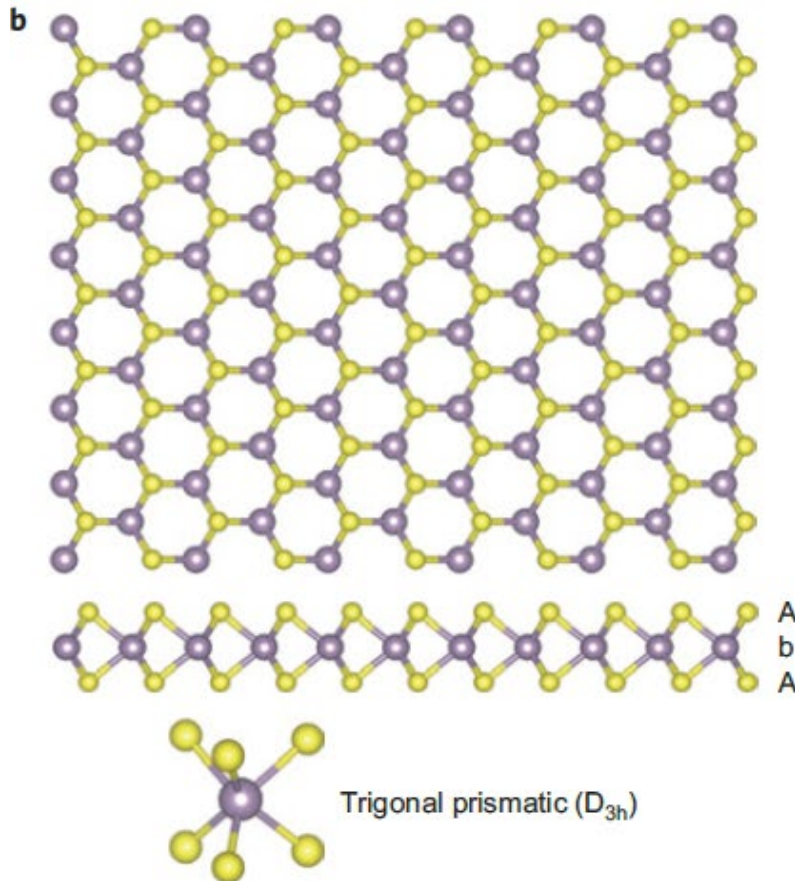


- The bulk material is an indirect gap semiconductor having a bandgap of ~ 1 eV with a valence band maximum (VBM) at the Γ point and a conduction band minimum (CBM) at the midpoint along Γ -K symmetry lines.
- In contrast, an isolated monolayer of the same material is a direct-gap semiconductor with VBM and CBM coinciding at the K-point.

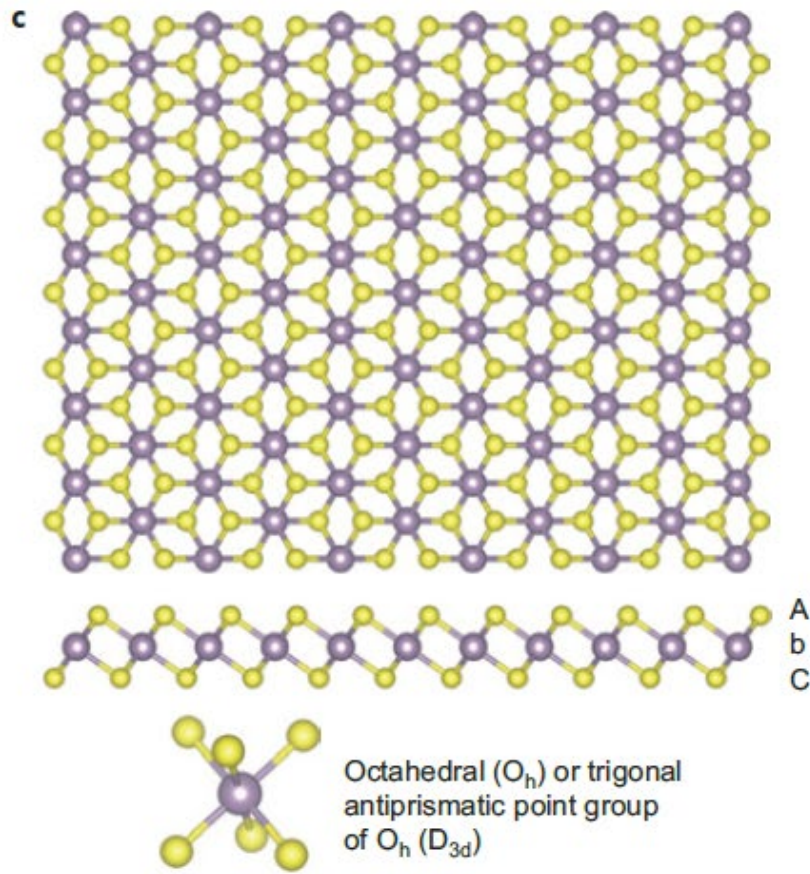
M. Chhowalla et al, Nature Chemistry (2013)

Crystal phases of monolayer TMD

1H phase



1T phase

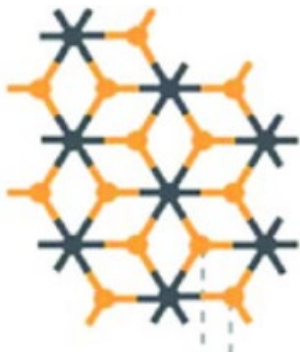
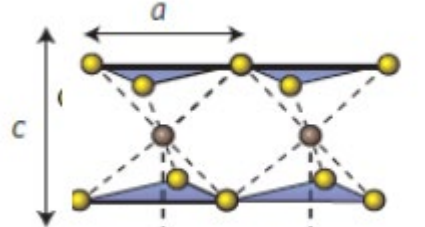


Monolayer TMDs exhibit two polymorphs: trigonal prismatic and octahedral (trigonal antiprismatic) structures. They are usually referred to as 1H and 1T phase, respectively.

M. Chhowalla et al, Nature Chemistry (2013)

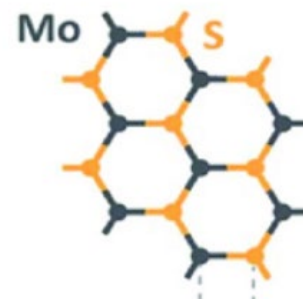
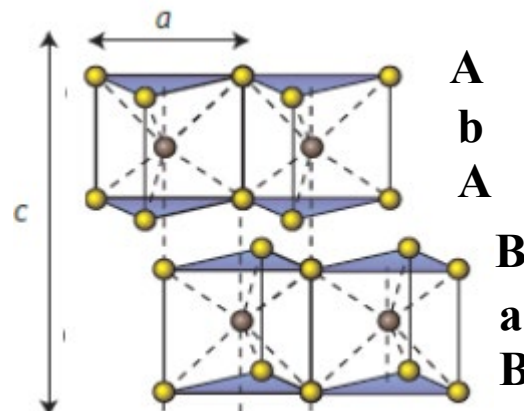
Crystal phases of bulk TMD

1T



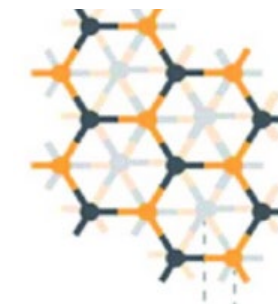
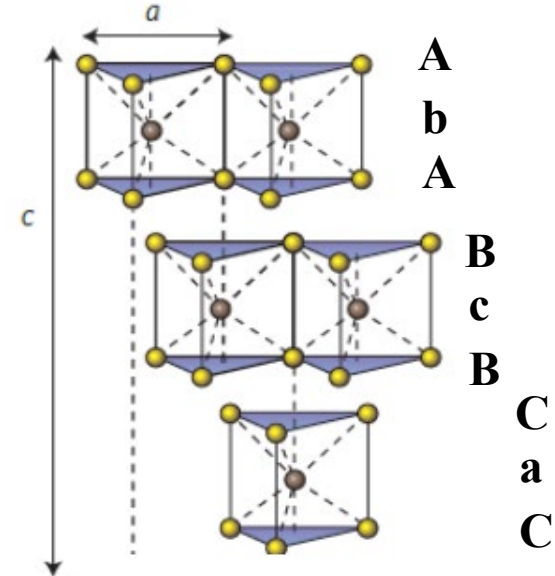
One layer per repeat unit
Tetragonal symmetry

2H



Two layers per repeat unit
Hexagonal symmetry

3R



Three layers per repeat unit
Rhombohedral (trigonal) symmetry

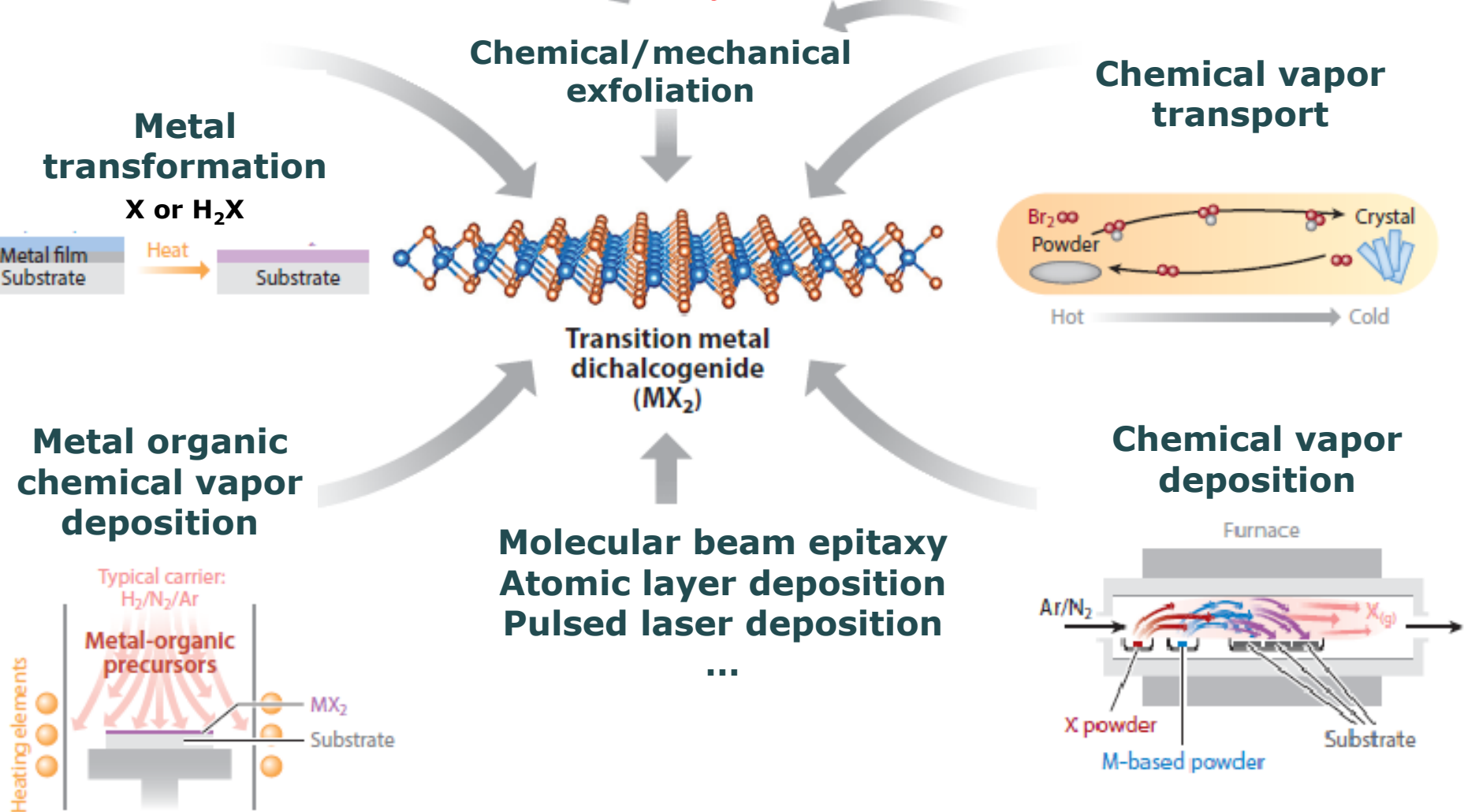
(In the atom position sequence, the capital and lower case letters denote chalcogen and metal atoms respectively)

Qing Wang, Michael Strano, Nature Nanotechnology, 7, 699, 2012

Outline

- Introduction of transition metal dichalcogenides (TMDs)
- • Synthesis of TMDs
- Current transport and electronic devices
- Optical properties and photonic devices

TMD synthesis



S. Das, et.al., Annu. Rev. Mater. Res. 45:1–27, 2015.

Y. Zhan, et.al., Small, 2012

Y. Lee, et.al., Advanced Materials, 2012;

A. Ubaldini, Crystal growth & design, 2013

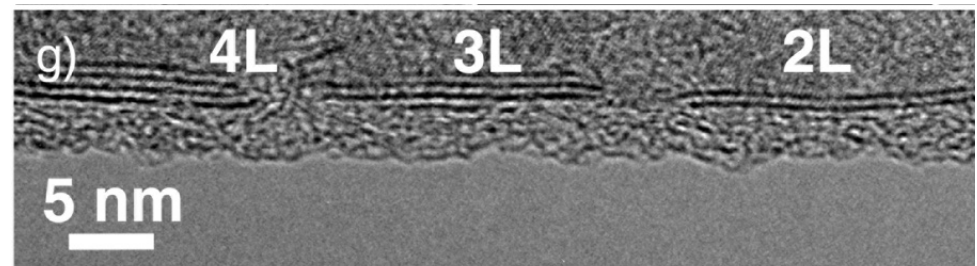
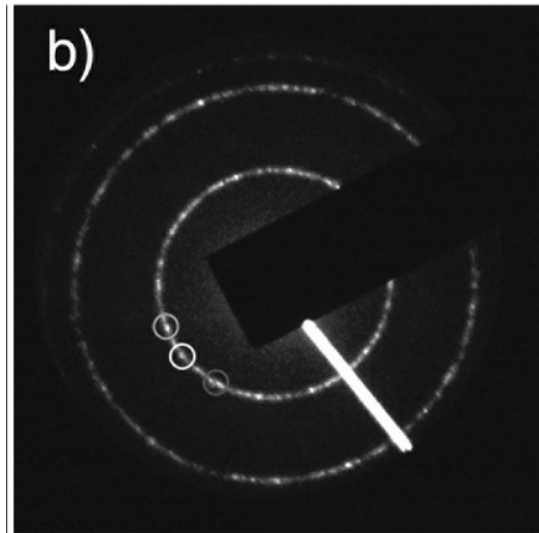
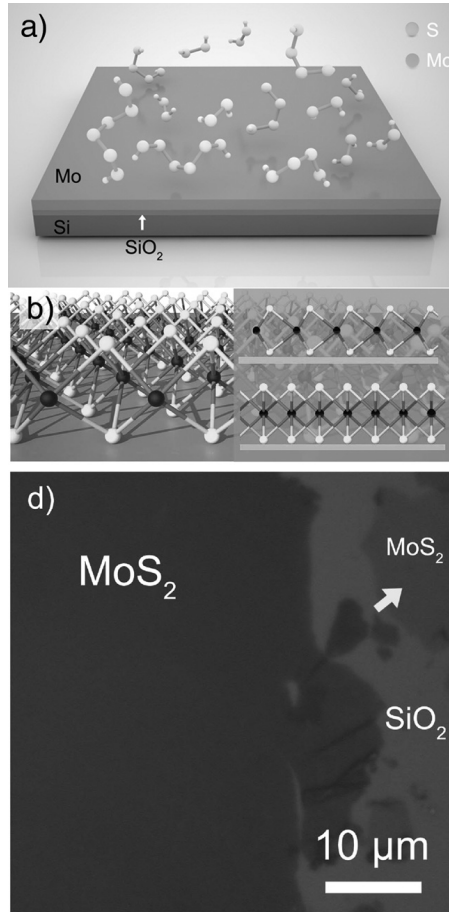
K. Kang, et.al., Nature, 2015;

S Das, et.al., Annu. Rev. Mater. Res. 2015;

Outline

- Introduction of transition metal dichalcogenides (TMDs)
- Synthesis of TMDs
 - ■ Synthesis of binary TMDs
 - Synthesis of TMD ternary alloys
 - Synthesis of TMD heterostructures
- Current transport and electronic devices
- Optical properties and photonic devices

Metal transformation method

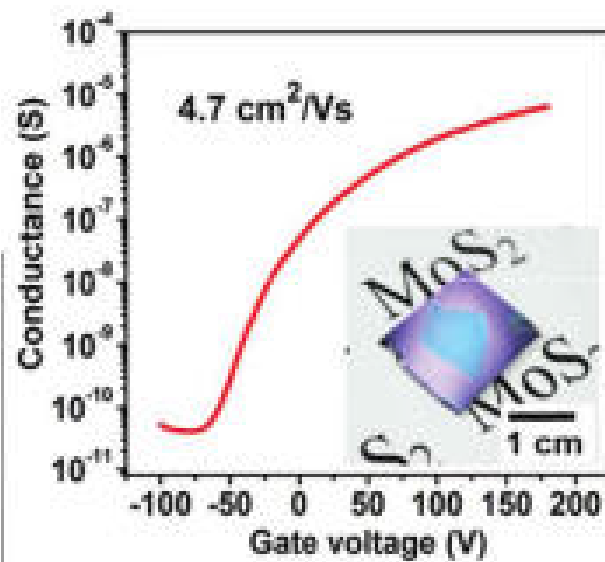
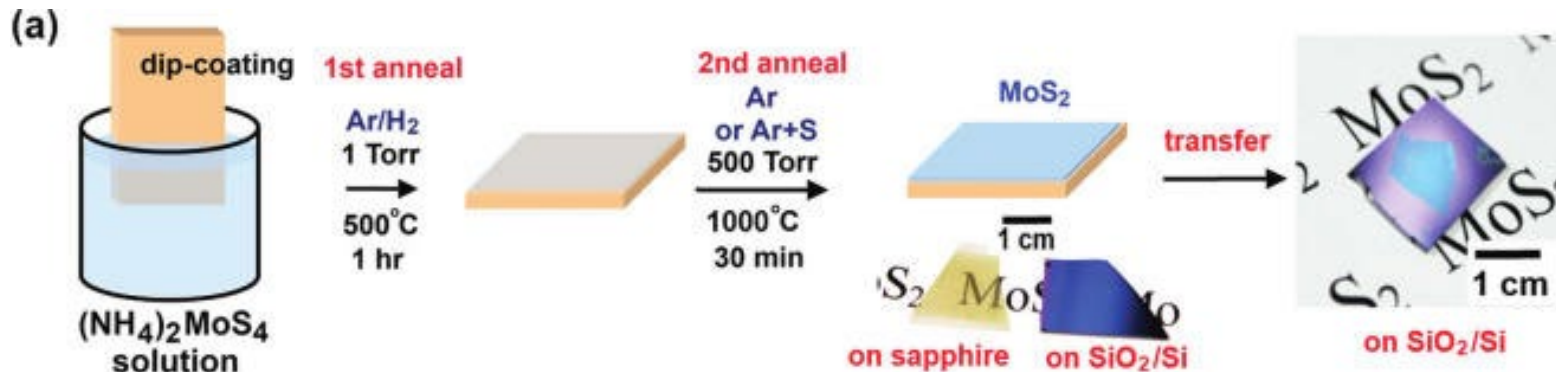


- A thin layer of Mo (~1–5 nm) was pre-deposited on SiO₂ by an e-beam evaporator. Sulfur is introduced and reacted with Mo at 750 °C forming very thin MoS₂ film (from single layer to few layers).
- Mobility is low: 0.004 to 0.04 cm²/V-s.

Y. Zhan, et.al., Small, 2012

CVD Synthesis of MoS₂ (1)

-- Two-step thermolysis process



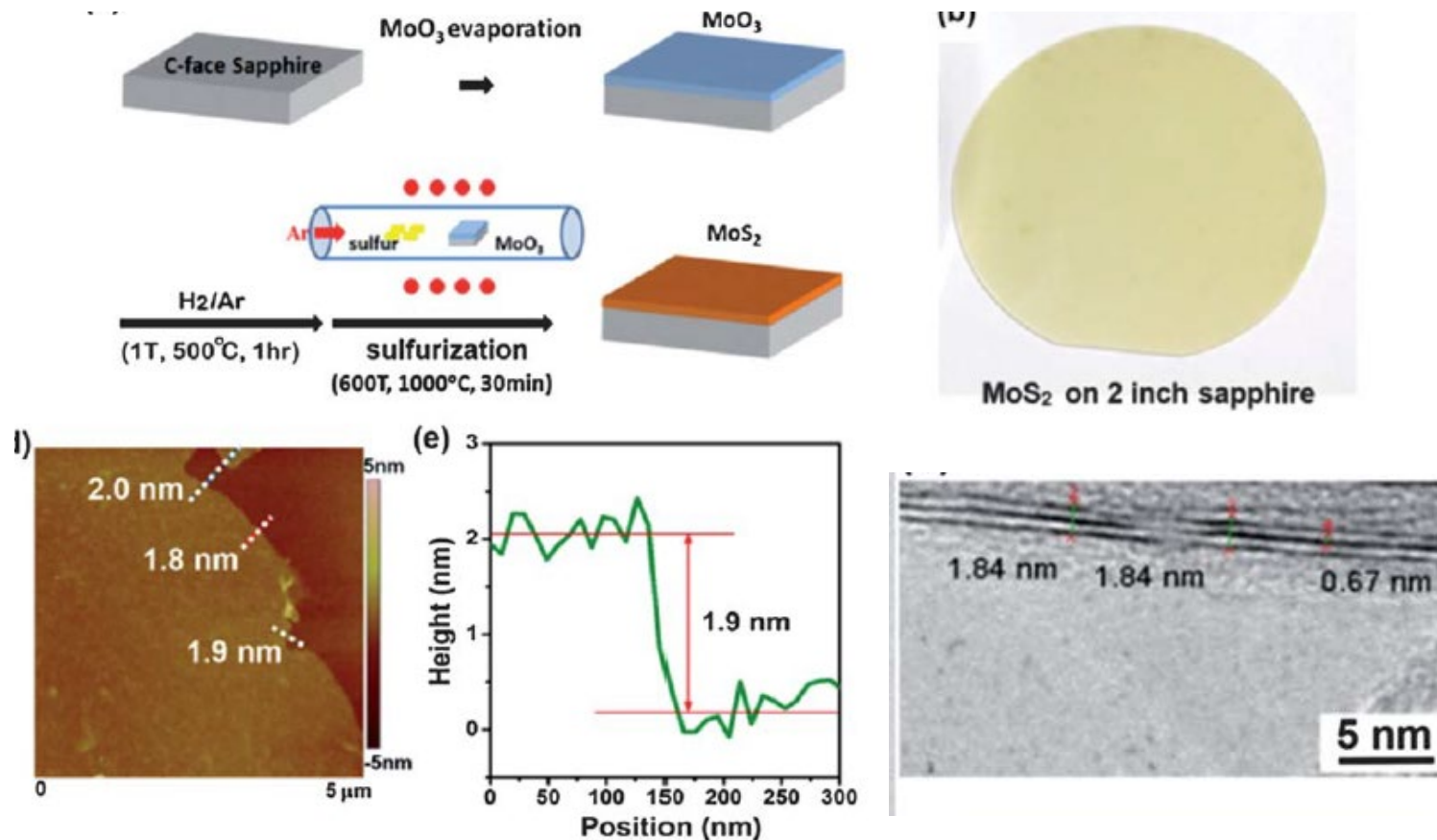
It was found that high temperature annealing of a thermally decomposed ammonium thiomolybdate layer in the presence of sulfur can produce large-area MoS₂ thin layers with superior electrical performance on insulating substrates.

Mobility: $\sim 6 \text{ cm}^2/\text{V}\cdot\text{s}$.

Keng-Ku Liu, Lain-Jong Li, et.al., Nano Letters, 12, 1538, 2012

CVD synthesis of MoS₂ (2)

--- sulfurization of metal oxide

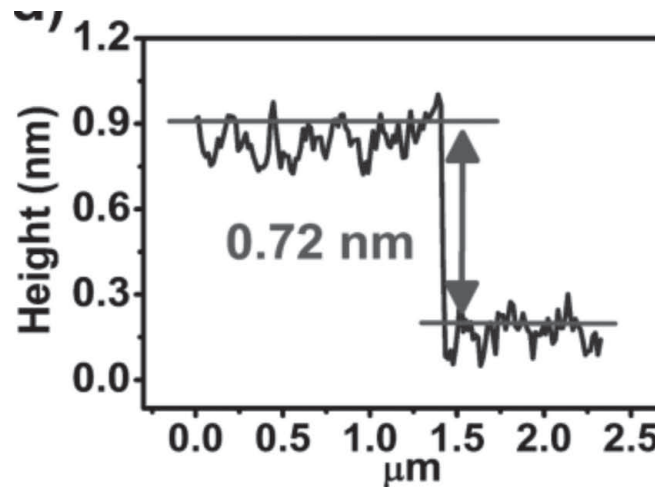
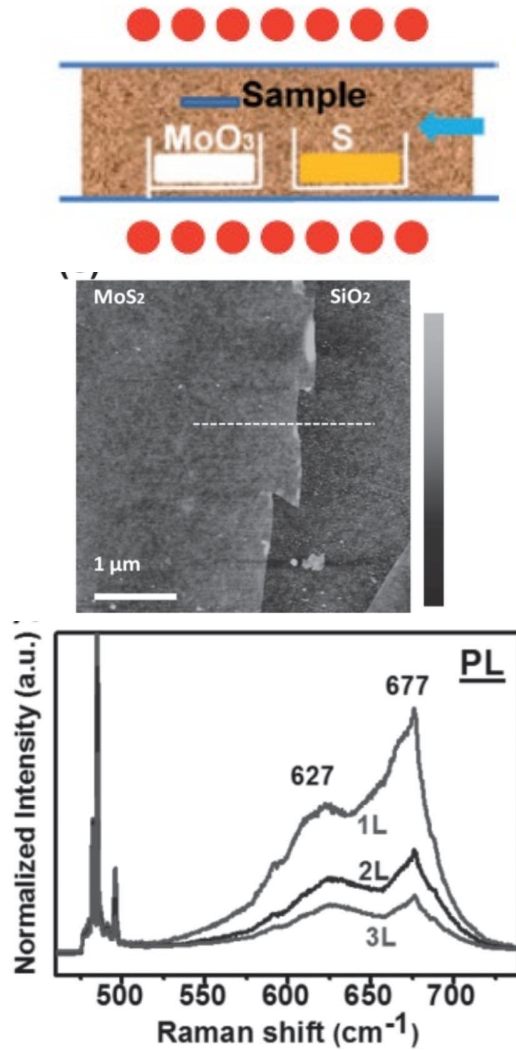


- Wafer-scale MoS₂ thin layers were synthesized on sapphire substrates by depositing MoO₃ thin films followed by thermal reduction of MoO₃ at 500 °C in hydrogen and sulfurization at 1000 °C in the presence of sulfur.
- Mobility: 0.8 cm²/V-s.

Yu-Chuan Lin, Lain-Jong Li, Nanoscale, 4, 6637, 2012

CVD synthesis of MoS₂ (3)

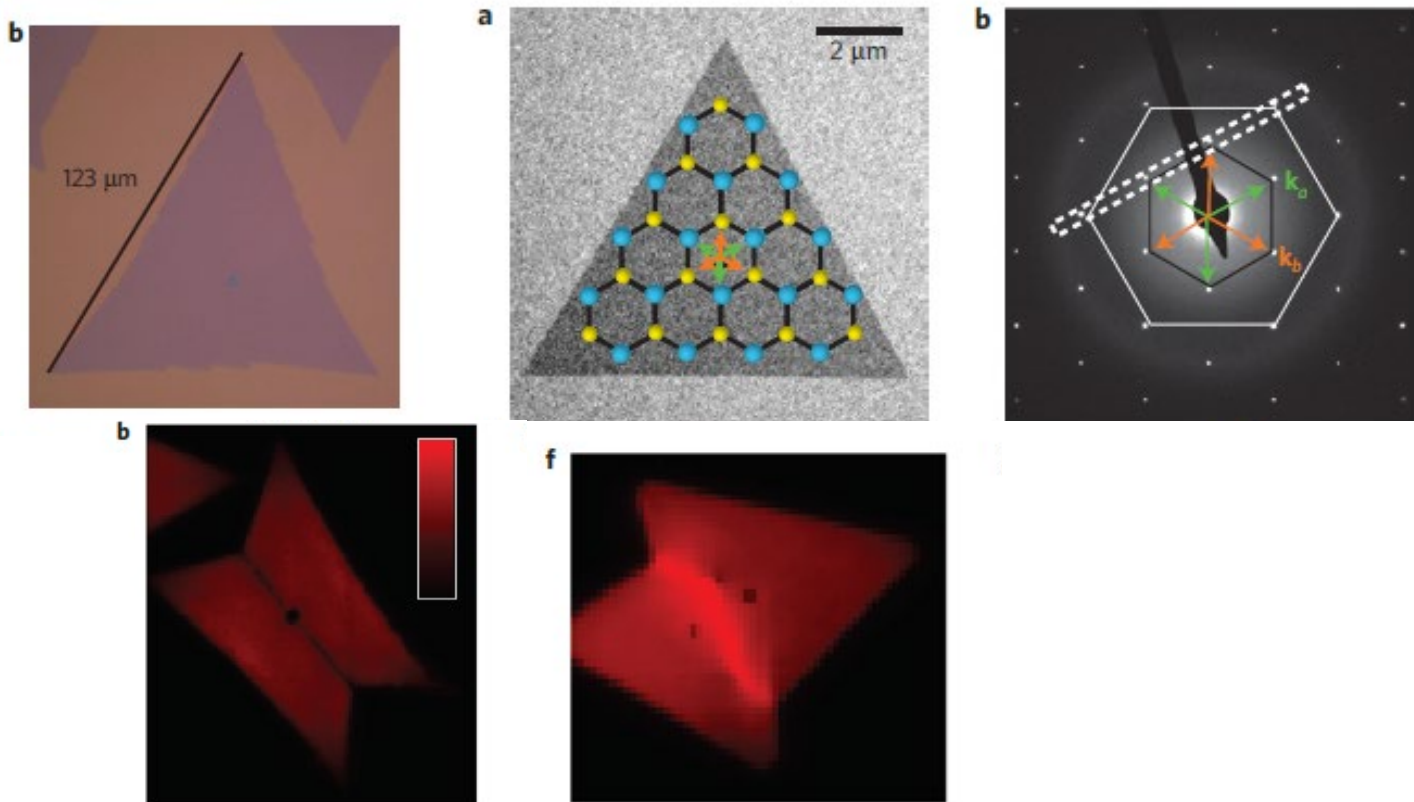
-- Gas-phase reaction of solid precursors



- Large-area monolayer MoS₂ films are directly synthesized on SiO₂ /Si substrates using with chemical vapor deposition.
- The use of graphene-like molecules for the substrate treatment, such as perylene-3,4,9,10-tetracarboxylic acid tetrapotassium salt (PTAS) and perylene-3,4,9,10-tetracarboxylic dianhydride (PTCDA), promotes the layer growth of MoS₂.
- Mobility: 0.02 cm²/V-s.

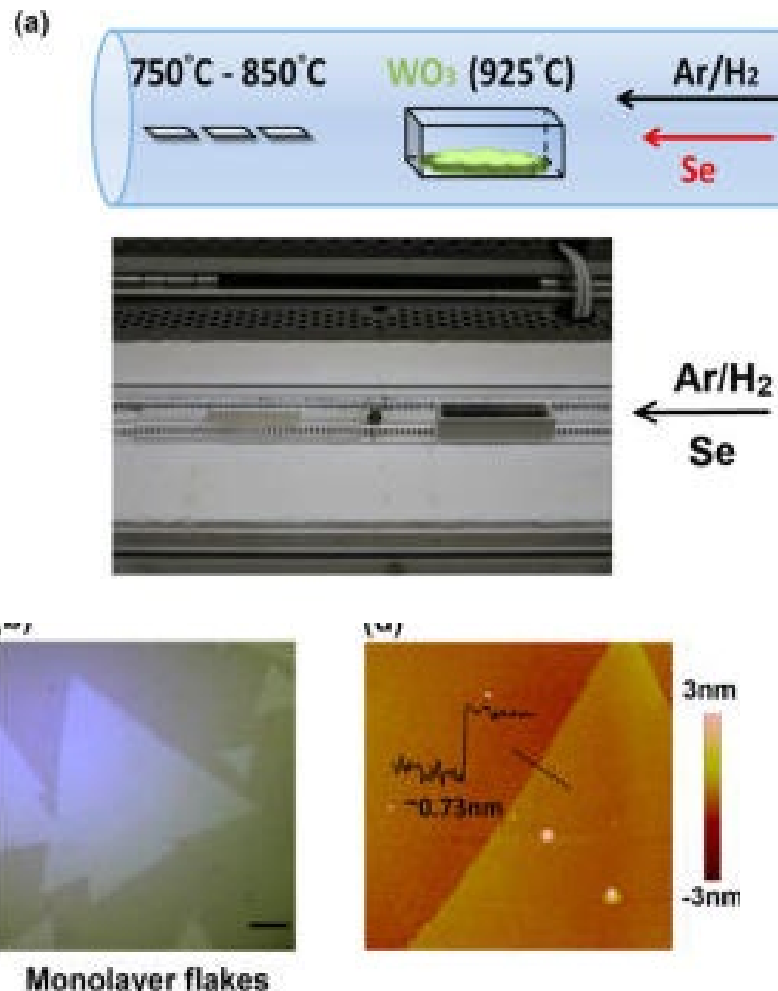
Yi-Hsien Lee, Tsung-Wu Lin, et.al., Advanced Materials, 24, 2320, 2012

CVD synthesis of MoS₂ (3)



- Monolayer MoS₂ with domain size up to 120 μm was synthesized without PTAS seed. The best growths were obtained with carefully cleaned substrates and by minimizing the exposure of the precursors to air during storage.
- The mirror twin boundaries cause strong photoluminescence quenching whereas tilt boundaries cause strong enhancement.
- Mobility: 1~8 $\text{cm}^2/\text{V}\cdot\text{s}$. Arend van der Zande, James Hone, et.al., Nature Materials, 12, 554, 2013

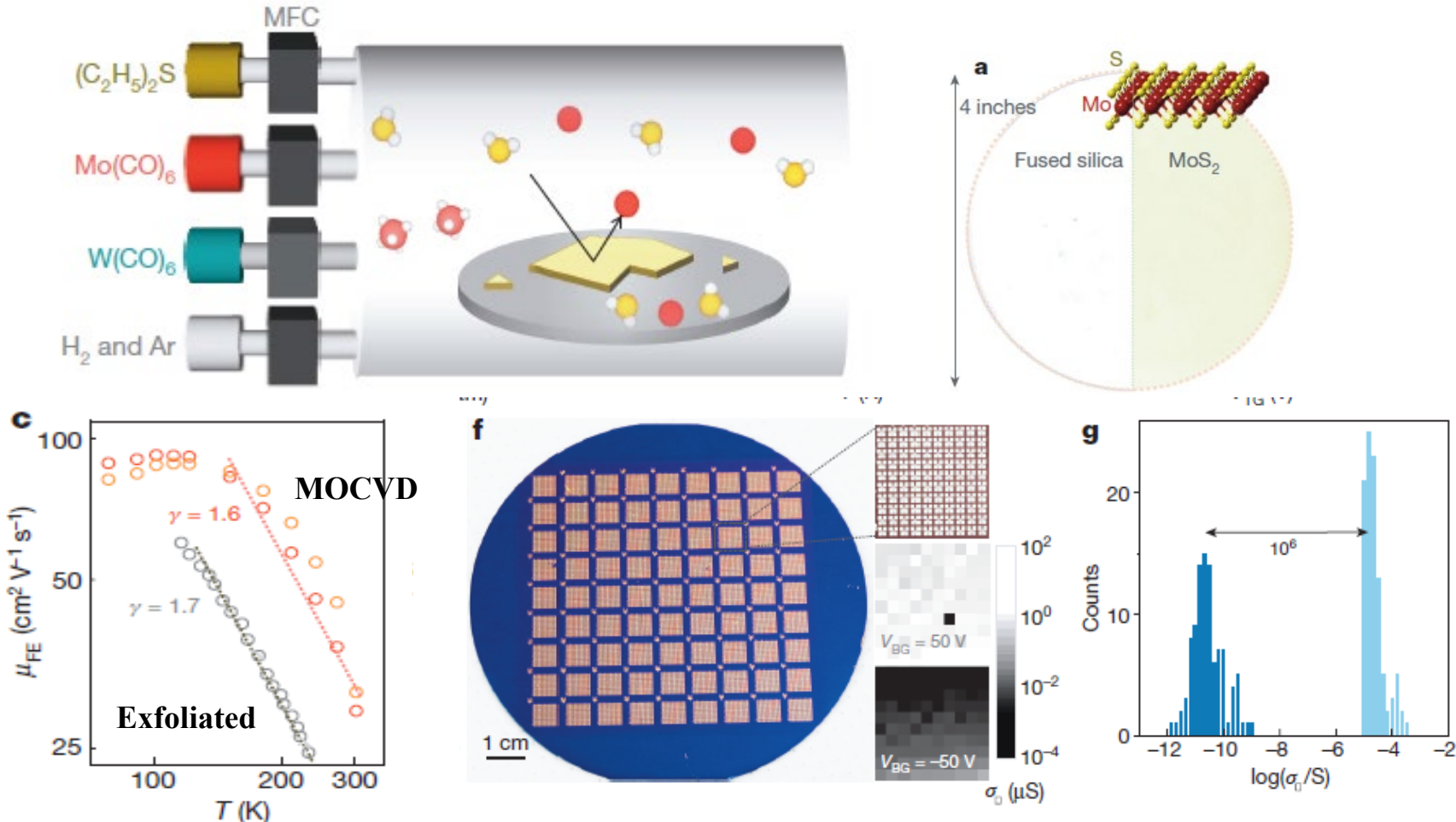
CVD synthesis of WSe₂



- Monolayer WSe₂ was synthesized on sapphire substrates via CVD using WO₃ and Se powder as precursors.
- The top-gated field-effect transistors based on WSe₂ monolayers using ionic gels as the dielectrics exhibit ambipolar characteristics, where the hole and electron mobility values are up to 90 and 7 cm²/Vs, respectively.

Jing-Kai Huang, Lain-Jong Li, et.al., 8, 923, 2014

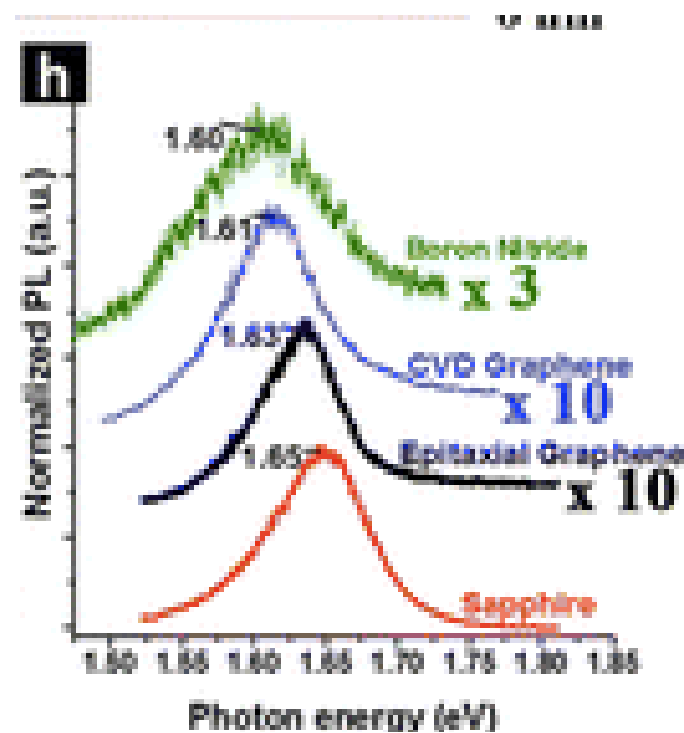
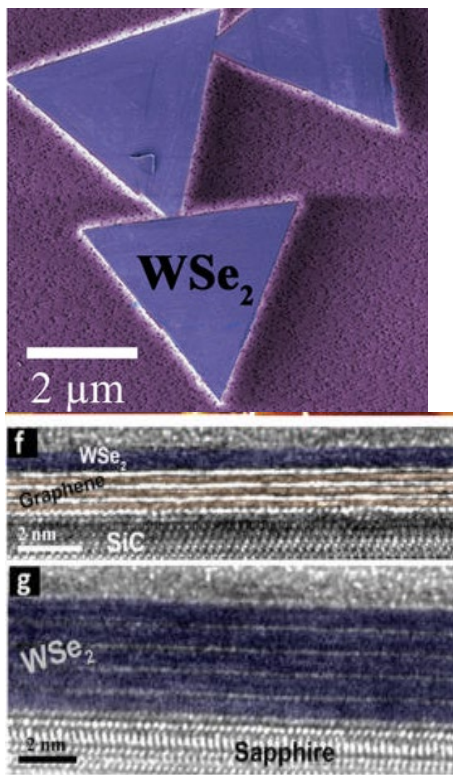
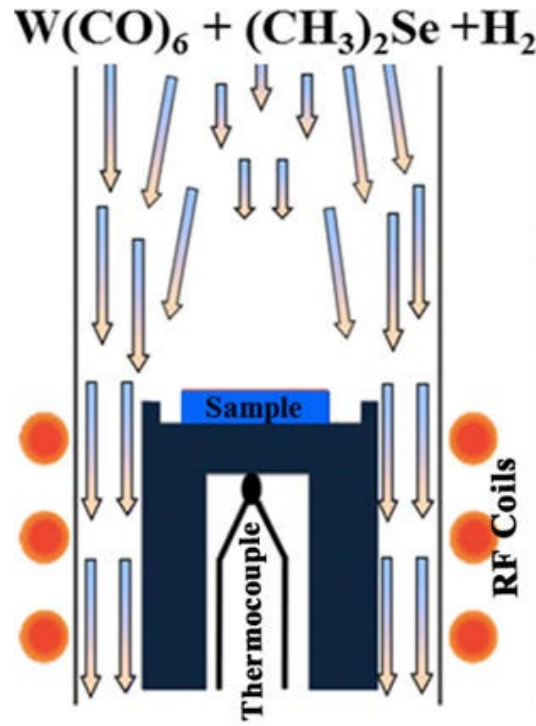
MOCVD synthesis of MoS₂ and WS₂



- 4-inch wafer-scale films of monolayer MoS₂ and WS₂ were grown via metal–organic chemical vapour deposition (MOCVD). The electron mobility is ~ 30 cm²/V-s at room temperature for MoS₂ with good uniformity.

Kibum Kang, Jiwoong Park, et.al., Nature, 520, 656, 2015

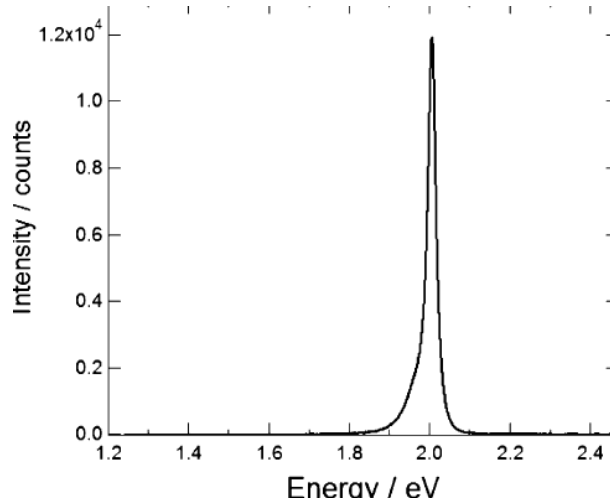
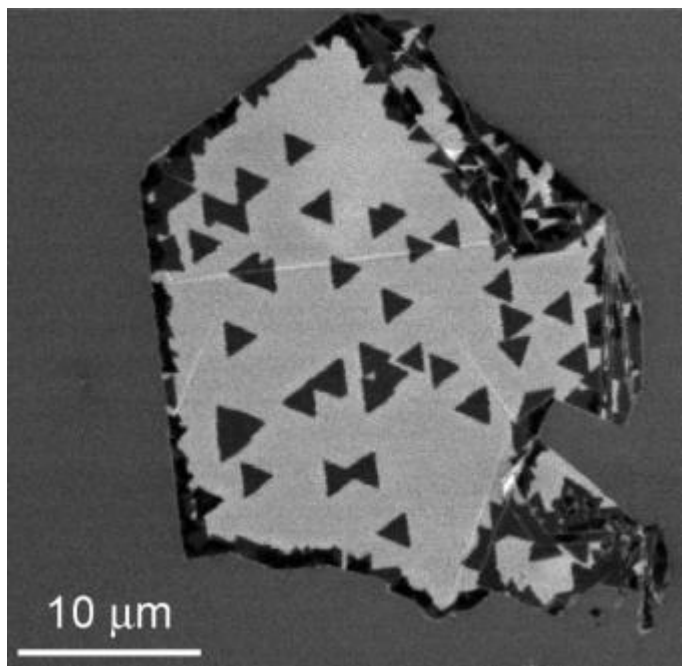
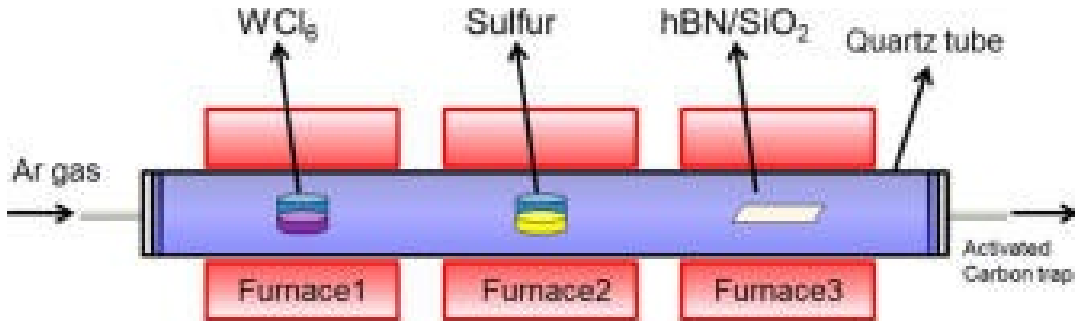
MOCVD synthesis of WSe₂



- The authors reported scalable synthesis of large-area, mono and few-layer WSe₂ via metal organic chemical vapor deposition using tungsten hexacarbonyl (W(CO)₆) and dimethylselenium ((CH₃)₂Se).
- WSe₂/graphene heterostructures were also synthesized.

Sarah Eichfeld, Joshua Robinson, et.al., ACS Nano, 9, 2080, 2015

Direct growth of WS_2 on boron nitride



- WS_2 was grown directly onto high-quality hBN using CVD process.
- Triangular crystals of WS_2 grown on hBN is limited to two different orientations with a relative angle of 60° .
- Photoluminescence spectra of the WS_2 show an intense emission peak at 2.01 eV with a quite small full width half maximum (fwhm) of 26 meV. The sharp emission peak indicates the high quality of the present WS_2 atomic layers with high crystallinity and clean interface.

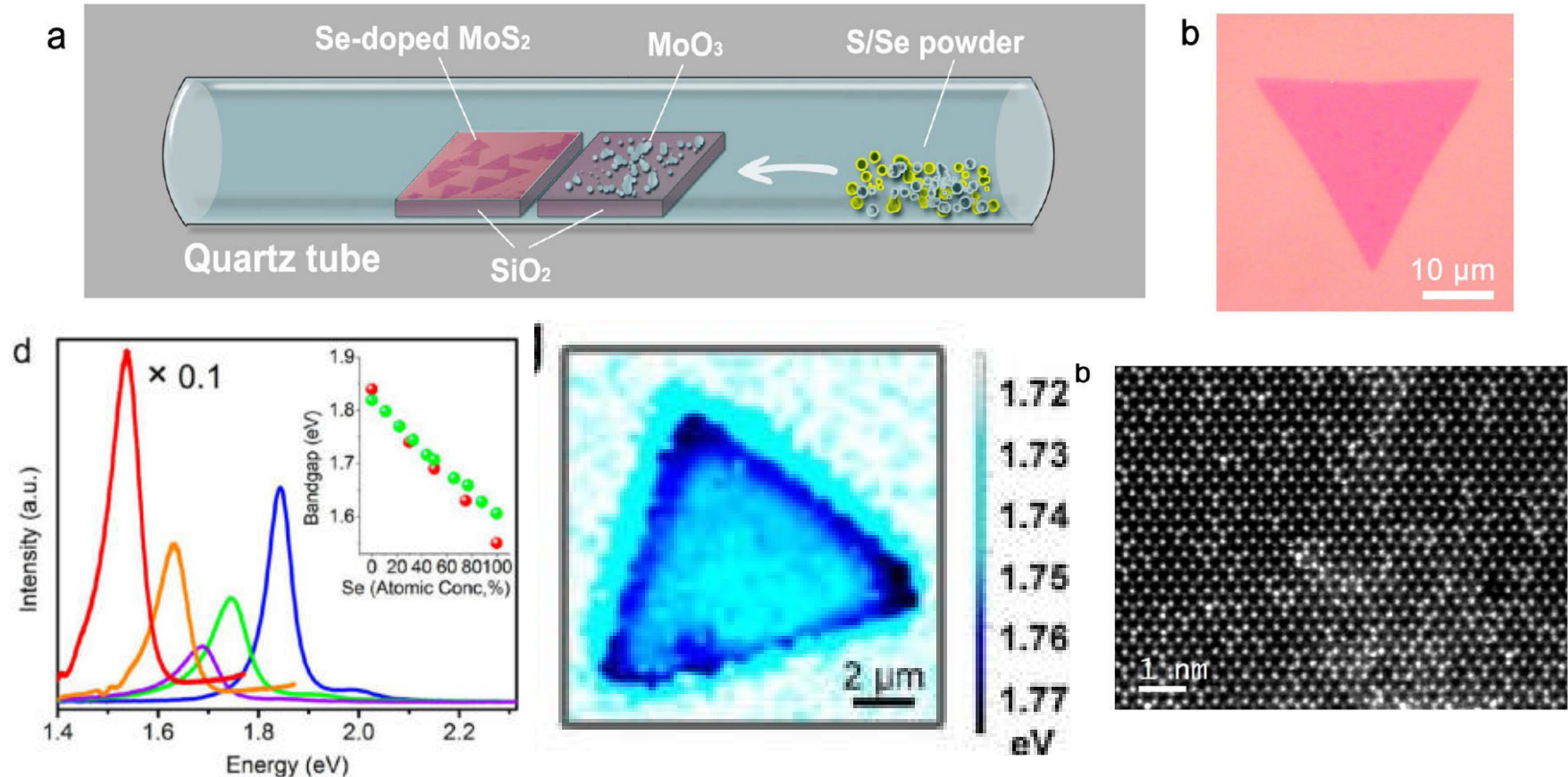
Mitsuhiro Okada, Ryo Kitaura, et.al., ACS Nano, 8, 8273, 2014

Outline

- Introduction of transition metal dichalcogenides (TMDs)
- Synthesis of TMDs
 - Synthesis of binary TMDs
 - Synthesis of TMD ternary alloys
 - Synthesis of TMD heterostructures
- Current transport and electronic devices
- Optical properties and photonic devices



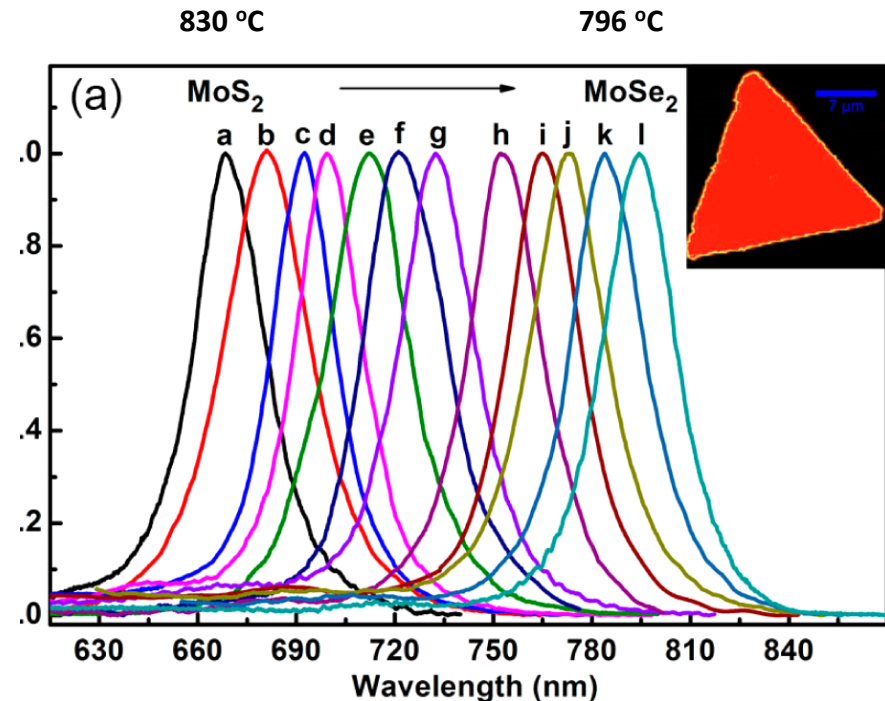
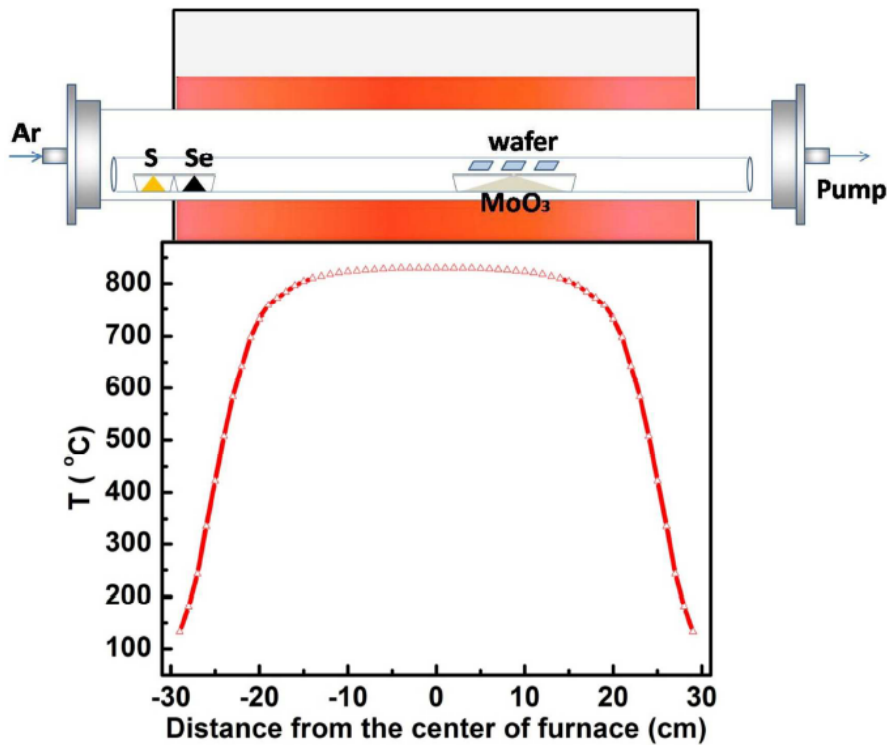
TMDC ternary alloy: $\text{MoS}_{2x}\text{Se}_{2-2x}$



- The authors synthesized MoS_2 substitutionally doped with a broad range of selenium concentrations, resulting in over 10% optical band gap modulations in atomic layers. Chemical analysis using Z-contrast imaging provides direct maps of the dopant atom distribution in individual MoS_2 layers.

Yongji Gong, Pulickel Ajayan, et.al. Nano Letters, 14, 442, 2014

TMDC ternary alloy: $\text{MoS}_{2x}\text{Se}_{2-2x}$



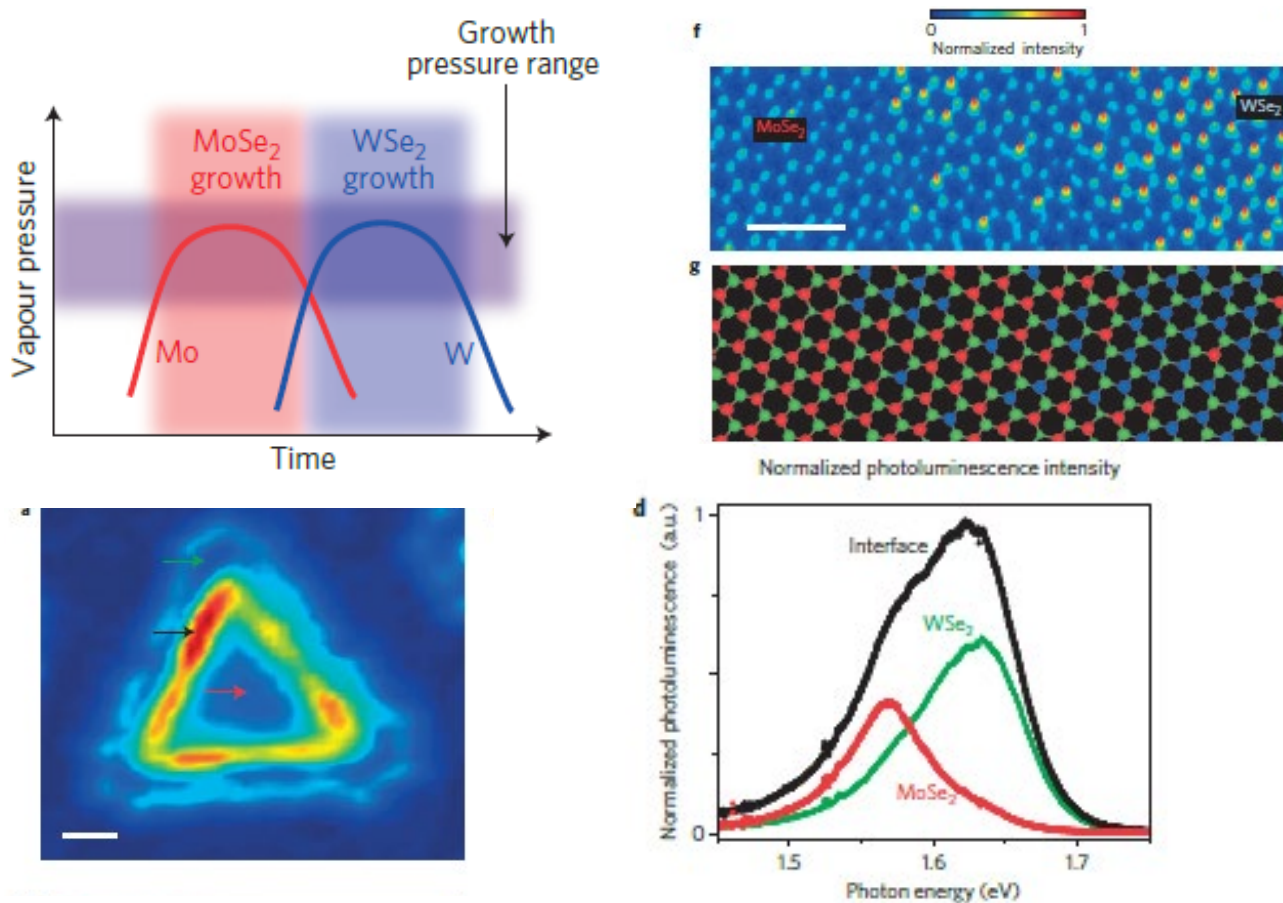
- A simple one-step chemical vapor deposition approach was demonstrated for the simultaneous growth of alloy $\text{MoS}_{2x}\text{Se}_{2(1-x)}$ triangular nanosheets with composition tunability.
- The samples show a single band edge emission peak, with the spectral peak position shifting from 668 nm (for pure MoS_2) to 795 nm (for pure MoSe_2).

Honglai Li, Xiangfeng Duan, et.al., Journal of the American Chemical Society, 136, 3756, 2014

Outline

- Introduction of transition metal dichalcogenides (TMDs)
- Synthesis of TMDs
 - Synthesis of binary TMDs
 - Synthesis of TMD ternary alloys
 - Synthesis of TMD heterostructures
- Current transport and electronic devices
- Optical properties and photonic devices

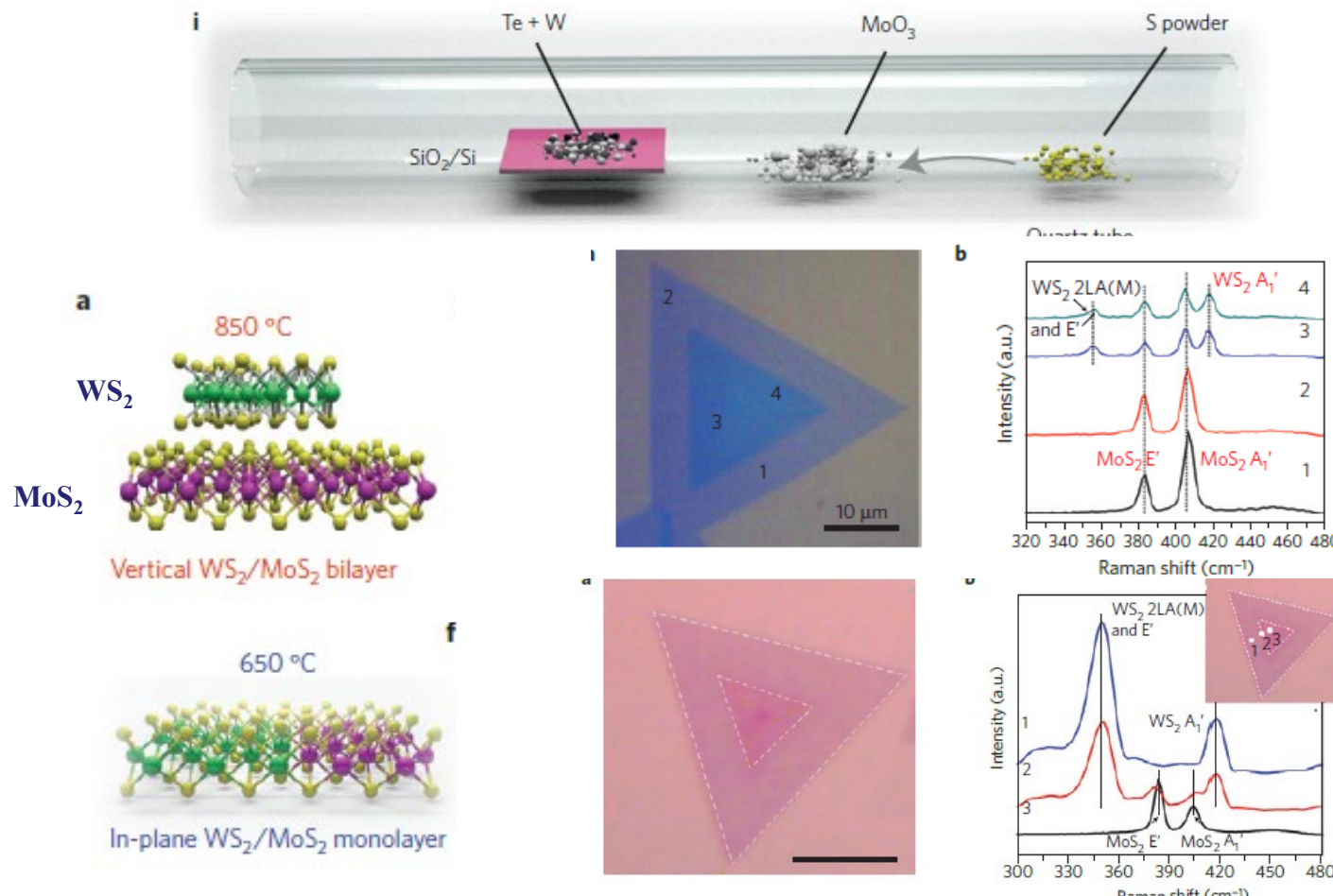
Lateral heterostructure synthesis: One-step process



- MoSe₂/WSe₂ heterojunctions was grown using physical vapour transport.
- The MoSe₂ and WSe₂ powder were loaded in the tube at the same time. MoSe₂ evaporates more rapidly at first, so initially growth is dominated by MoSe₂, After MoSe₂ precursor are depleted, WSe₂ start to grow.

Chunming Huang, Xiaodong Xu, et.al., Nature Materials, 13, 1096, 2014

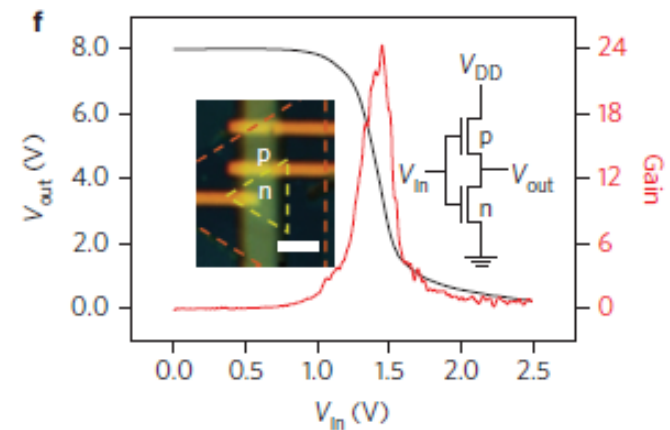
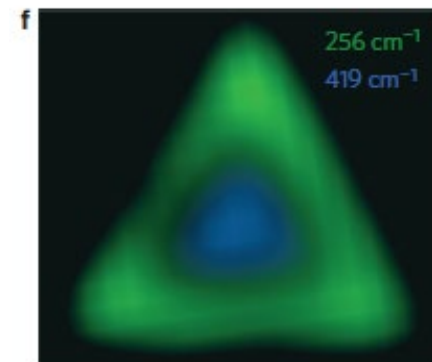
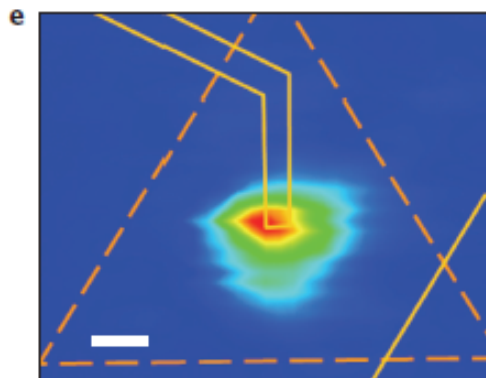
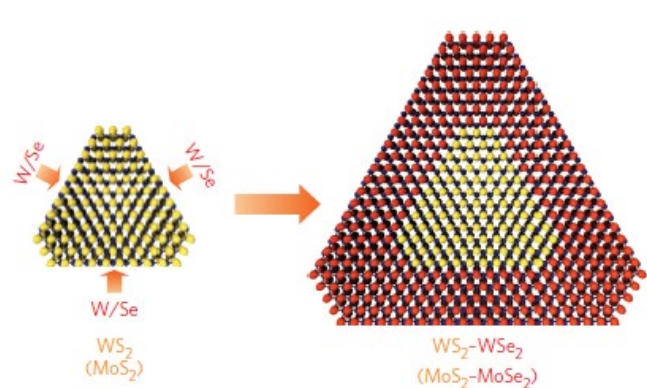
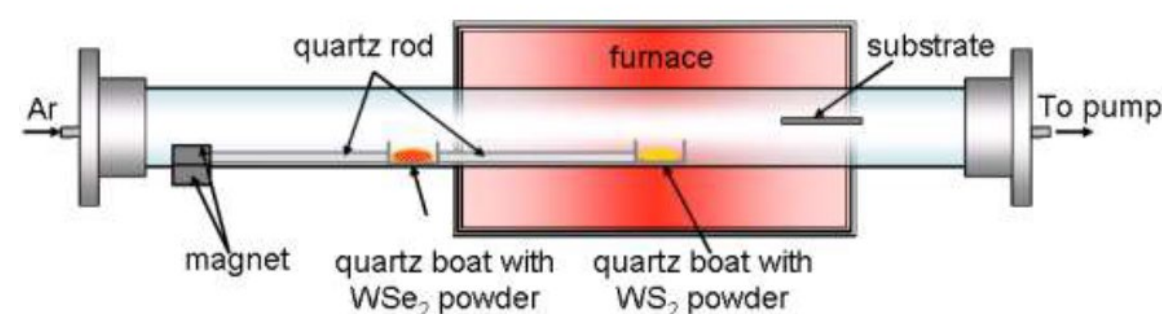
Synthesis of vertical and lateral heterostructure



- Vertical and lateral WS₂/MoS₂ heterostructures were grown using one-step process.
- At high temperature, vertically heterostructure with WS₂ epitaxially grown on top of the MoS₂ monolayer are formed. At low temperature, lateral epitaxy of WS₂ on MoS₂ edges were formed.

Yongju Gong, Pulickel Ajayan, Nature Materials, 13, 1135, 2014

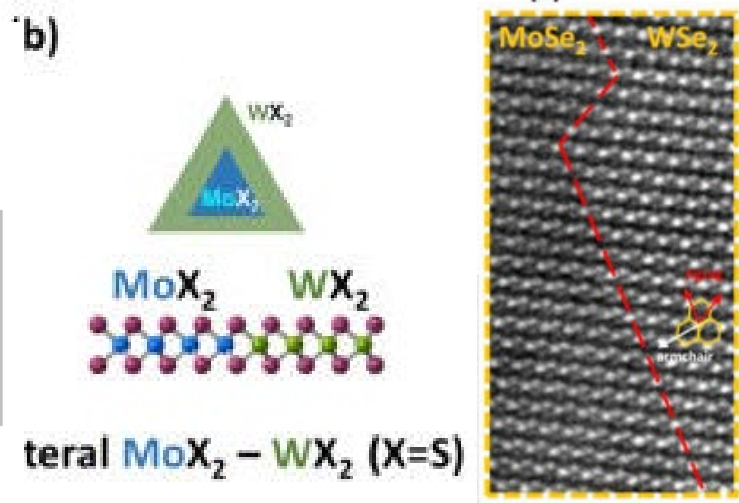
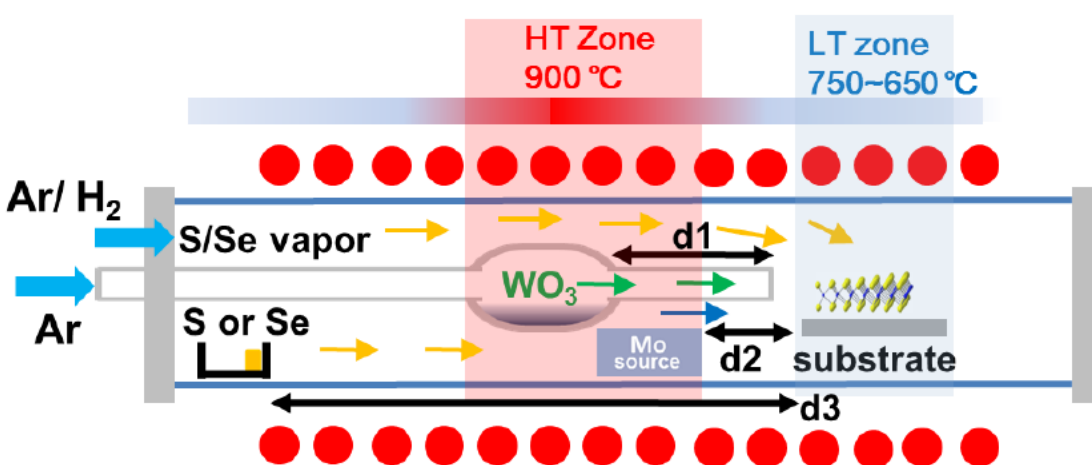
Synthesis of lateral heterostructure



- By *in situ* transfer of the WS₂ solid source out of the hot zone and the WSe₂ solid source into the hot zone without exposure to ambient conditions, WS₂–WSe₂ lateral heterostructures was produced.
- The WSe₂–WS₂ heterojunctions form lateral p–n diodes and photodiodes, and can be used to create complementary inverters with high voltage gain.

Xidong Duan, Xiangfeng Duan, et.al., Nature Nanotechnology, 9, 1024, 2014

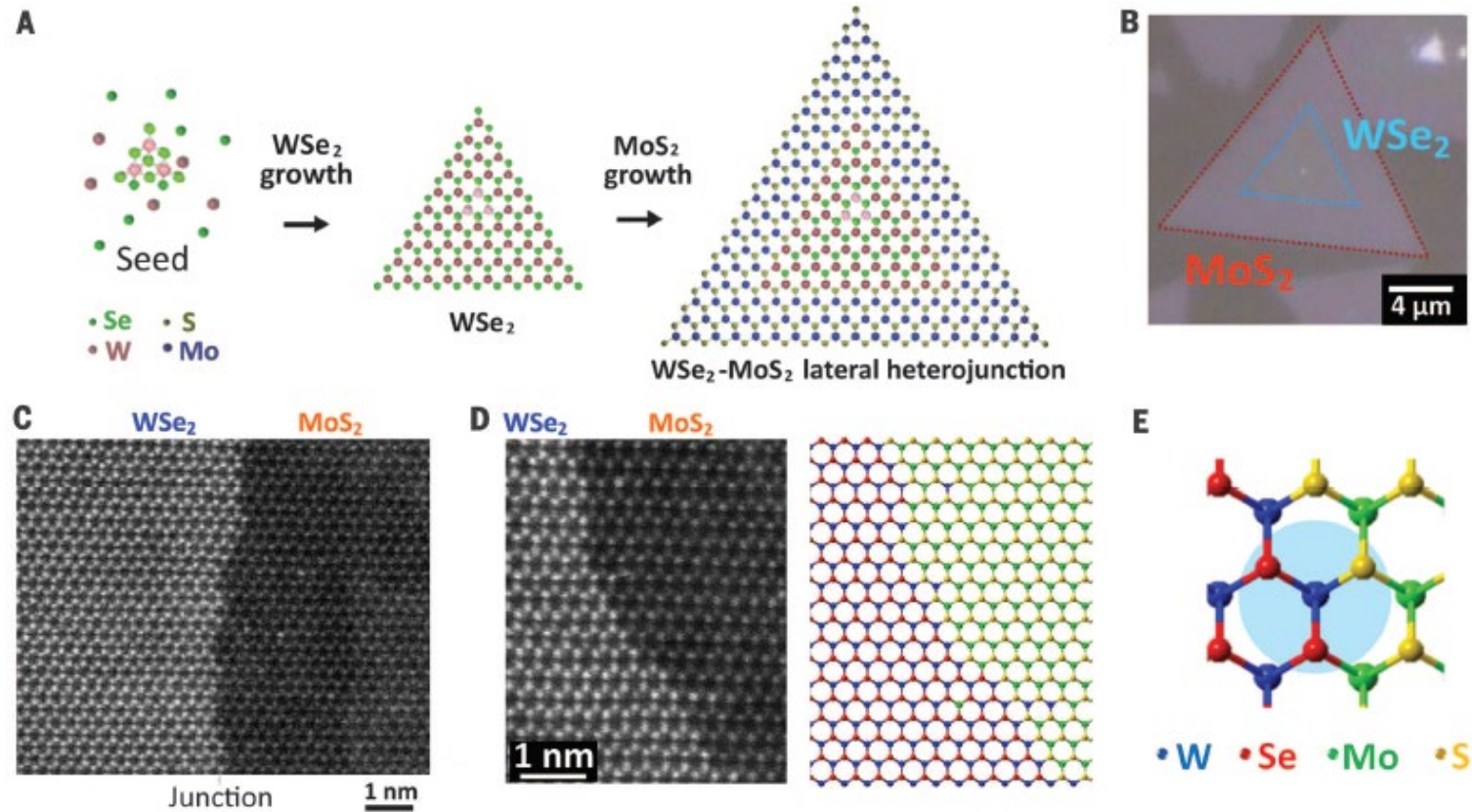
Synthesis of lateral heterostructure



- Monolayer TMDs: MoS_2/WS_2 and $\text{MoSe}_2/\text{WSe}_2$ lateral heterostructure were synthesized by CVD.
- The WO_3 powders were filled in the quartz reactor with a transfer tube in tunable length. By controlling the amount of reactants, lateral heterostructures of different TMD atomic layers can be synthesized.

Xin-Quan Zhang, Yi-Hsien Lee, Nano Letters, 15, 410, 2015

Lateral heterostructure synthesis: 2-step process



- Two-step epitaxial growth was used to grow lateral WSe₂-MoS₂ heterojunction, where the edge of WSe₂ induces the epitaxial MoS₂ growth despite a large lattice mismatch.
- The epitaxial growth process offers a controllable method to obtain lateral heterojunction with an atomically sharp interface.
- WSe₂ was grown on the sapphire substrate first, then the sample was put into a separate furnace for the 2nd step MoS₂ growth.

Ming-Yang Li, Lain-Jong Li, et.al., Science, 349, 524, 2015

Outline

- **Introduction of TMDs**
- **Synthesis of TMDs**
- **Electronic properties and electronic devices**
 - **Electronic properties**
 - • Carrier mobility
 - Metal-TMD contact
 - **Electronic devices**
- **Optical properties and photonic devices**

Mobility characterization methods

- Effective mobility

$$\mu_{eff} = \frac{L}{W} \frac{I_D}{V_D |Q_I|} \approx \frac{L}{W V_D} \frac{I_D}{C_i (V_G - V_T)}$$

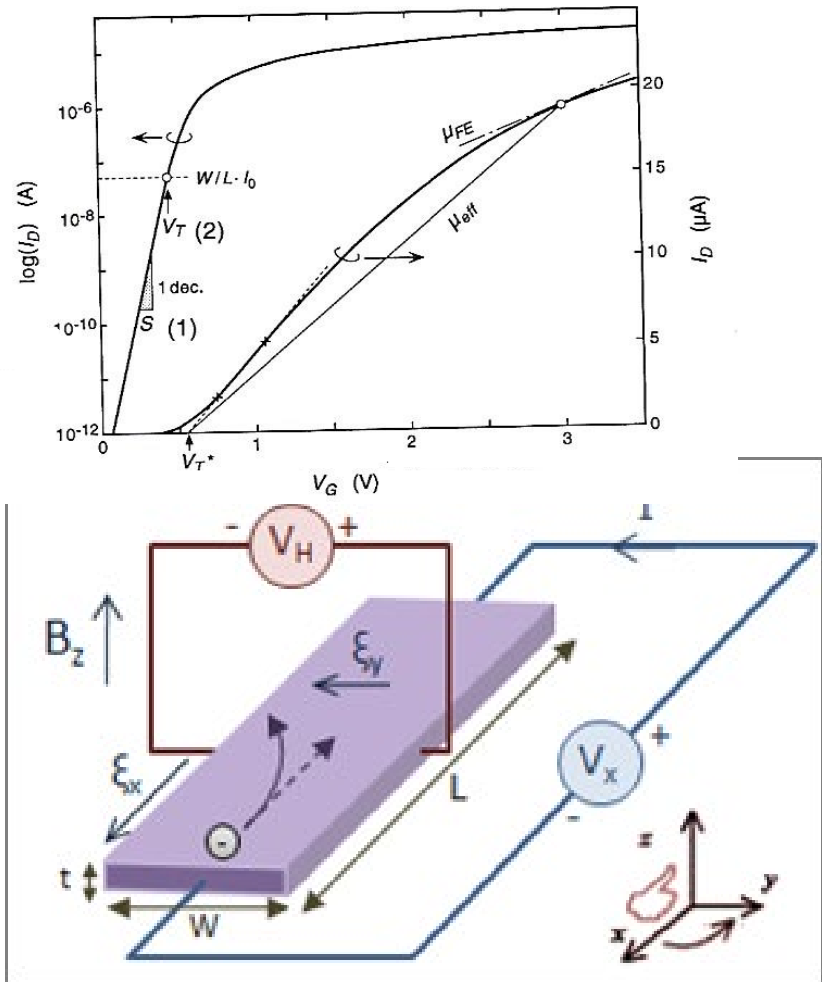
- Field Effect Mobility

$$\mu_{FE} = \frac{L}{W V_D C_i} g_m$$

- Hall mobility

$$n = \frac{J_x B}{q \epsilon_H}$$

$$\mu_{Hall} = \frac{\sigma_x}{qn}$$



Trapped charge and contact resistance can result in underestimate of mobility using effective and field effect mobility methods. Hall effect measurement can directly measure mobile carrier density and channel resistance, i.e. more accurate.

To extract mobility accurately

1. For effective and field effect mobility extraction, it is important to use the correct oxide capacitance.

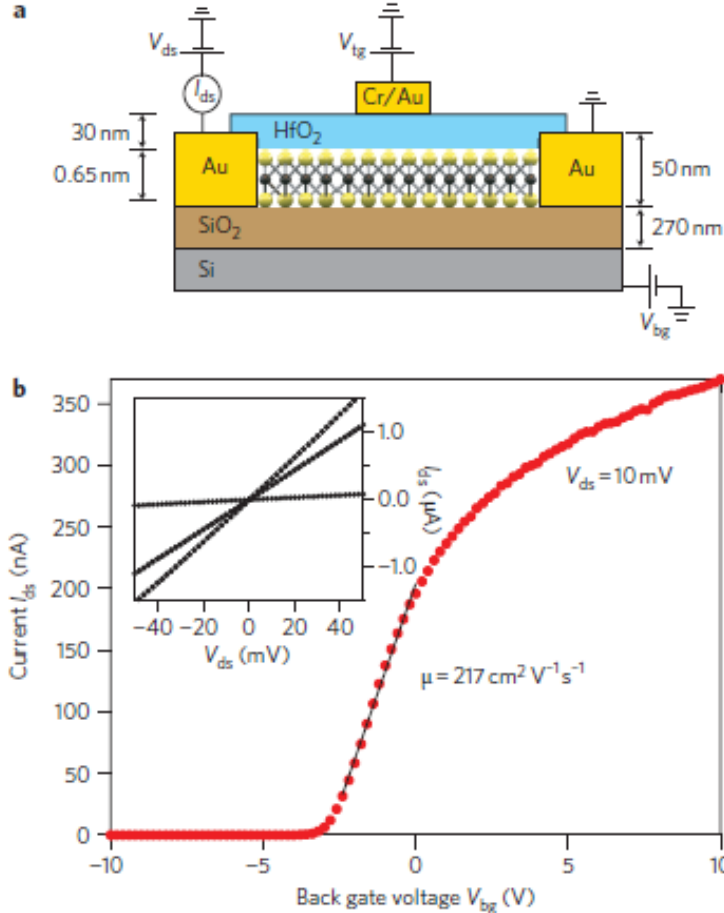
In a double gated transistor, the voltage applied to the back gate can be coupled to the top gate. If the thickness of the top gate dielectric is much thinner than the back gate oxide, then the top gate capacitance needs to be used in the mobility extraction.

2. Distinguish the mobile carrier from the trapped carriers

Carriers trapped in the localized states in TMDs do not contribute to the drive current of a transistor. Using capacitance to directly estimate the carrier density can lead to overestimation of carriers and underestimation of mobility. To extract mobility accurately, measurement of trap charge density is needed.

3. Hall measurement can provide more accurate information on the carrier density and mobility

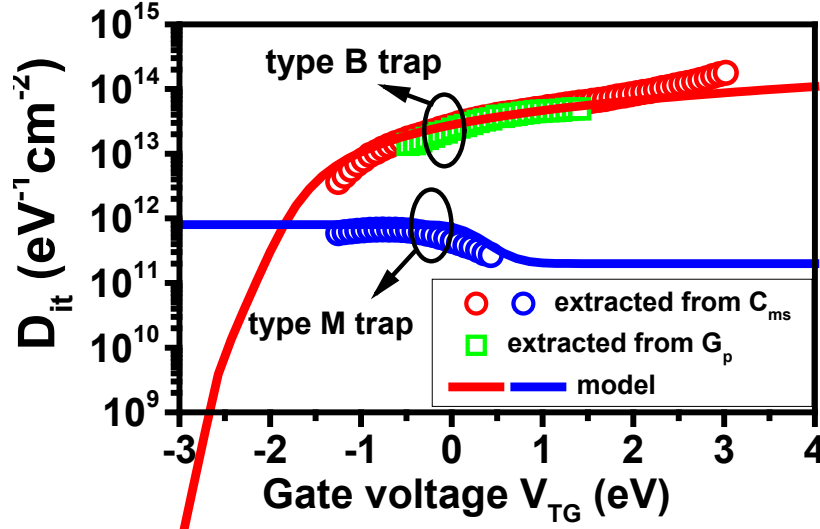
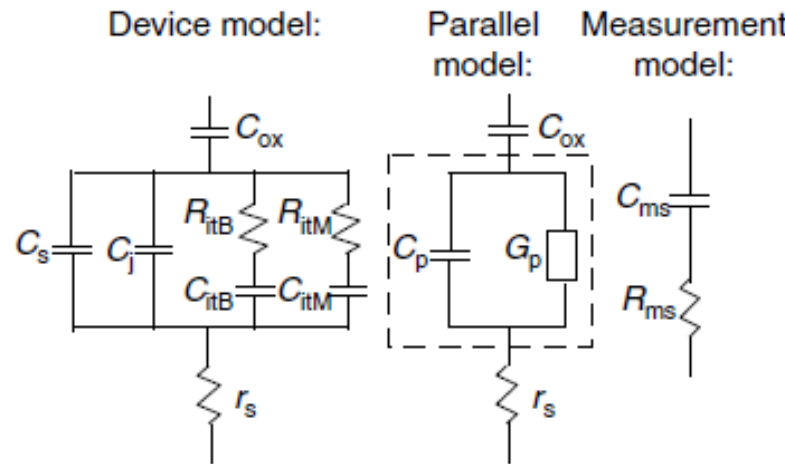
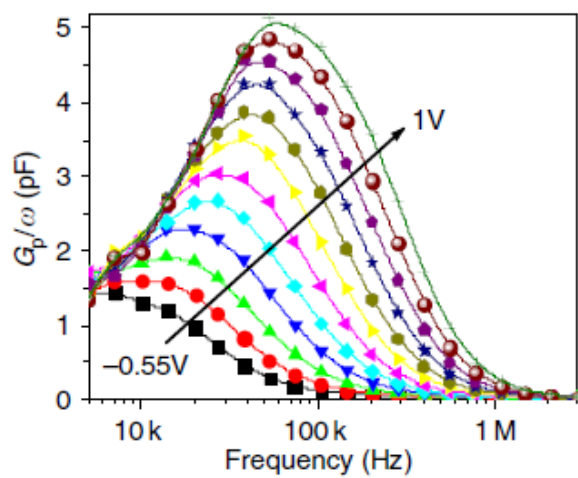
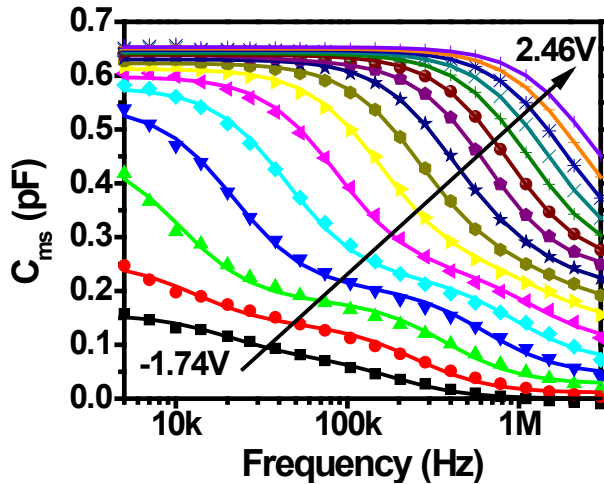
Mobility of MoS₂ transistor



- The authors demonstrate a room-temperature single-layer MoS₂ of on/off ratios of 10⁸.
- Mobility measured in back-gated transistor: 0.1–10 cm²/V-s
- Mobility measured using back gate in a top-gated transistor: ~200 cm²/V-s.

B. Radisavljevic, A. Kis, Nature Nanotechnology, 6, 147, 2011

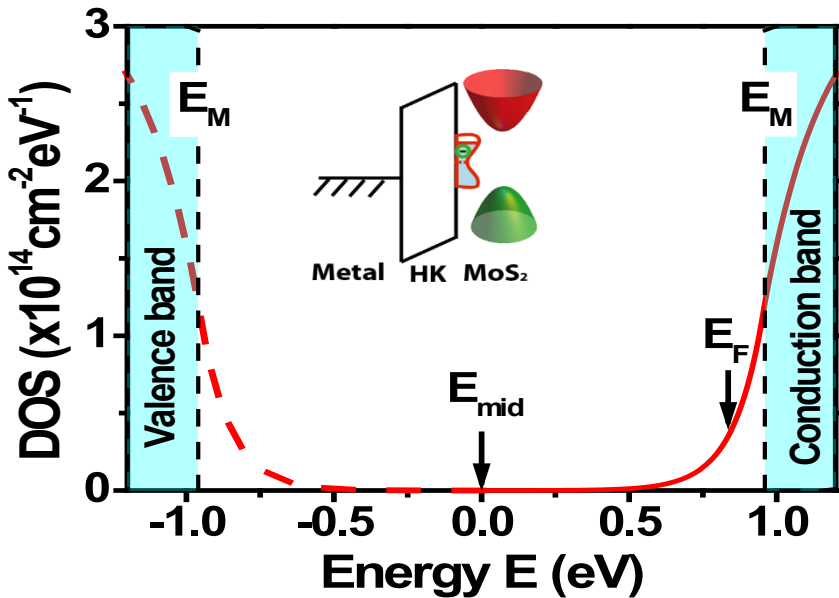
Measurement of interface traps in MoS₂ devices



- Density of gap state in MoS₂ can be measured using ac conductance method.

W. Zhu, et.al. Nature Communications, 2014

Extract band mobility of MoS₂

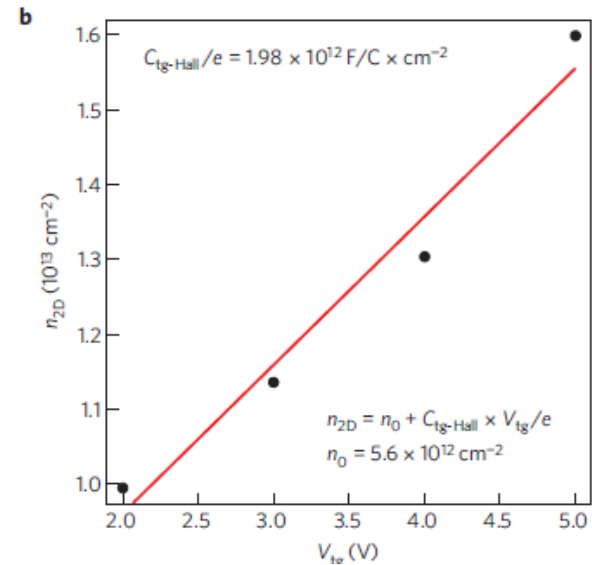
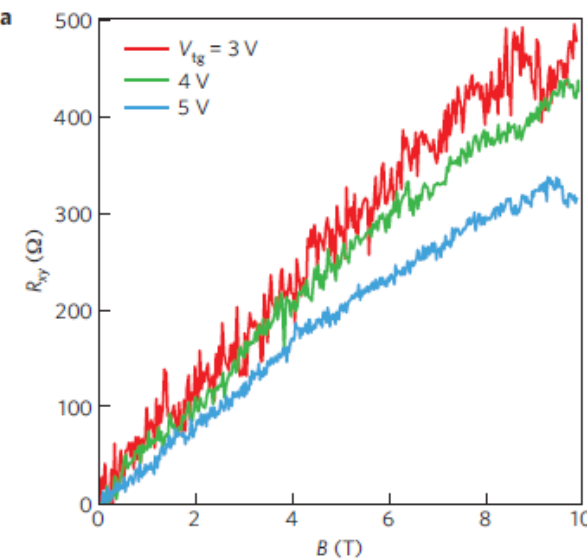
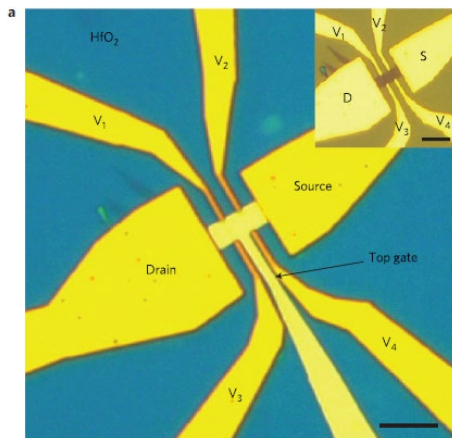


$$\mu_{band} = \frac{\sigma}{en_{band}} = \mu_{eff} \frac{n_{loc} + n_{band}}{n_{band}}$$

- By considering the carriers trapped in the localized state, the number of mobile carrier and the corresponding band mobility can be extracted.
- The band mobility is several times higher than the effective mobility.

W. Zhu, et.al. Nature Communications, 2014

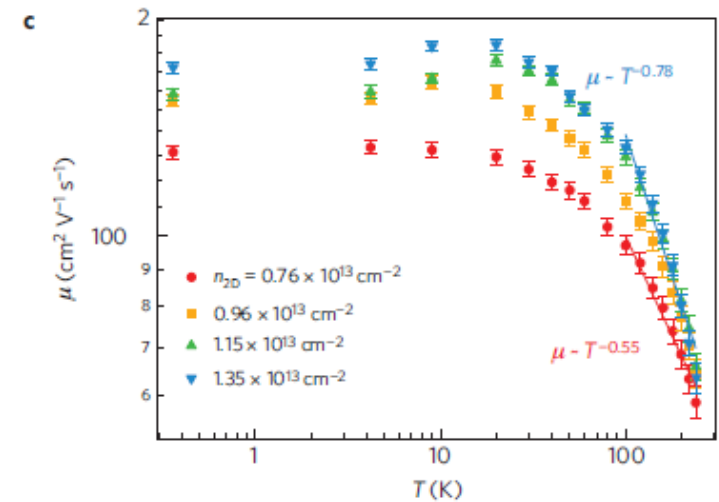
Mobility of MoS₂ measured using Hall effect



The mobility is extracted using the expression for field-effect mobility:

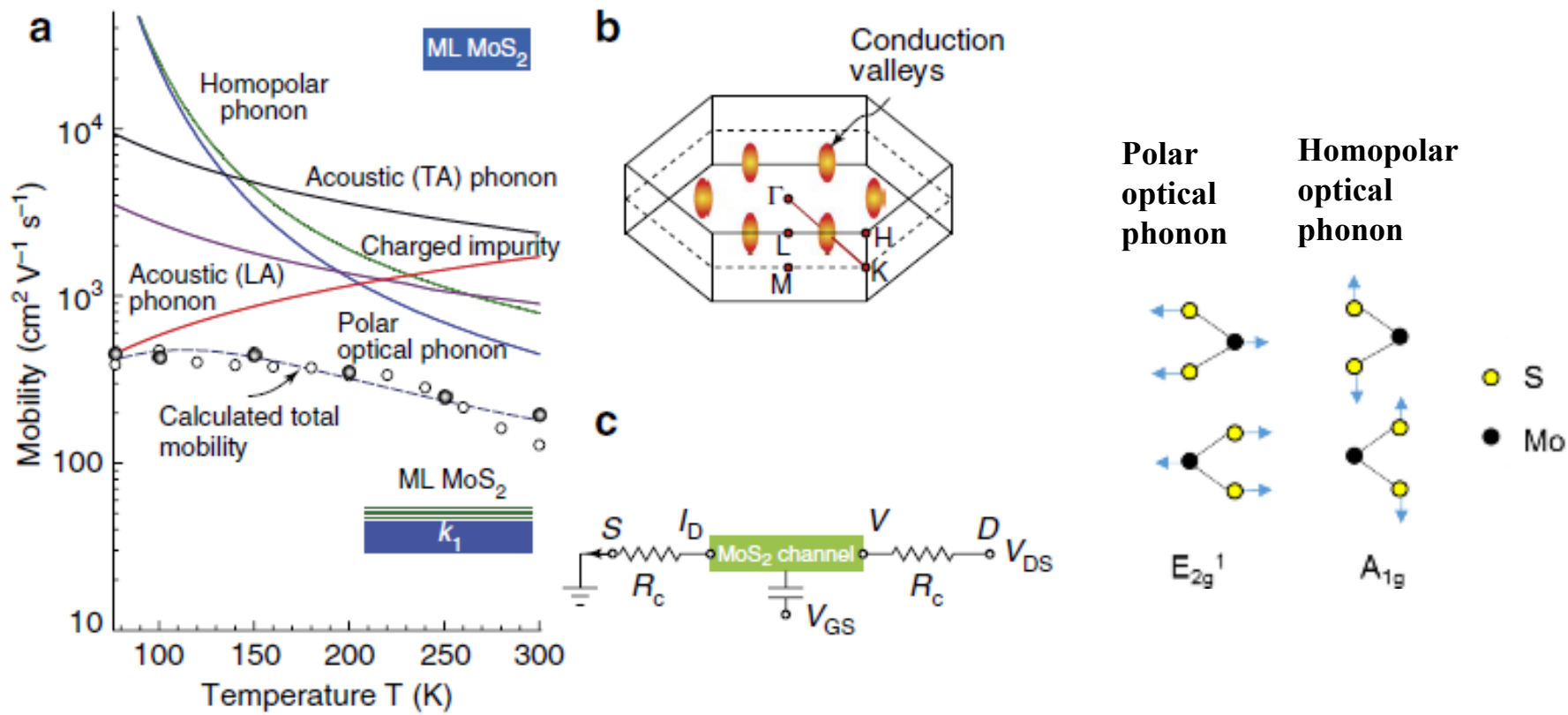
$$\mu = [dG/dV_{bg}] \times [L_{12}/WC_{tg_Hall}]$$

where the capacitance C_{tg_Hall} is extracted from the slope of carrier density versus gate voltage, where the carrier density is extracted from the Hall coefficient as a function of magnetic field.



Branimir Radisavljevic and Andras Kis, Nature Materials, 12, 815, 2013

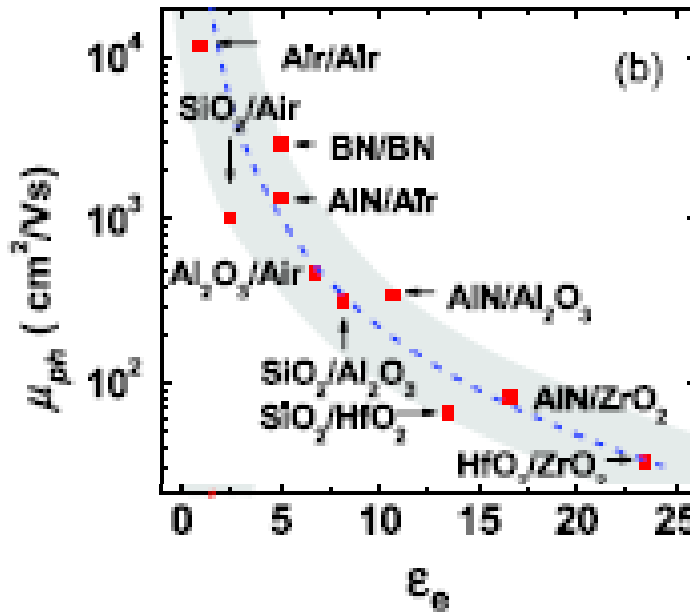
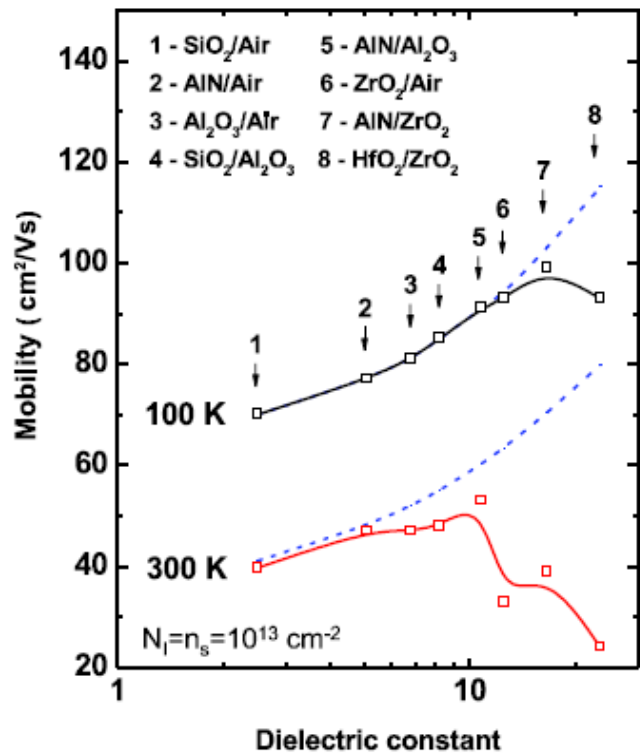
Mobility degradation mechanisms in MoS₂



- At low temperatures, the mobility is limited by ionized impurity scattering. At room temperature, the mobility decreases by enhanced optical phonon and acoustic phonon scattering.

Sunkook Kim, Kinam Kim, et.al., Nature Communications, 3, 1011, 2012

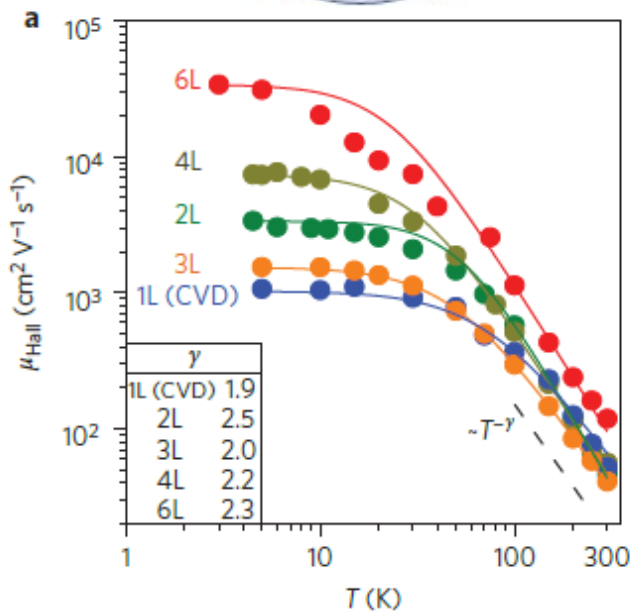
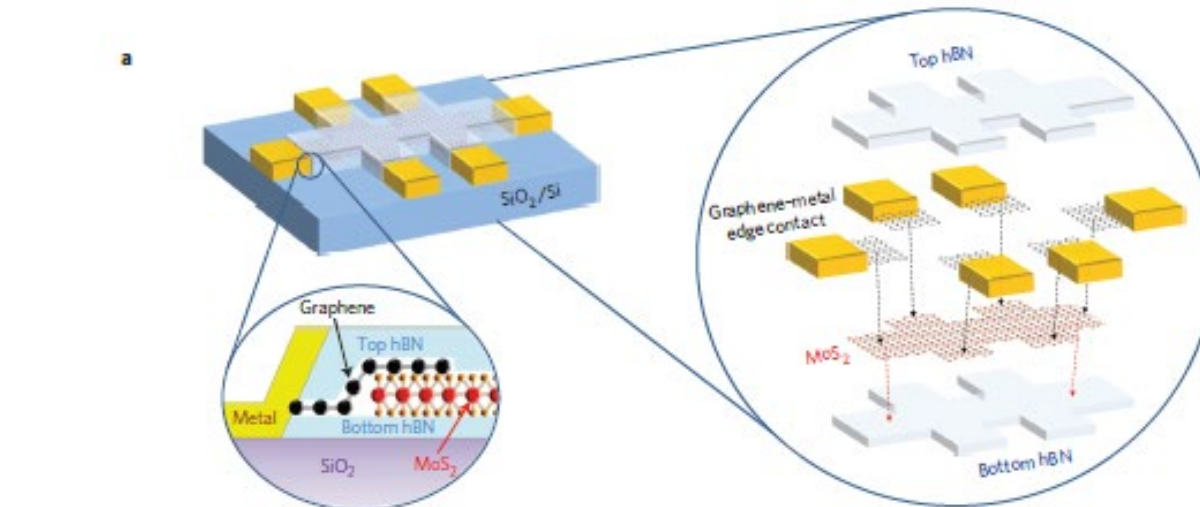
Impact of dielectric constant on mobility



- When surface optical (SO) phonon scattering is absent, the electron mobility is limited almost entirely by impurity scattering, which increases with dielectric constant because of the reduction of Coulomb scattering by dielectric screening.
- However, when the SO phonon scattering is in action, single layer MoS₂ layers suffer from enhanced SO phonon scattering if they are in close proximity to high-κ dielectrics that allow low-energy polar vibrational modes.

Nan Ma, Debdeep Jena, Physical Review X, 4, 011043, 2014

Mobility of MoS₂ encapsulated by hBN



- MoS₂ layers are fully encapsulated within hexagonal boron nitride and electrically contacted in a multi-terminal geometry using gate-tunable graphene electrodes.
- Magneto-transport measurements show Hall mobility reaching 34,000 cm²/V-s for six-layer MoS₂ at low temperature, 40~120 cm²/V-s at room temperature.

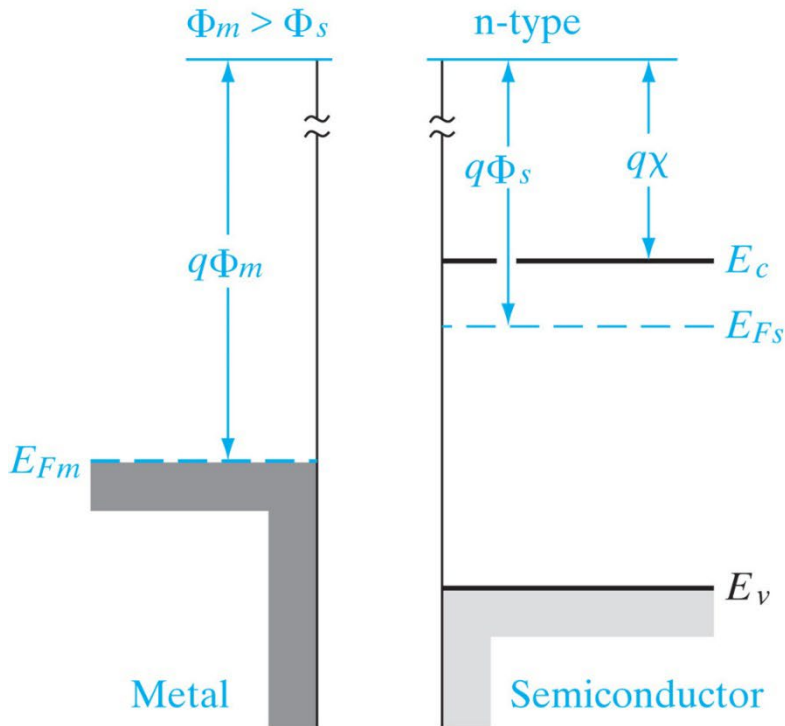
Xu Cui, James Hone, Nature Nanotechnology, 10, 534, 2015

Outline

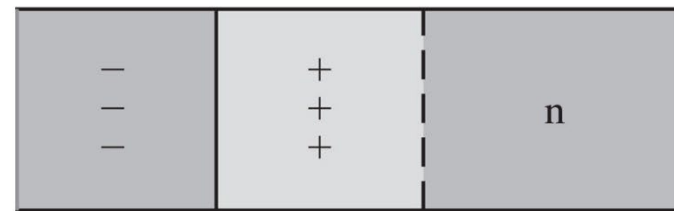
- Introduction of TMDs
- Synthesis of TMDs
- Electronic properties and electronic devices
 - Electronic properties
 - Carrier mobility
 - Metal-TMD contact
 - Electronic devices
- Optical properties and photonic devices

Recap: Schottky Barrier formation — n type semiconductor

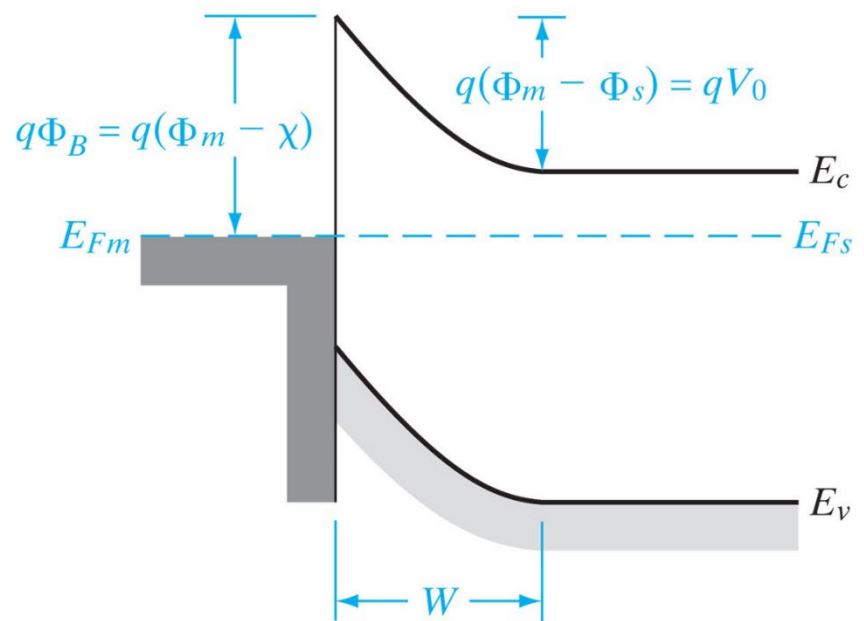
Metal/Semiconductor Not in Contact



Metal Semiconductor

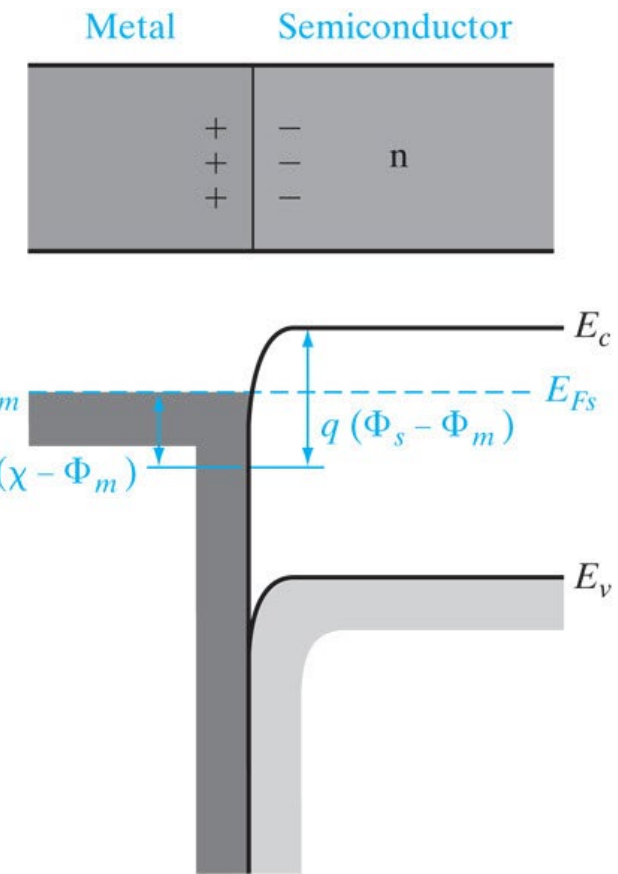
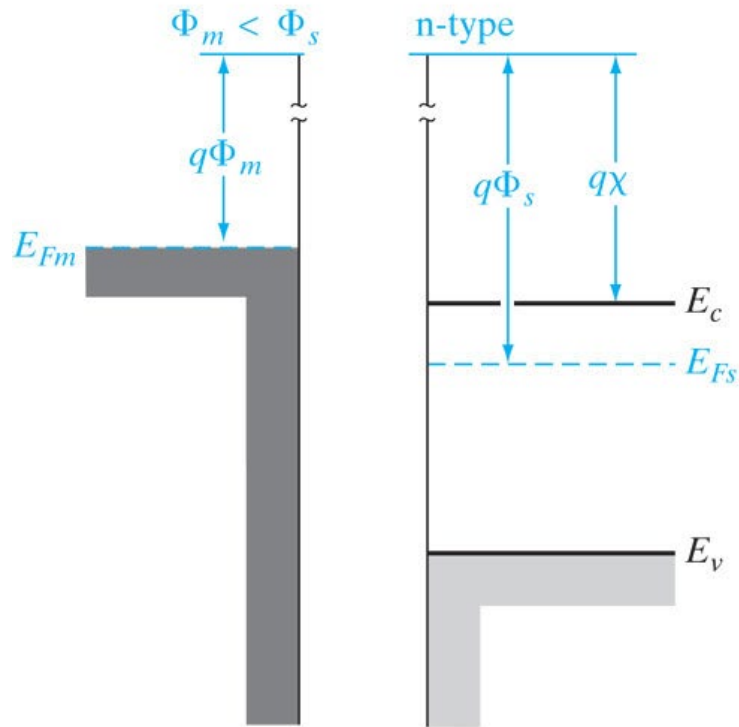


Metal/Semiconductor in Contact



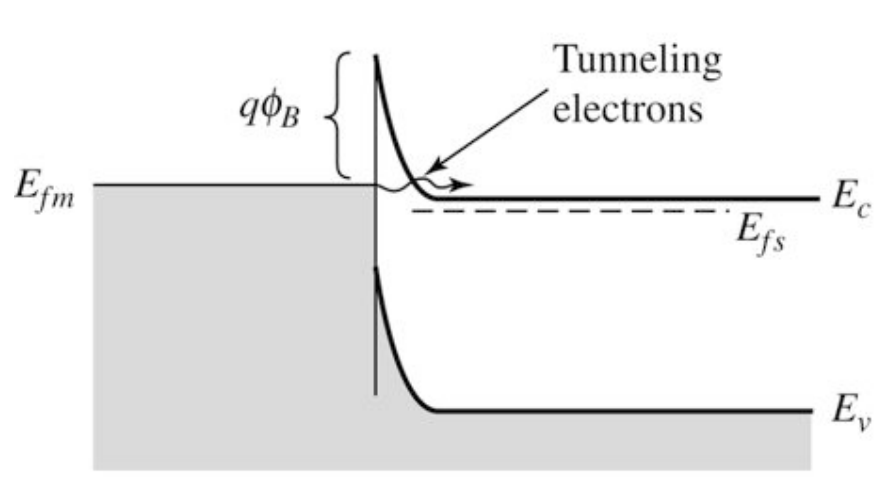
For n type semiconductor, if $\Phi_M > \Phi_s$, majority carrier in the n type silicon is depleted from the metal-semiconductor interface. This type of contact is called Schottky contact.

Recap: Ohmic contact — n type semiconductor

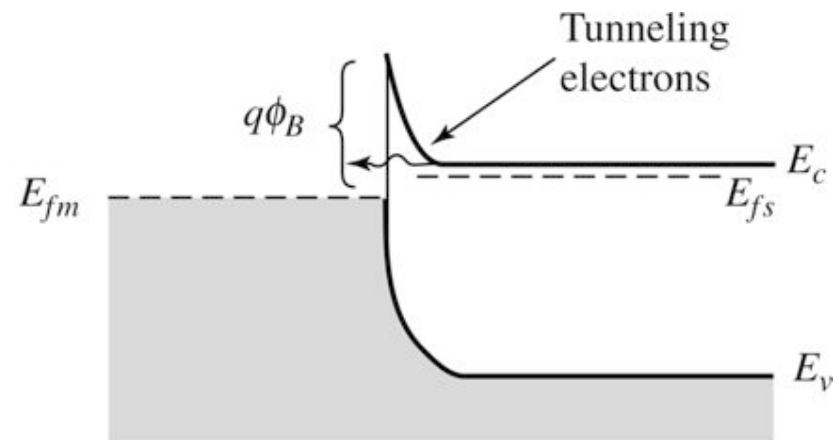


- For n type semiconductor, if $\Phi_M < \Phi_s$, majority carrier electrons are more numerous near the contact than they are in the bulk of the semiconductor, forming Ohmic contact.

Recap: Ohmic contact — Tunnel contact



(a)



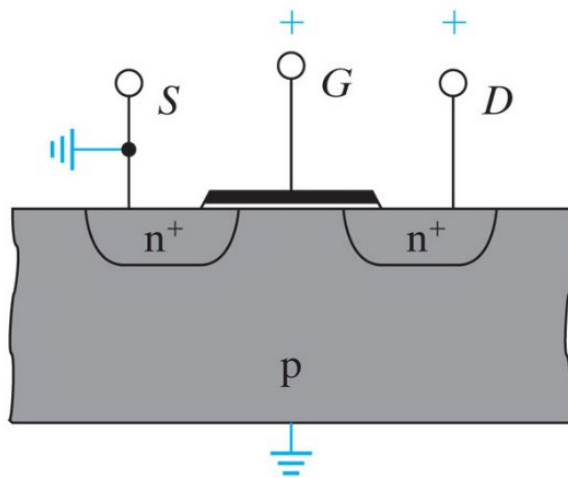
(b)

$$x_d = \sqrt{2\epsilon_s\phi_i/qN_d}$$

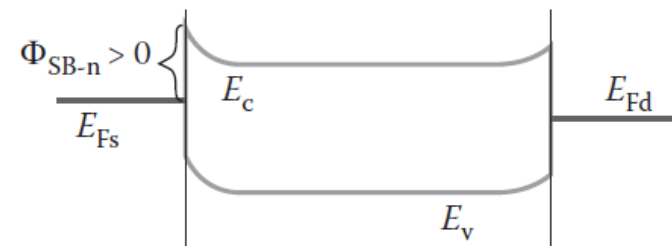
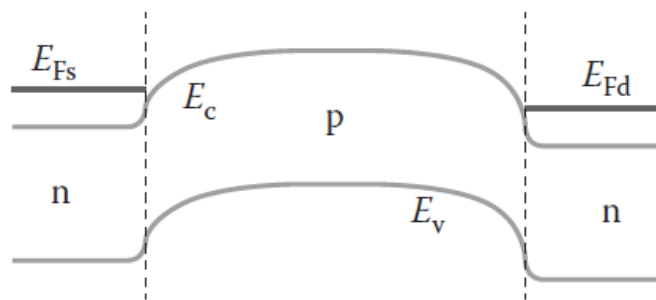
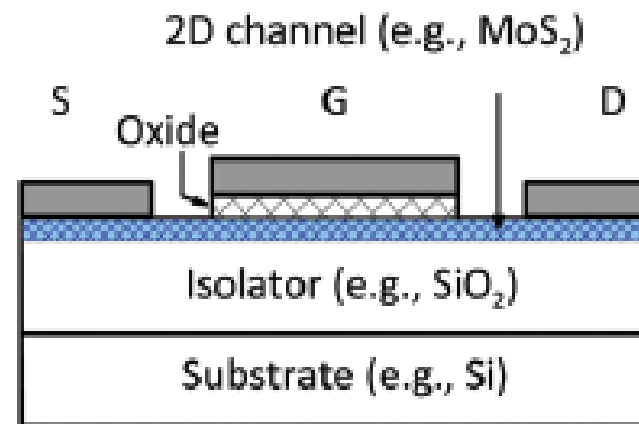
- Heavily doping the semiconductor in the contact region → depletion width is small enough for carrier to tunnel through the barrier → Ohmic contact

Comparison of TMD and Si transistors

Si transistor



TMD transistor

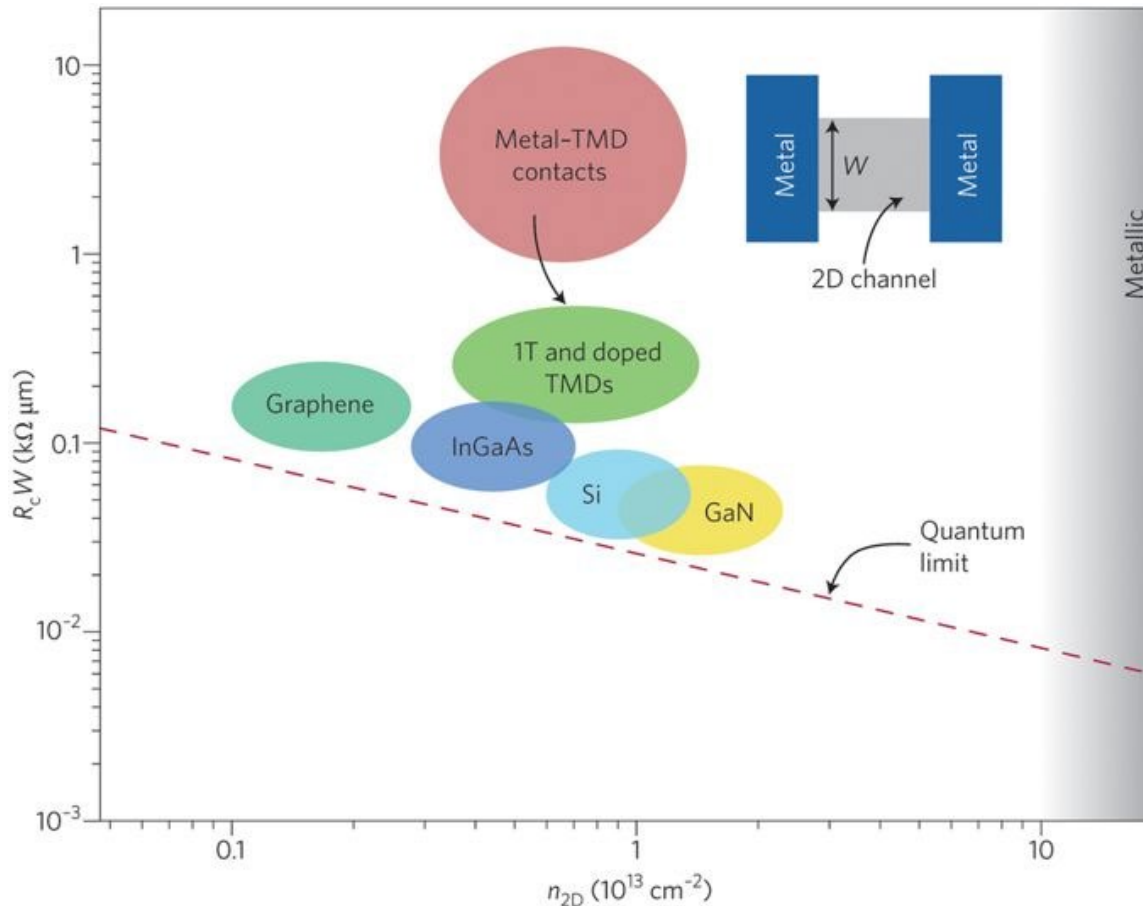


- Source/Drain: Ohmic contact
- Unipolar transport

- Source/Drain: Schottky contact
- Allow ambipolar transport

“Schottky barrier transistor”

Contact resistance in TMD transistors

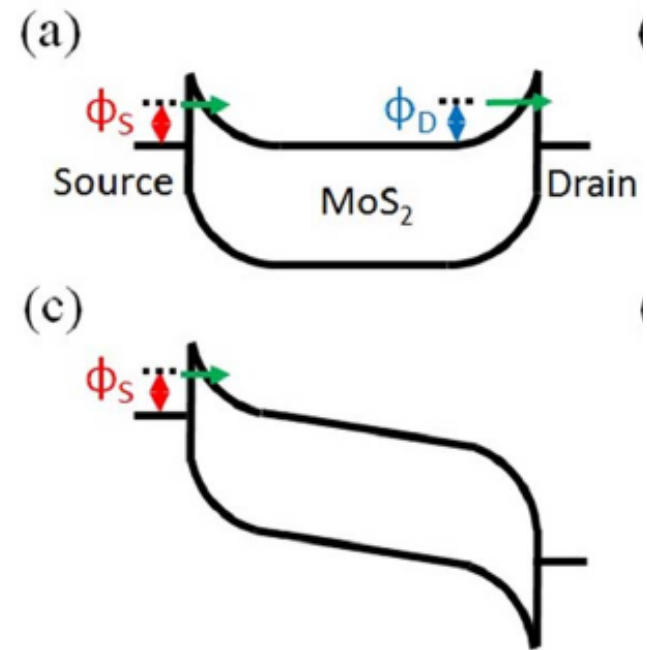


The contact resistance in TMD transistors are significantly higher than that in silicon and graphene, which limits the performance of the electronic devices.

D. Jena, G. Xing, Nature Materials, 13, 1076, 2014

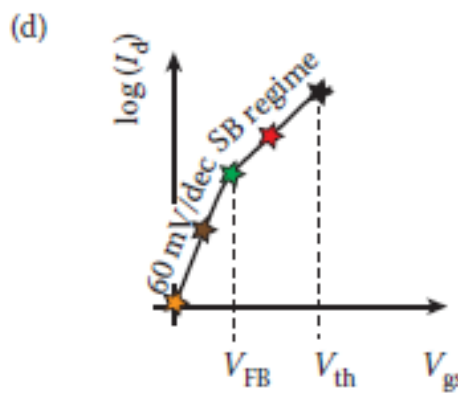
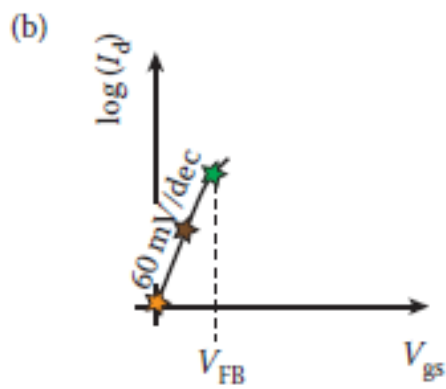
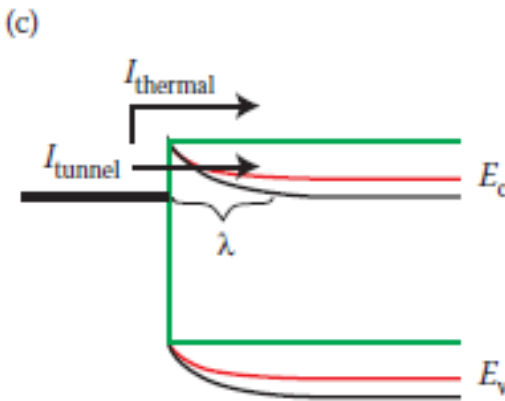
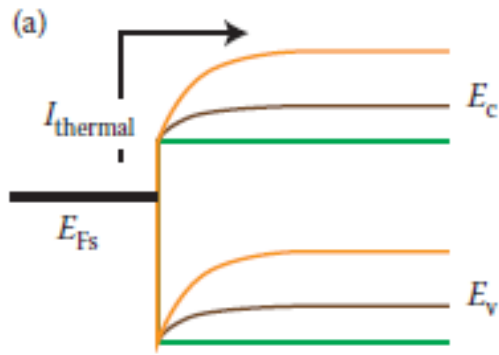
What is the root cause of the high contact resistance?

- Large bandgap and high Schottky barrier
- Low doping
- Atomic thin body
- High density of interface trap and Fermi level pinning



Y. Du, P. Ye, APL Materials, 2, 092510 (2014)

Band diagram and subthreshold current

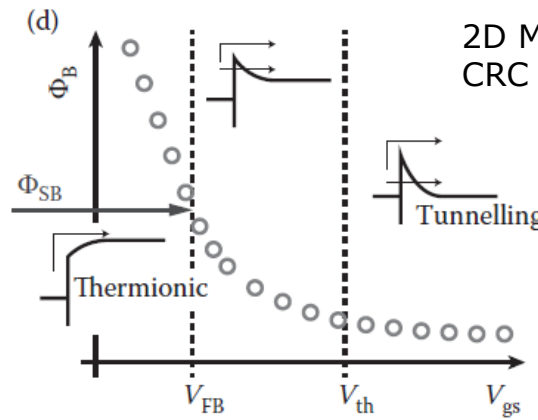
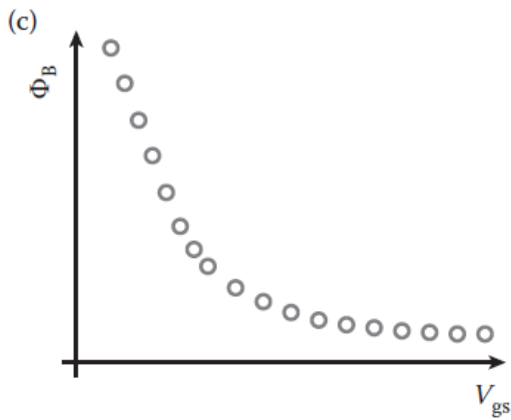
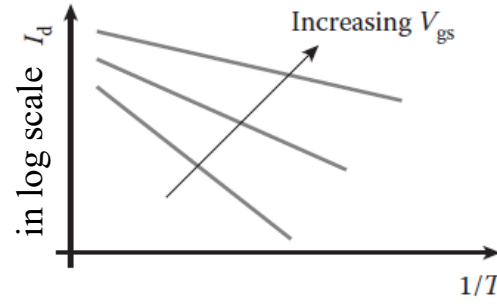
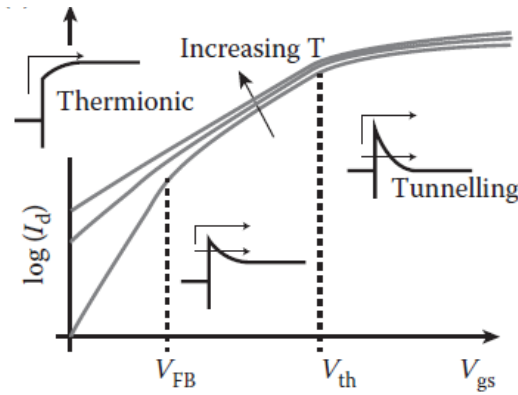


- The threshold voltage is approximately reached in Schottky barrier devices when the conduction band edge coincides with the source Fermi Level.

2D Materials for Nanoelectronics,
CRC Press Book, 2016

- When $V_{gs} < V_{FB}$, the carriers are injected through thermionic emission from source “over” the barrier. When the gate voltage increases, the conduction band move downwards allowing more carriers injected into the channel and the current increases exponentially.
- When $V_{FB} < V_{gs} < V_{th}$, in addition to the thermionic current “over” the barrier, thermal assisted tunneling current “through” the barrier will contribute to the total current as well.

Schottky barrier extraction

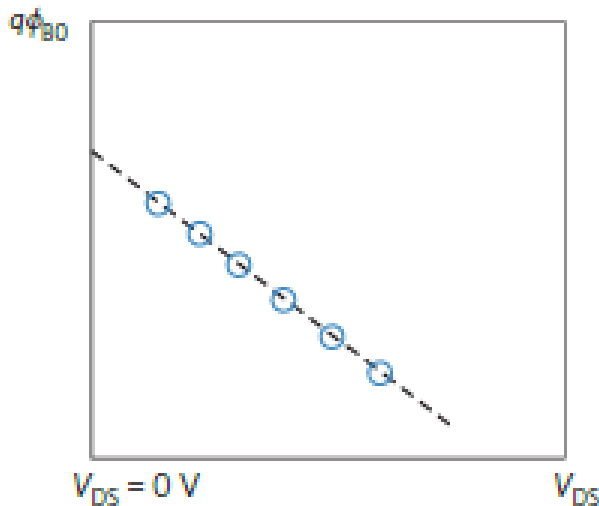
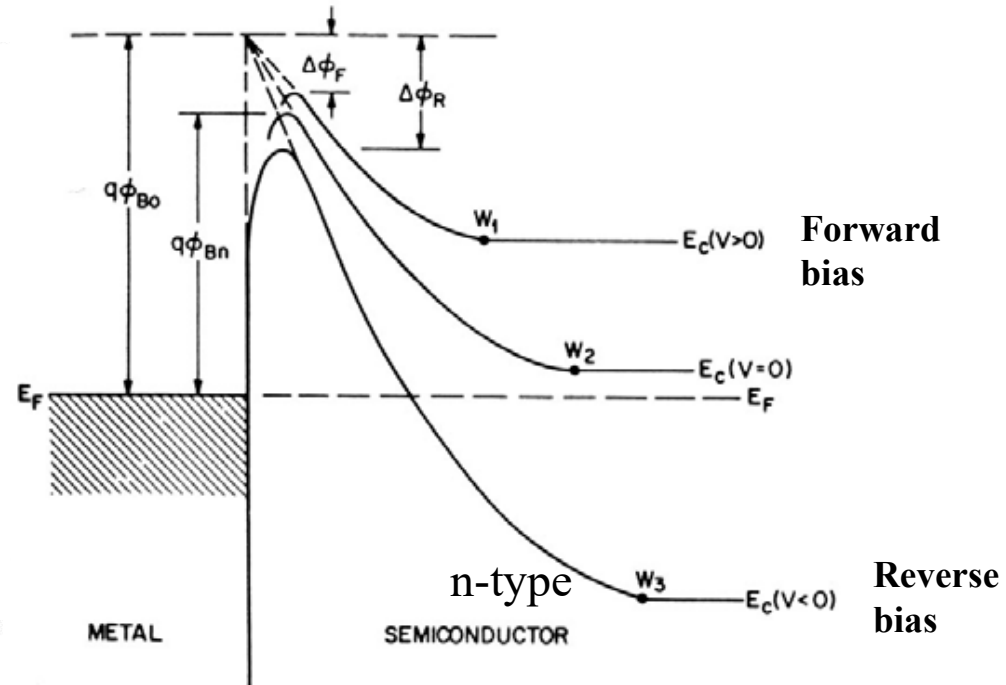
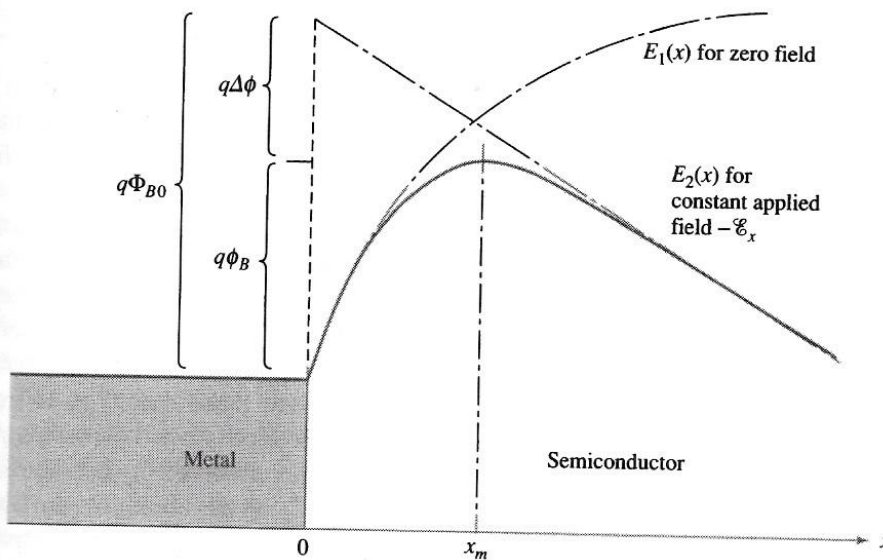


Thermionic emission current:

$$I_d = AT^{\frac{3}{2}} \exp\left(\frac{-q\varphi_B}{k_B T}\right) \left[\exp\left(\frac{qV_d}{nk_B T}\right) - 1 \right]$$

When $V_{gs} < V_{FB}$, Φ_B changes linearly with V_{gs} . Once $V_{gs} > V_{FB}$, the linear dependence no longer prevails. This can be used to determine the V_{FB} and the actual Φ_B .

Schottky barrier height lowering

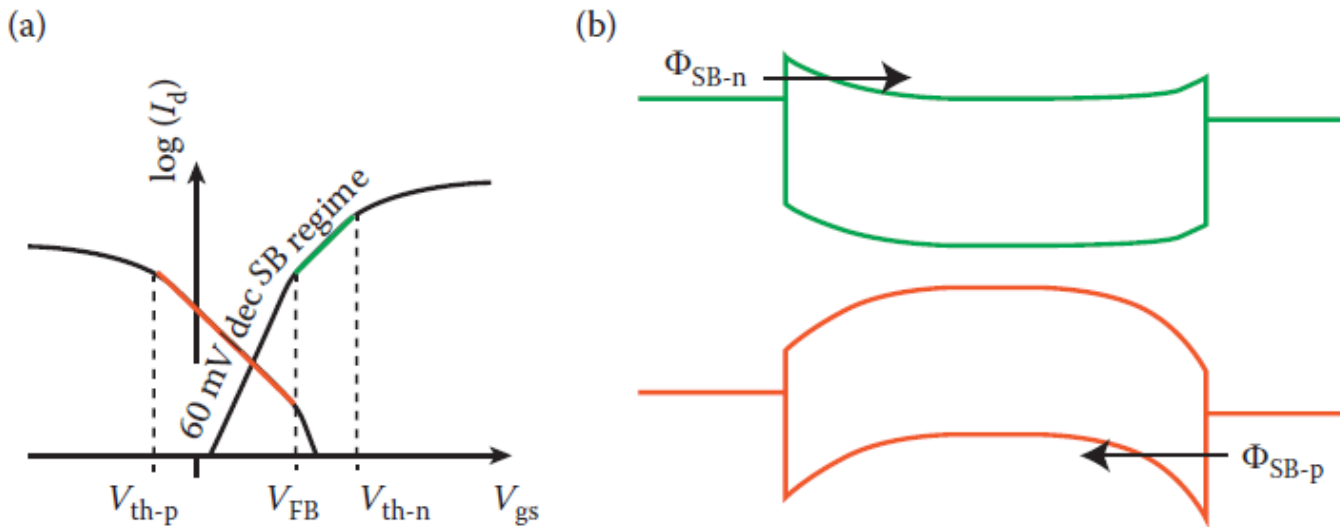


- Schottky barrier height lowering at finite source–drain bias V_{DS} due to image forces leads to an underestimation of the Schottky barrier height. The error can be decreased by extracting the Schottky barrier height at finite bias (blue circles) and then extrapolating it to zero drain bias

Adrien Allain, Andras Kis, et.al., Nature Materials, 14, 1195, 2015

S. Sze, Physics of Semiconductor Device, Chapter 5 Metal-Semiconductor Contacts, John Wiley & Sons, 1981

Ambipolar device characteristics



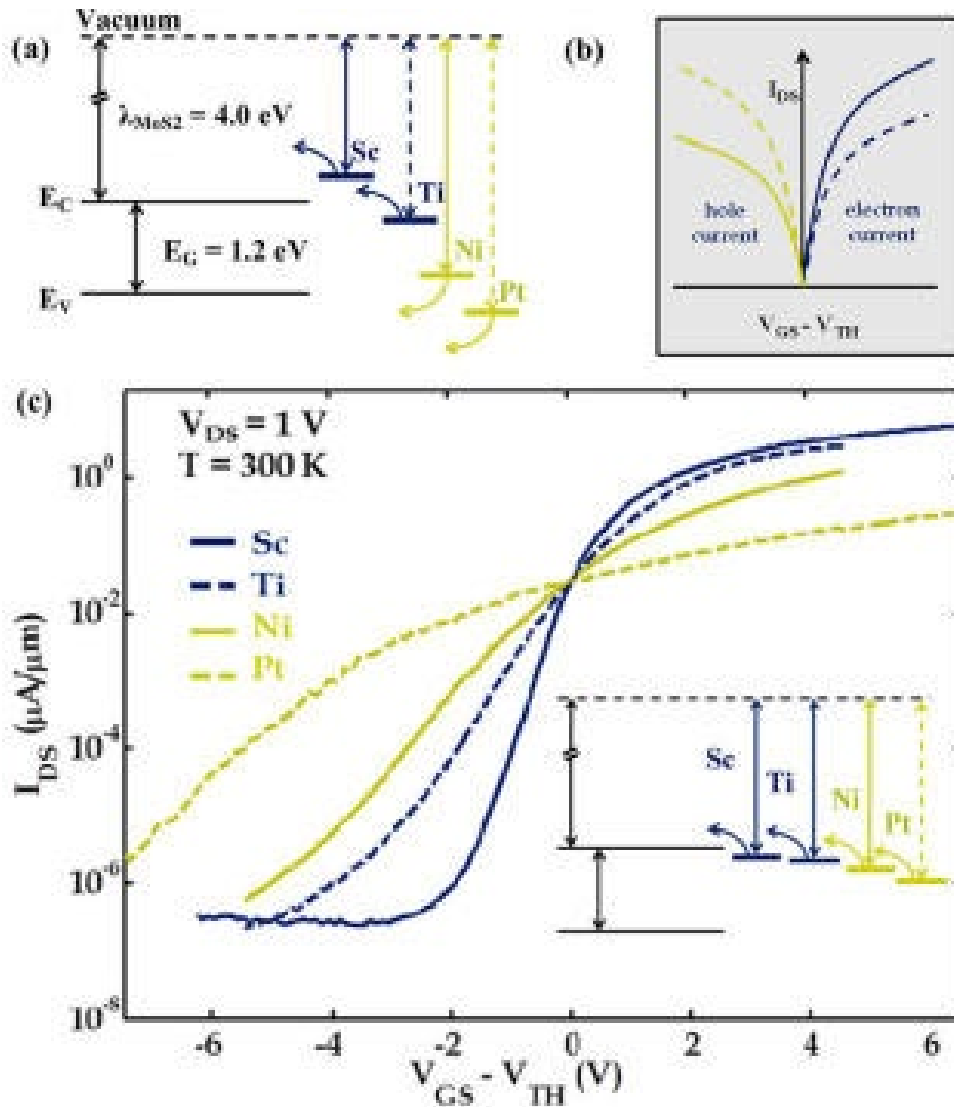
- The absence of a bandgap in the source/drain region of the Schottky barrier transistor allows for both electron and hole injection, resulting in “ambipolar” device characteristics.
- The bandgap of the TMDs is the sum of the barrier height for electrons and holes

$$E_g = \Phi_{SB_n} + \Phi_{SB_p}$$

How to reduce contact resistance?

- For silicon, the traditional method to lower the contact resistance are:
 - Heavily dope silicon at the contact region
 - Choose the metal based on its work function to form an Ohmic contact.
- For TMDs, chemical doping is still very challenging. Following approaches have been explored.
 - Vary metal work function
 - Use graphene contact
 - Convert TMD at contact region from 2H to 1T phase
 - 2D/2D contact with heavily doped TMD layer

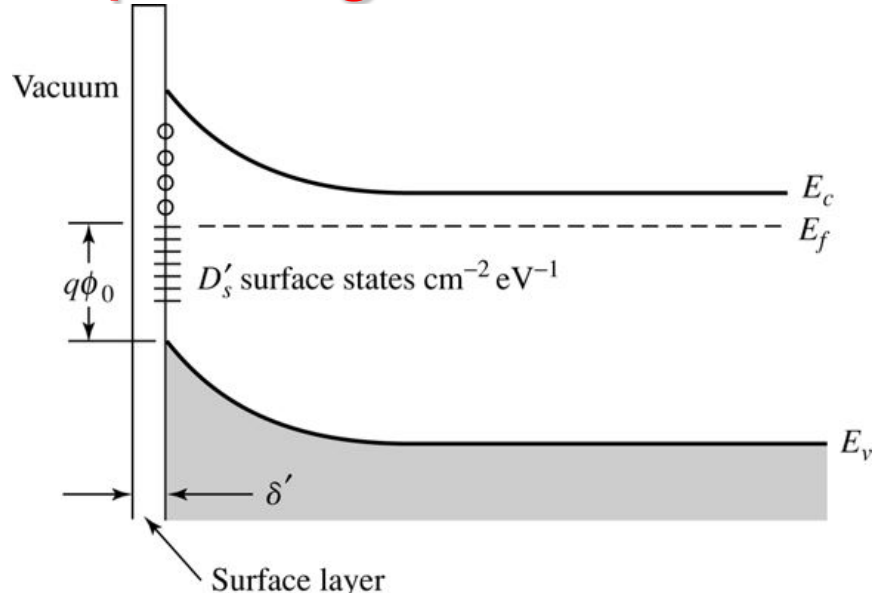
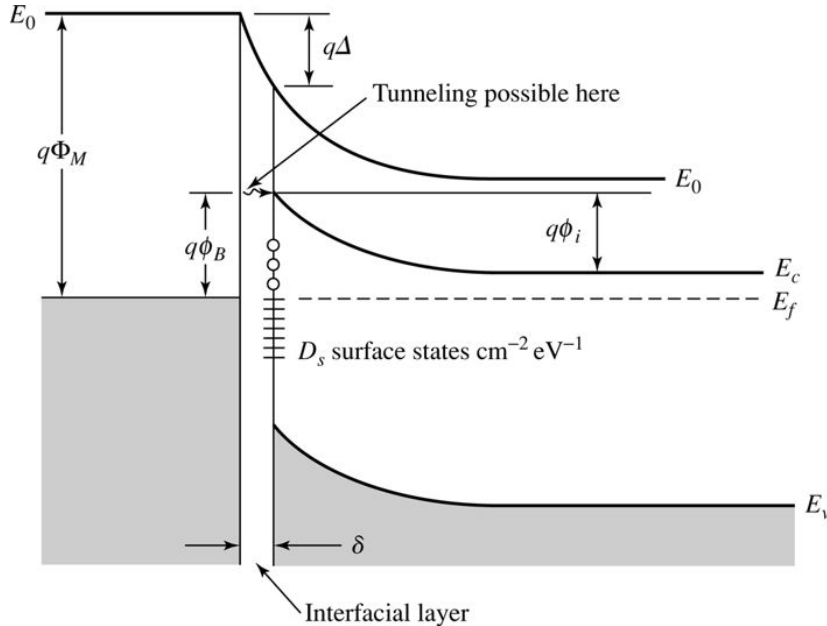
Vary metal work function



- Pt, Ni, Ti, and Sc are used as metal contacts. All transistors exhibit n-type FET characteristics, which indicate that the Fermi levels for all of these metals line-up close to the conduction band edge of MoS₂
- The metal work function has very little impact on the barrier height, indicates strong Fermi-level pinning at the metal/MoS₂ interface

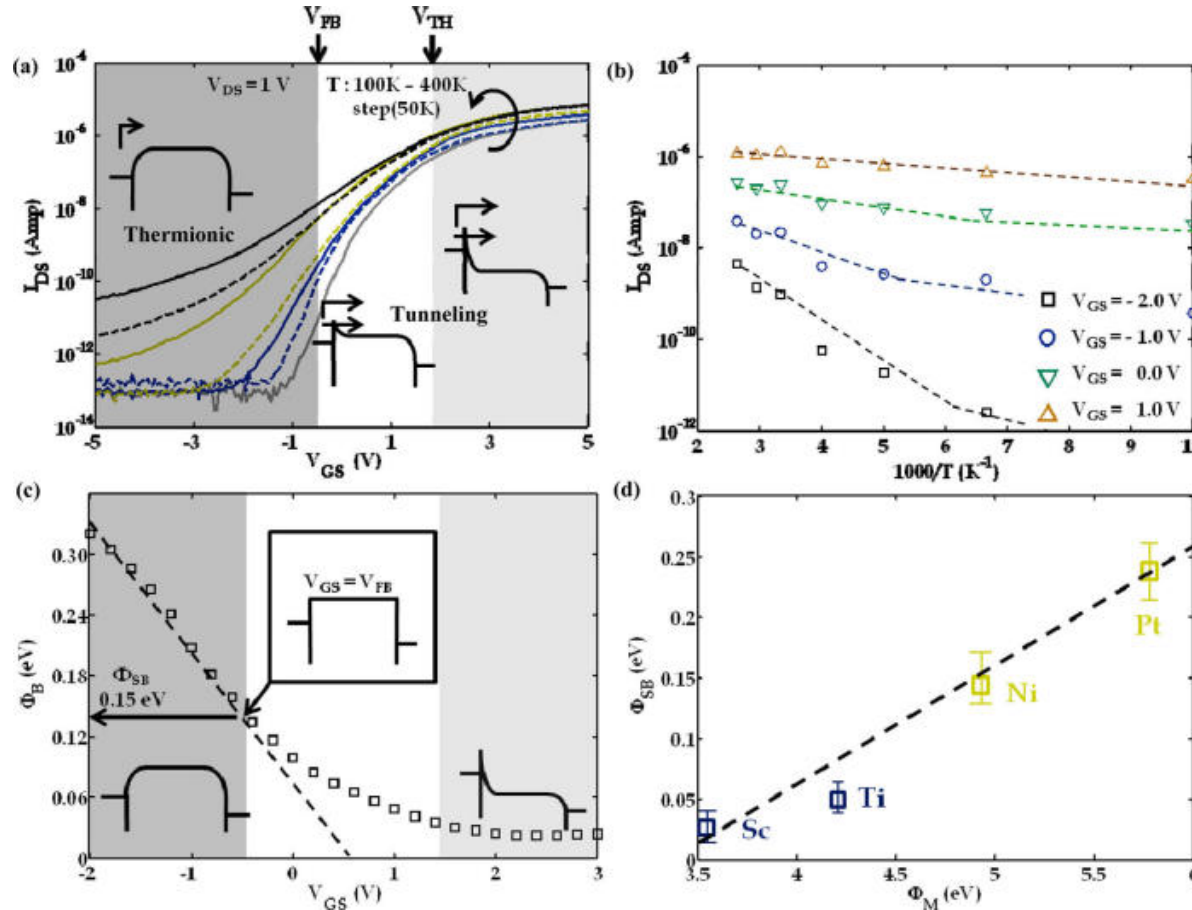
Saptarshi Das, Joerg Appenzeller, et.al.,
Nano Letters, 13, 100, 2013

Fermi-level pinning



- If $\Phi_M > \Phi_s$, transfer electrons from semiconductor to metal bends the conduction band away from the Fermi level. This removes charge from some of the surface states.
- The larger the surface state density D_s , the greater the amount of charges are removed for each incremental energy increase in Ec near the contact.
- If D_s is large, a negligible movement of Fermi level at the surface transfer sufficient charges to equalize the Fermi levels. In this case, the Fermi level is said to be “Pinned” by the surface states.

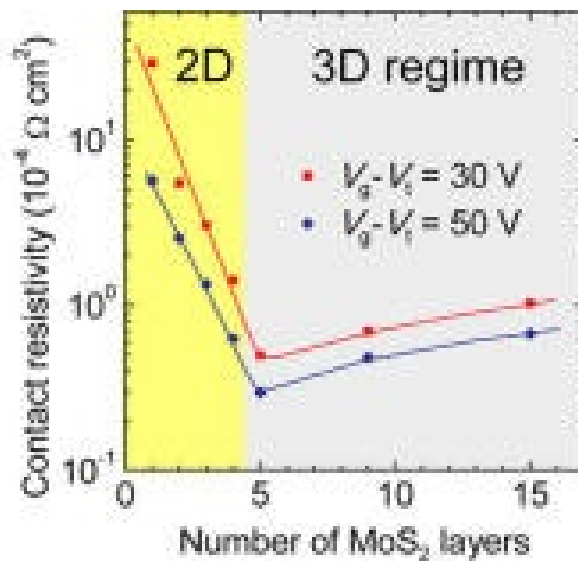
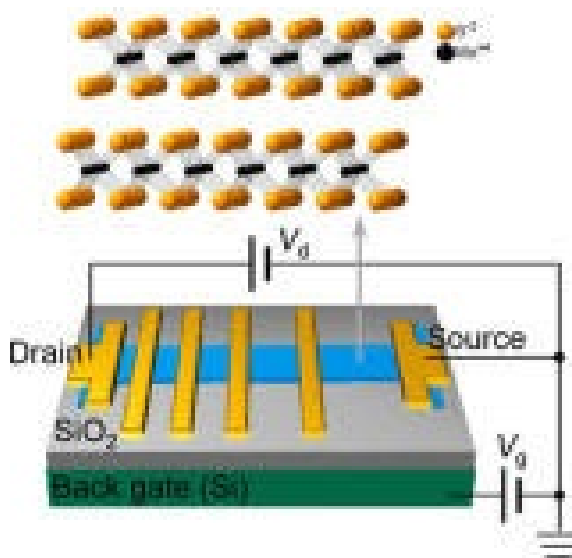
Barrier height of MoS₂ Schottky contacts



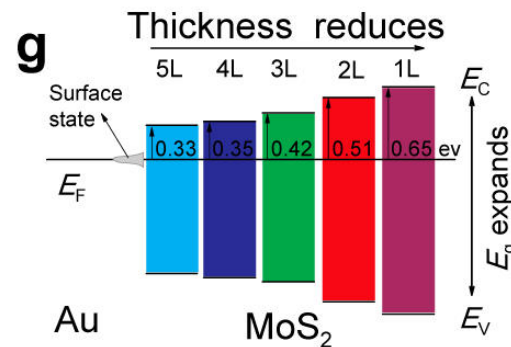
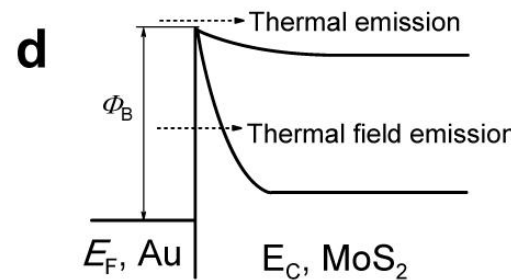
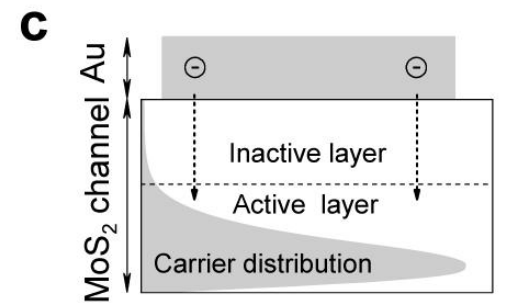
- The extracted slope $d\Phi_{SB}/d\Phi_M$ of around 0.1 indicates that strong pinning at the metal/MoS₂ interface determines the line-up between the metal Fermi level and the conduction band of MoS₂

Saptarshi Das, Joerg Appenzeller, et.al., Nano Letters, 13, 100, 2013

Thickness dependence of contact resistance

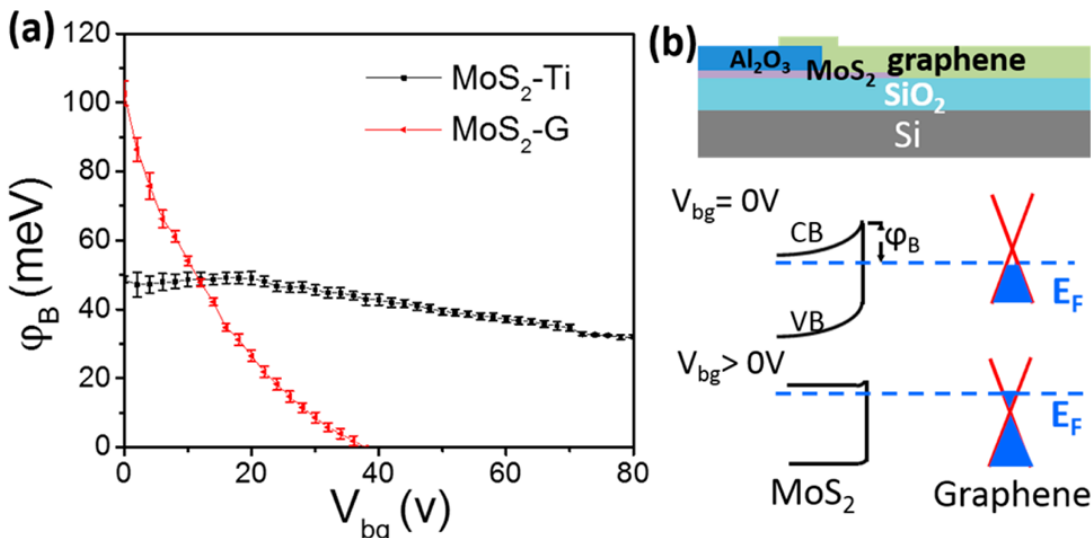
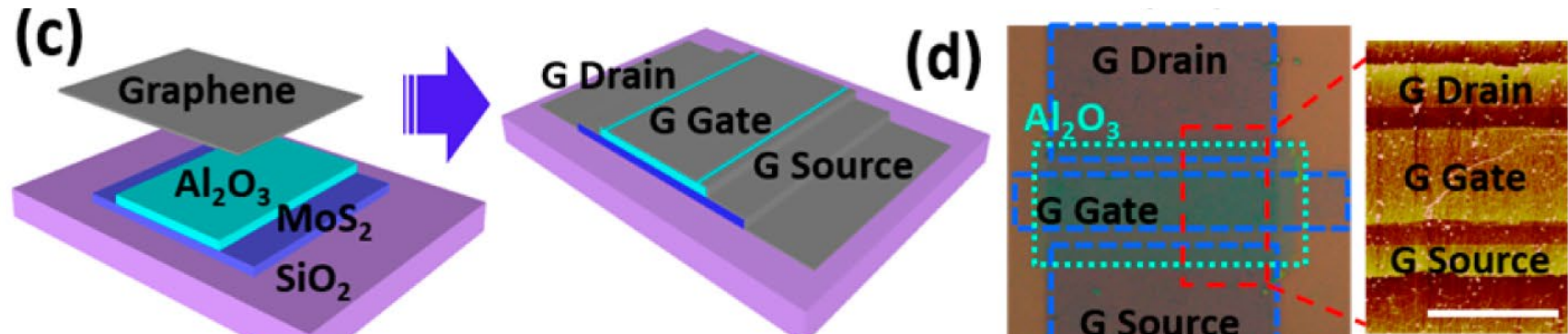


- For MoS₂ thicker than 5 layers, the contact resistivity slightly decreases with reducing MoS₂ thickness.
- By contrast, the contact resistivity sharply increases with reducing MoS₂ thickness below 5 layers, mainly governed by the quantum confinement effect and the resulting band gap change.



Song-Lin Li, Kazuhito Tsukagoshi, ACS Nano, 8, 12836, 2014

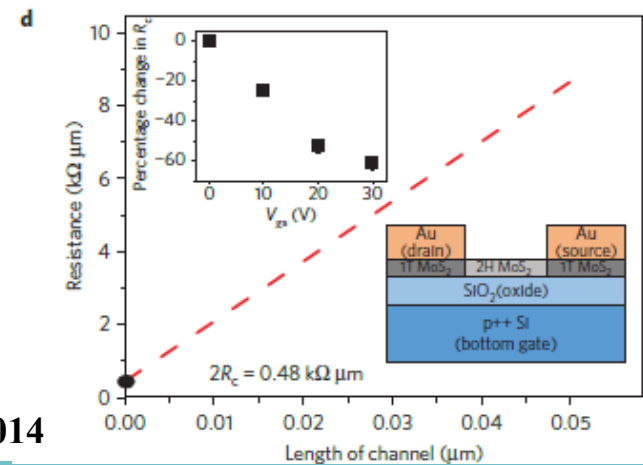
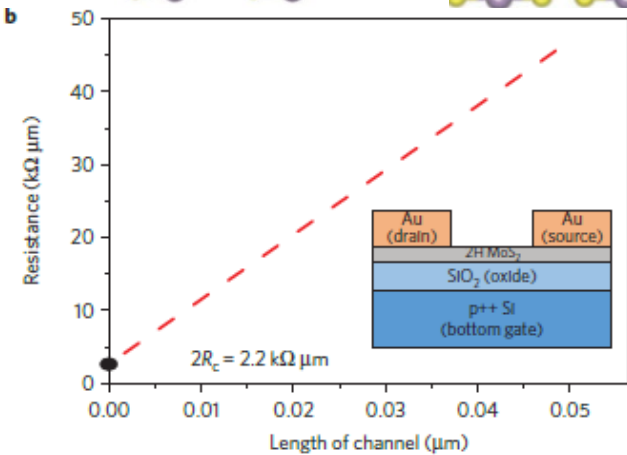
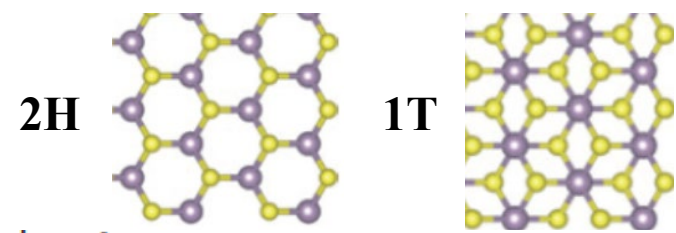
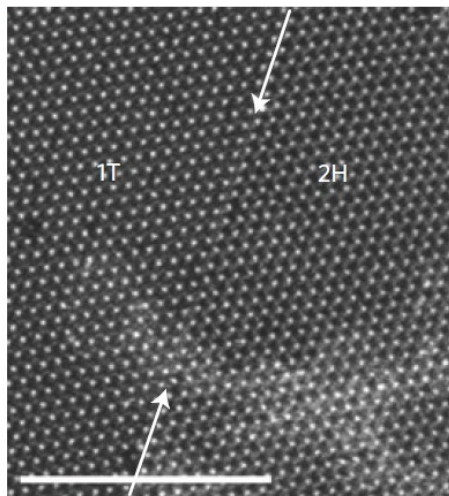
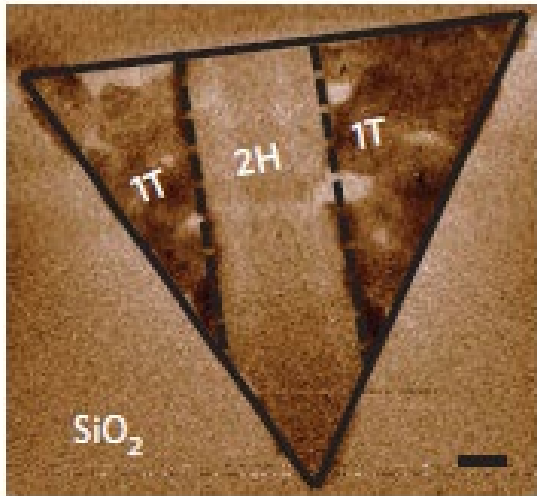
Graphene contact for TMD



- MoS₂ is used as the transistor channel and graphene as contact electrodes and circuit interconnects.
- The tunability of the graphene work function with electrostatic doping significantly improves the Ohmic contact to MoS₂.

Lili Yu, Tomas Palacios, et.al., Nano Letters, 14, 2014

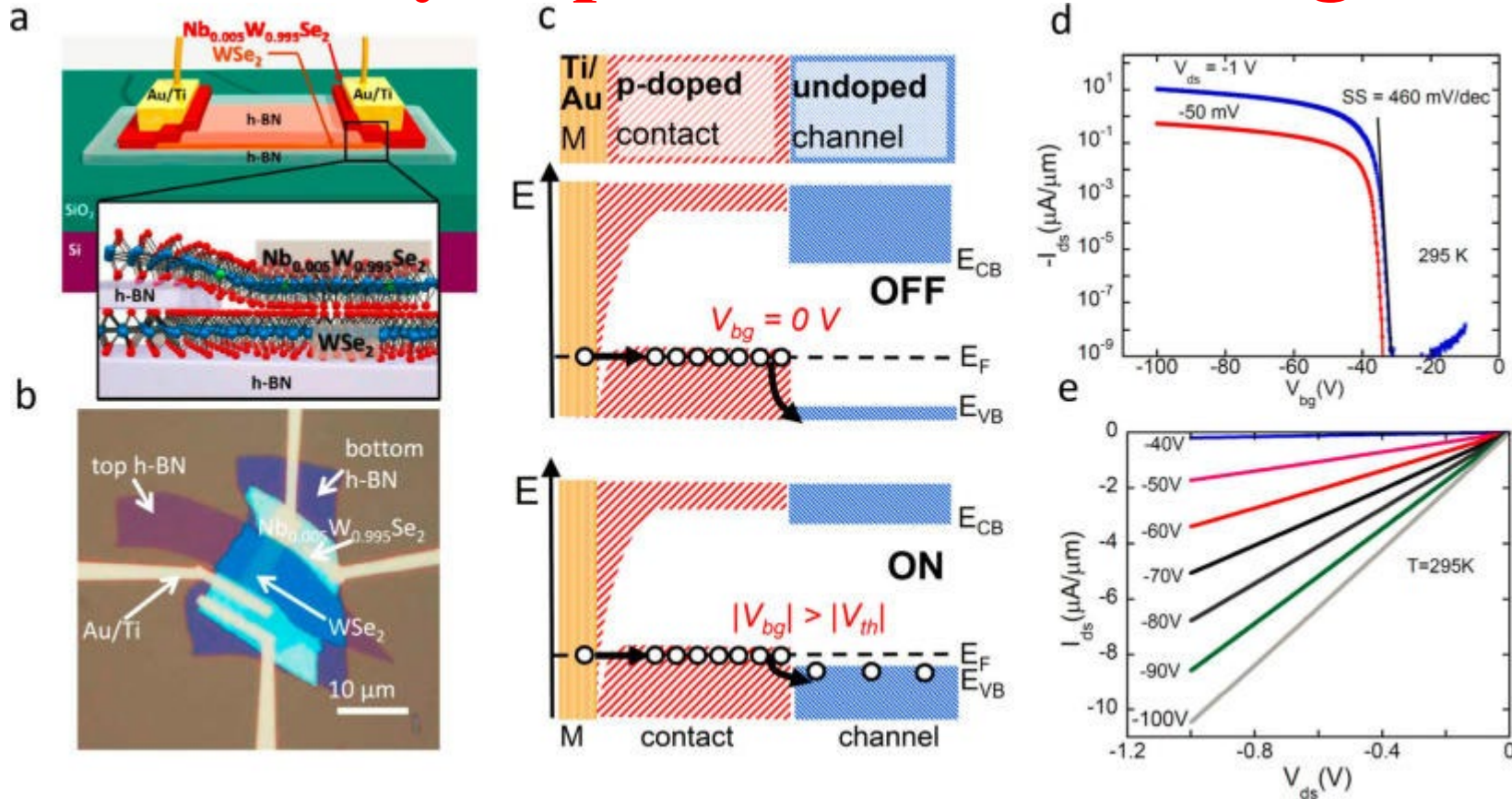
Convert MoS₂ from 2H to 1T at contact



- After lithography, samples were immersed into n-butyl lithium, which convert the MoS₂ from 2H phase to 1T phase.
- The resistance of the 1T contacts decreases by a factor of 5 from $1.1 \text{ k}\Omega\text{-}\mu\text{m}$ to $0.2 \text{ k}\Omega\text{-}\mu\text{m}$ at zero gate bias.

Rajesh Kappera, Manish Chhowalla, et.al., Nature Materials, 13, 1128, 2014

Heavily doped source/drain region



- Degenerately doped TMD flakes grown by CVT are used as source/drain contact, while TMDs with no intentional doping are used as channel.
- These few-layer WSe_2 field-effect transistors (FETs) with 2D/2D contacts exhibit low contact resistances of $\sim 0.3 \text{ k}\Omega \mu\text{m}$, high on/off ratios up to $> 10^9$.

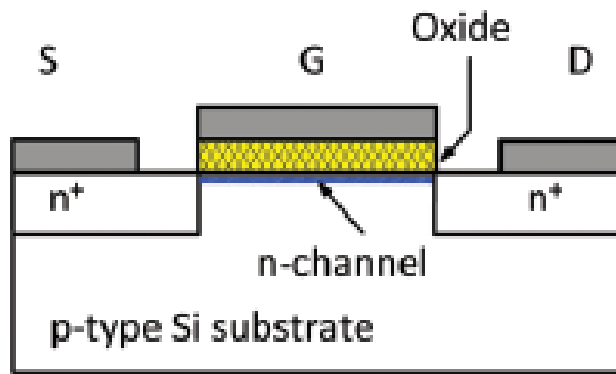
Hsun-Jen Chuang, Zhixian Zhou, et.al., Nano Letters, 16, 1896, 2016

Outline

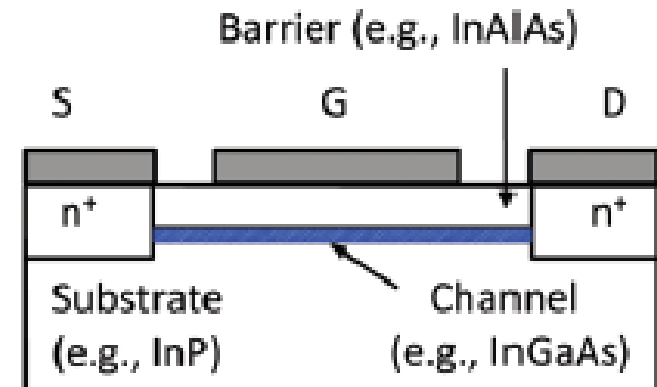
- **Introduction of TMDs**
- **Synthesis of TMDs**
- **Electronic properties and electronic devices**
 - **Electronic properties**
 - **Electronic devices**
- • **Logic devices**
 - **Tunneling field effect transistor**
 - **RF devices**
 - **Memory devices**
 - **Integrated circuits**
- **Optical properties and photonic devices**

Transistor structures

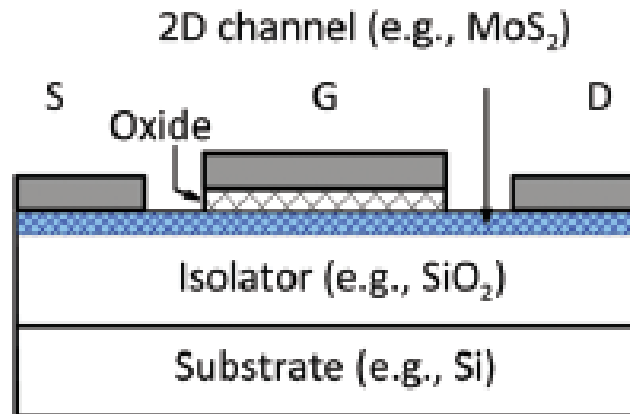
Si FET



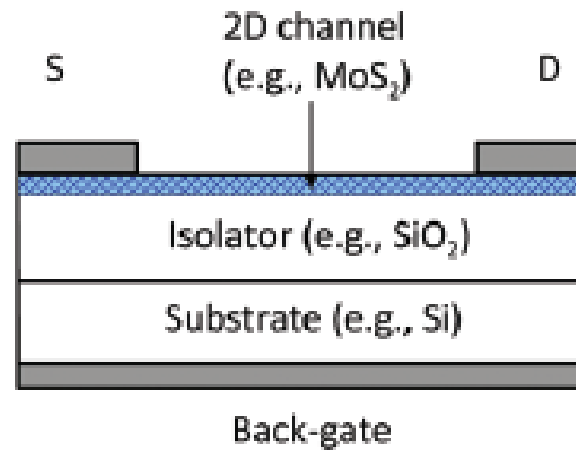
III-V HEMT (High Electron Mobility Transistor)



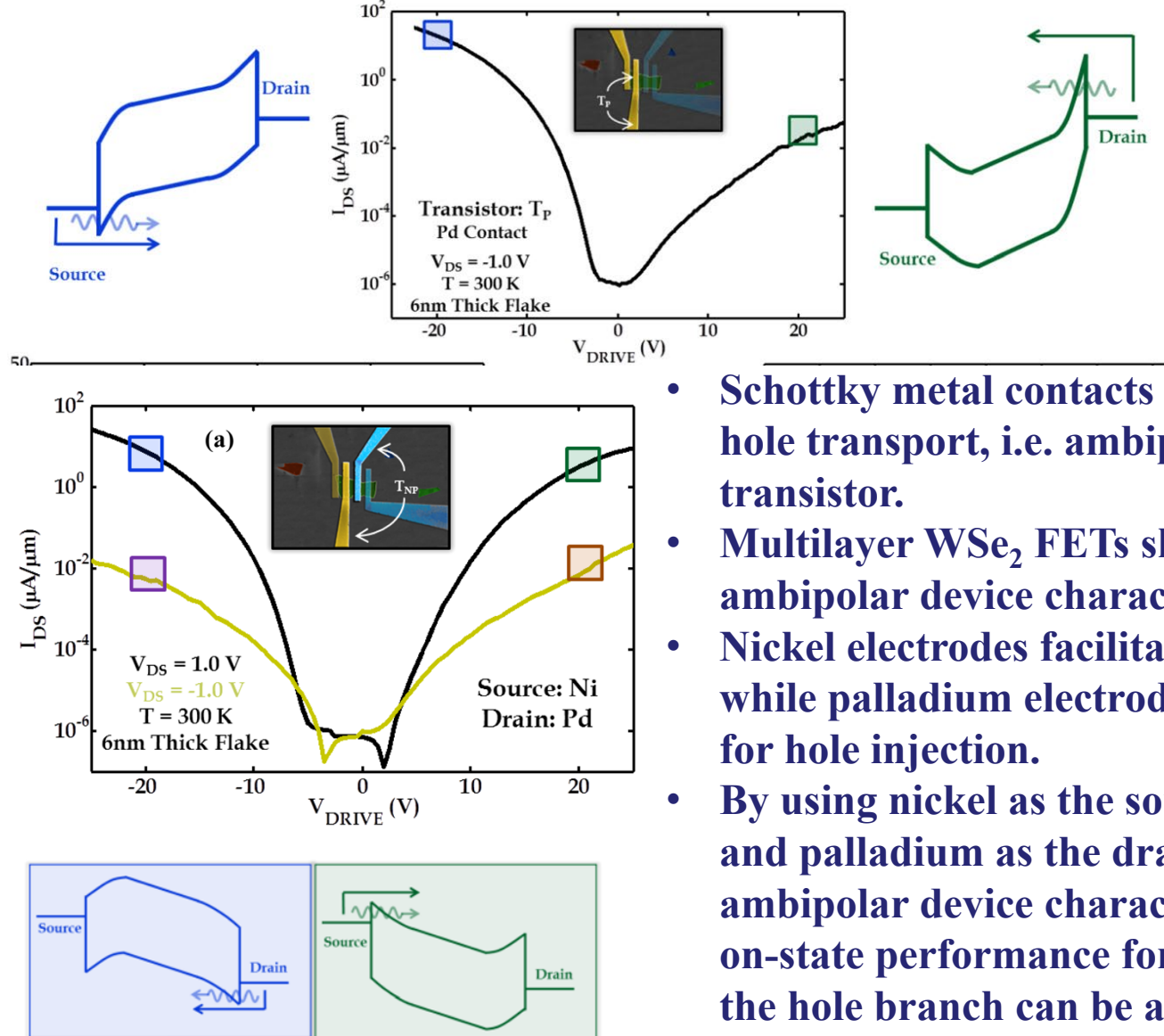
2D top-gated FET



2D back-gated FET



Transistors based on thick WSe₂ flake



- Schottky metal contacts allow both electron and hole transport, i.e. ambipolar transport in the transistor.
- Multilayer WSe₂ FETs show pronounced ambipolar device characteristics.
- Nickel electrodes facilitate electron injection while palladium electrodes are more efficient for hole injection.
- By using nickel as the source contact electrode and palladium as the drain contact electrode, ambipolar device characteristics with similar on-state performance for both the electron and the hole branch can be achieved in WSe₂ FETs.

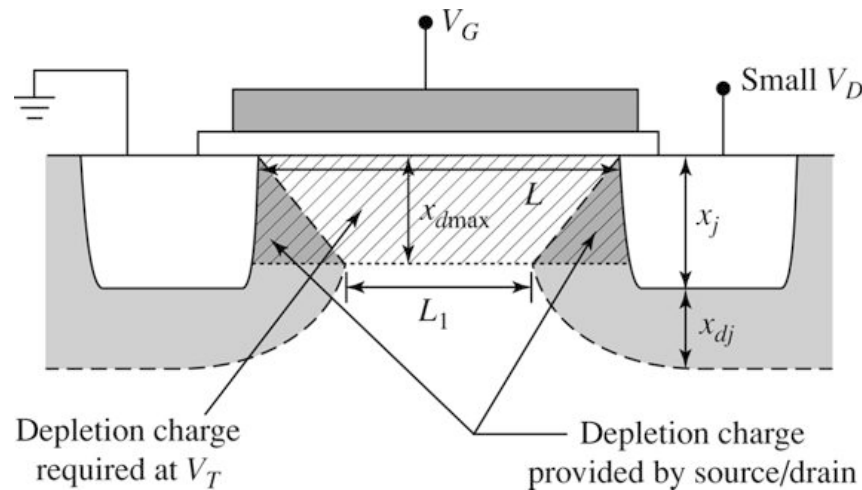
Saptarshi Das and Joerg Appenzeller, Applied Physics Letters, 103, 103501, 2013

Short-Channel Effects

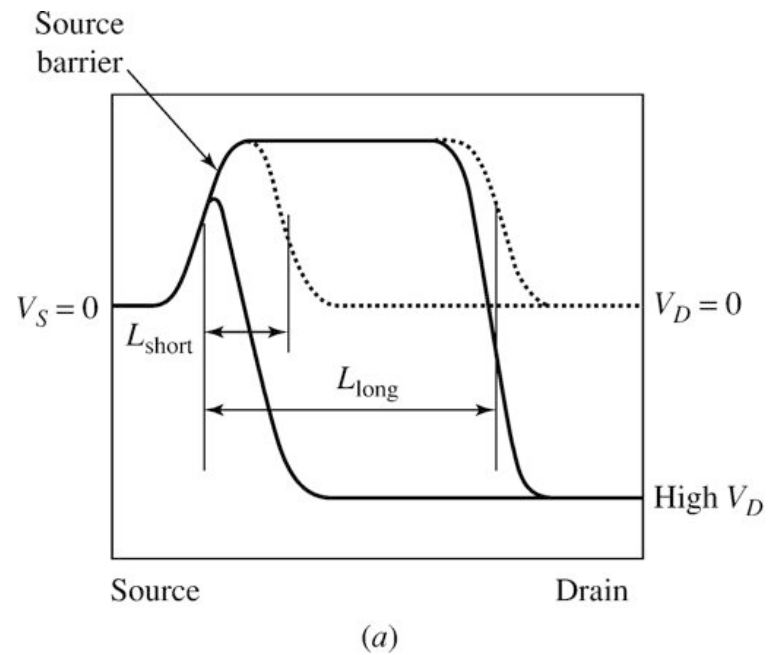
- In short-channel MOSFETs, the channel length L and the thickness of the drain space-charge region are the same order of magnitude.
- Short-channel effect refers to the changes of threshold voltage V_T that occurs when L decrease and the drain bias increases.
- The reduction in V_T results from the combination of three effects:
 - ✓ Source/drain charge sharing
 - ✓ Drain-induced barrier lowering
 - ✓ Subsurface punch-through

Short-channel effect

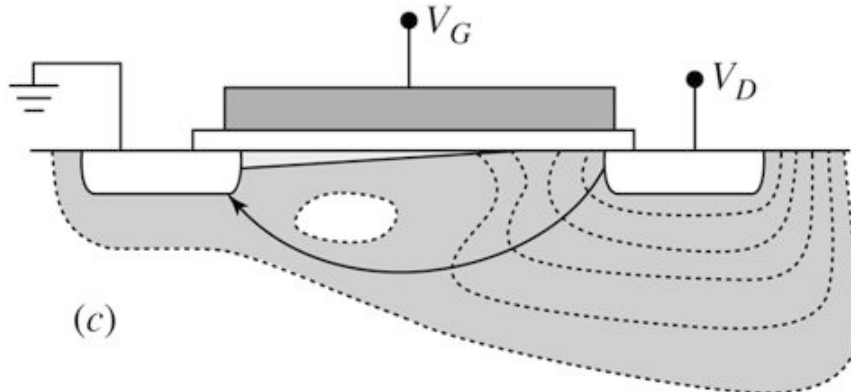
Source/drain charge sharing



Drain-induced Barrier Lowering



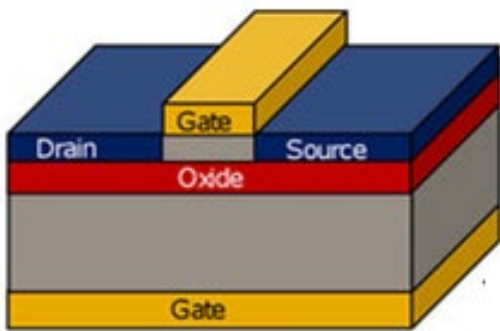
Subsurface Punch-through



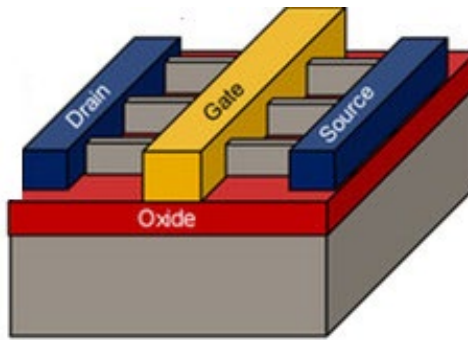
Approaches to suppress short-channel effect

Enhance gate control

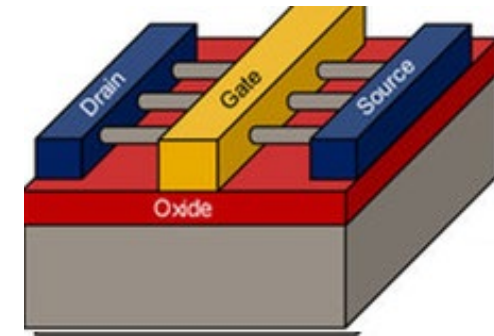
Double Gate



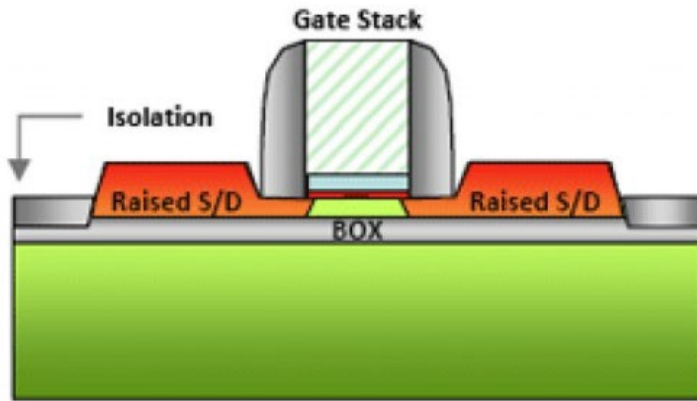
Tri-gate, FinFET



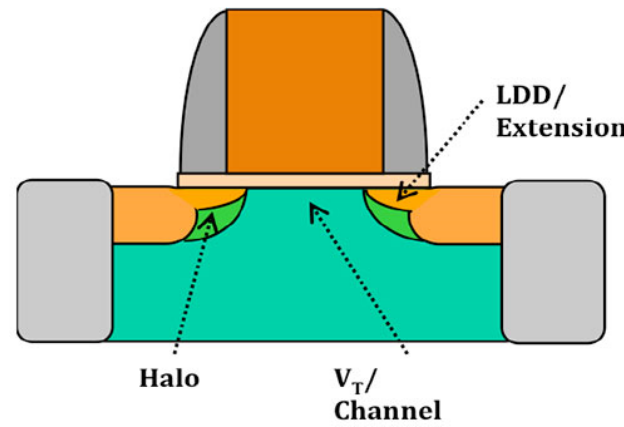
Gate-all-around



Reduce channel thickness

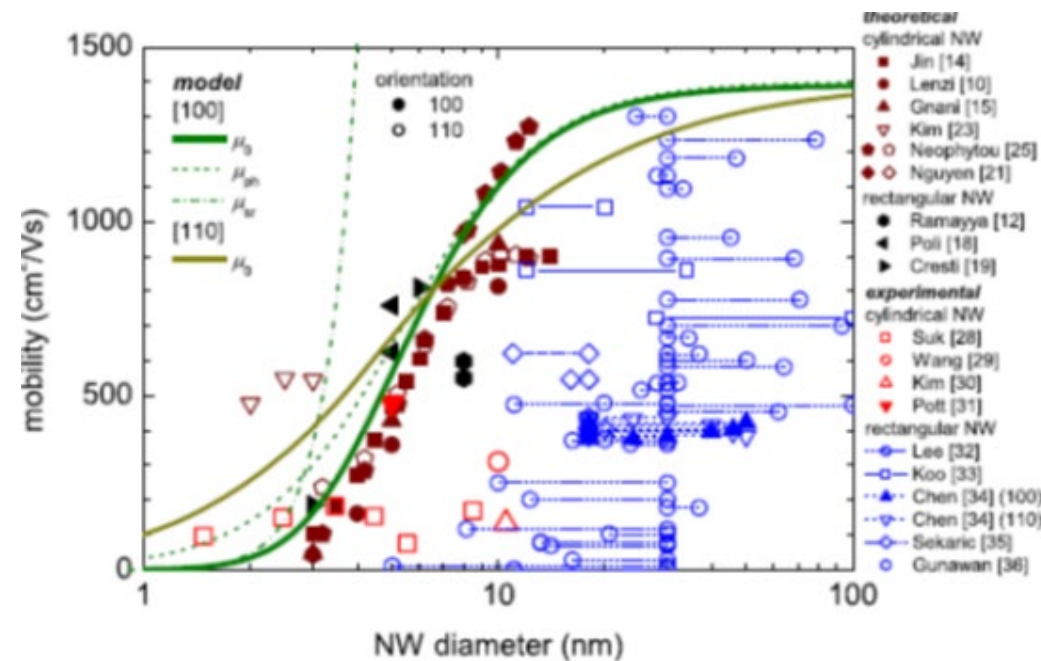
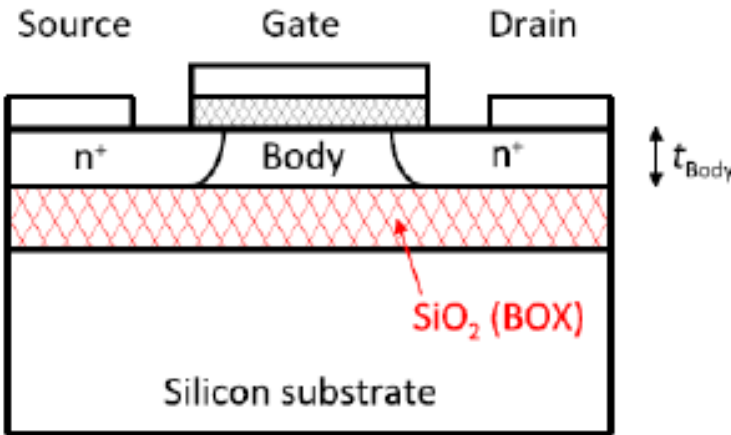


Halo implant



Enhance electrostatic control of channel

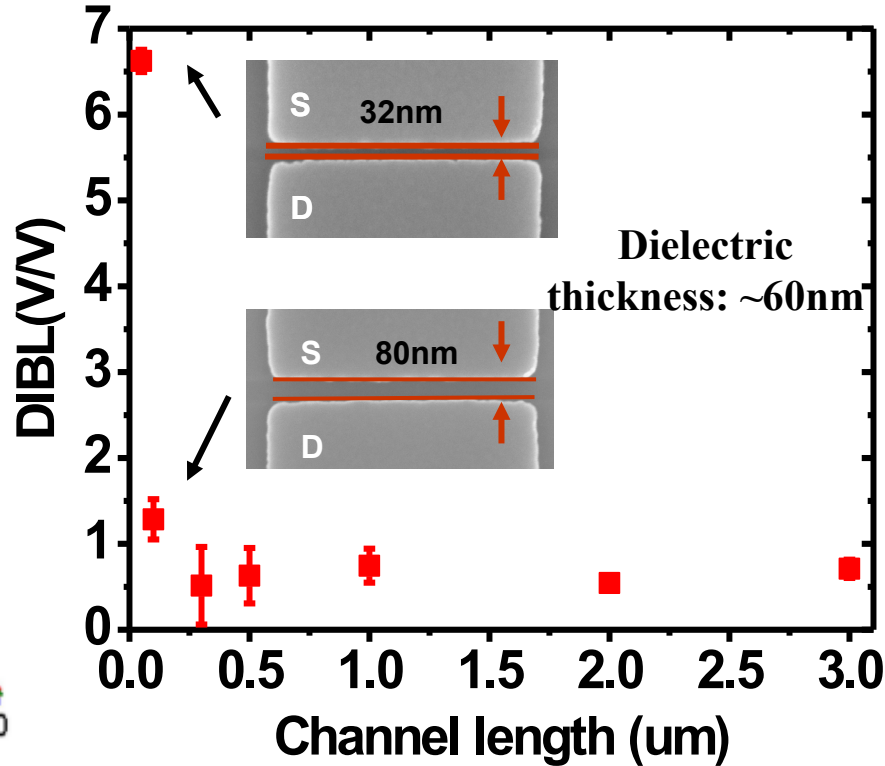
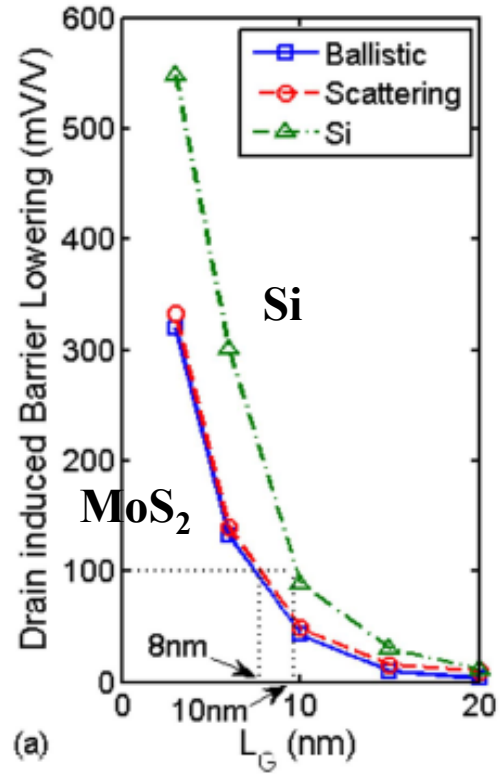
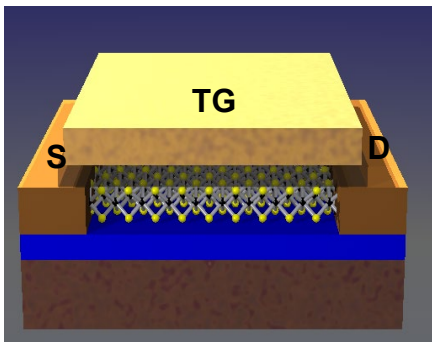
(i) UTB SOI MOSFETs (ultra-thin body)



- To maintain good electrostatic integrity, the conventional bulk MOSFETs was replaced with UTB SOI.
- However, thin and narrow bodies degrade mobility severely.
- 2D materials are atomically thin, which can effectively suppress short channel effect.

Granzner, et.al., IEEE Transaction of electron device, 2014

2D TMDs can suppress short-channel effect



Electrostatic scaling length $\lambda = \sqrt{\epsilon_s t_s t_{ox} / \epsilon_{ox}}$

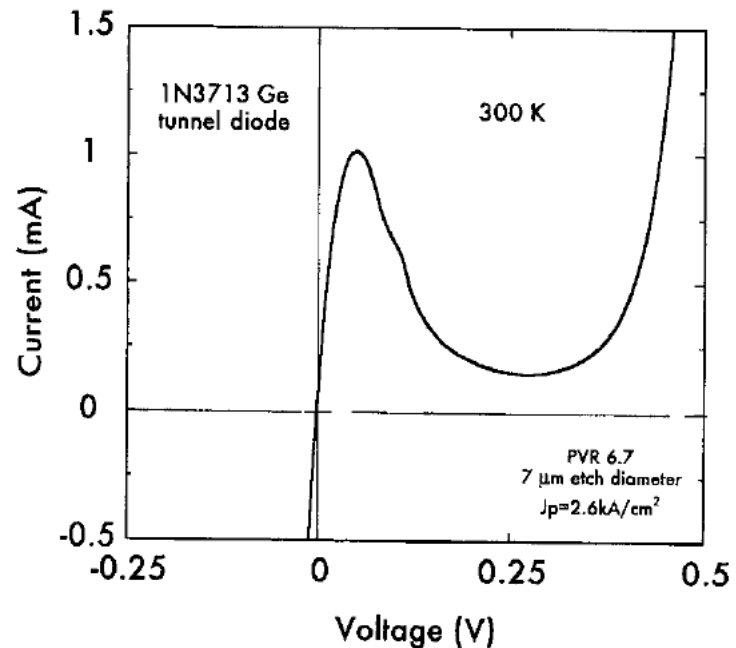
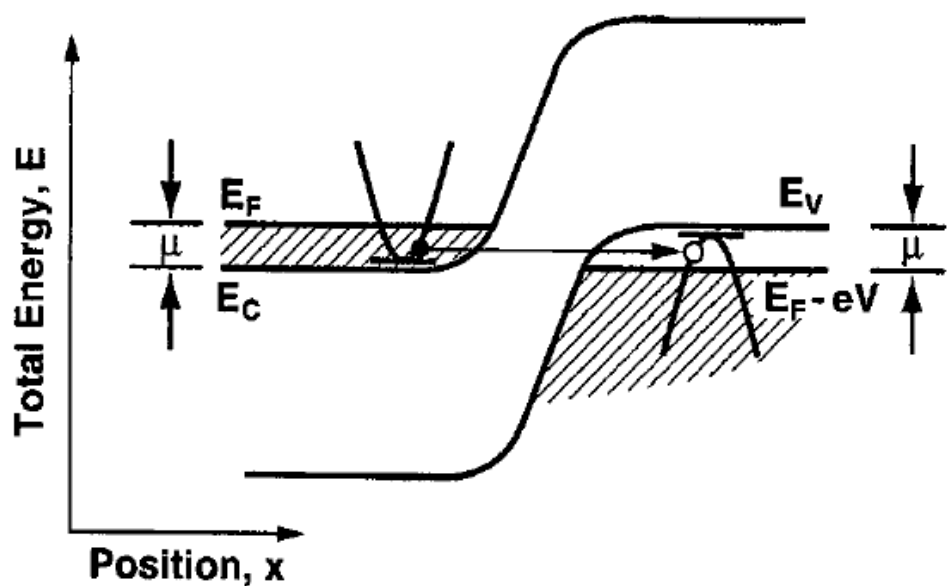
- Monolayer MoS₂ FETs show 52% smaller drain-induced barrier lowering (DIBL) and 13% smaller subthreshold swing (SS) than 3nm-thick-body Si FETs.
- The scaling limit of monolayer MoS₂ FETs is assessed to be 7 nm for 3nm hafnium oxide.

Wenjuan Zhu, Phaedon Avouris, et.al. Nature Communications, 5, 3087, 2014
Leitai Liu, Jing Guo, et.al., IEEE Transactions of Electron Devices, 60, 4133, 2013

Outline

- **Introduction of TMDs**
- **Synthesis of TMDs**
- **Electronic properties and electronic devices**
 - **Electronic properties**
 - **Electronic devices**
 - **Logic devices**
 - **Esaki diode and tunneling field effect transistor (TFET)**
 - **RF devices**
 - **Memory devices**
 - **Integrated circuits**
- **Optical properties and photonic devices**

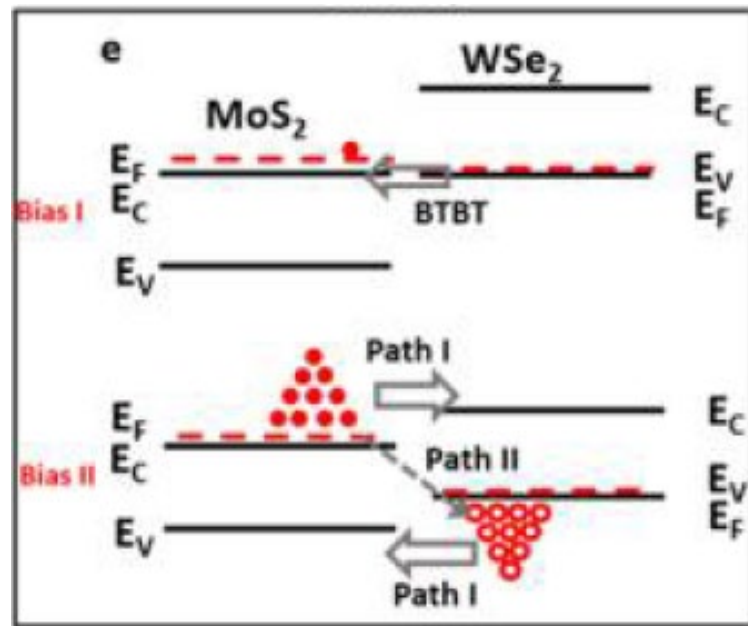
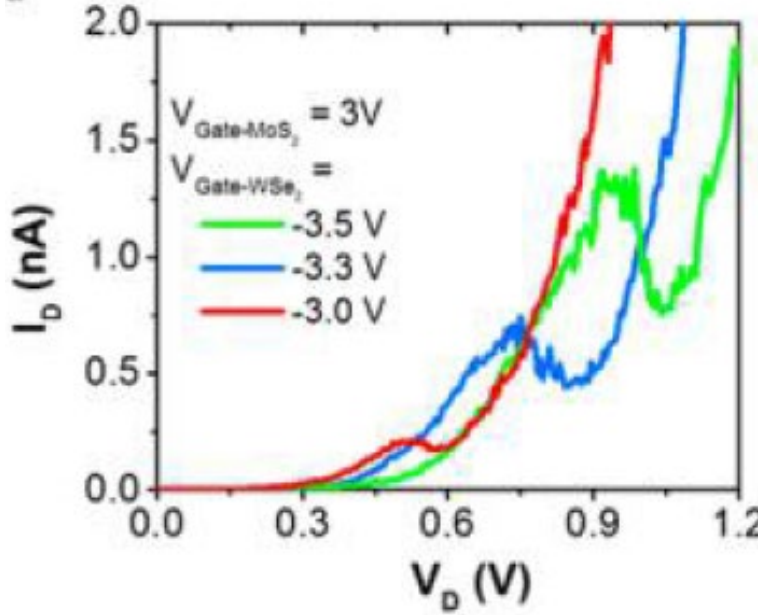
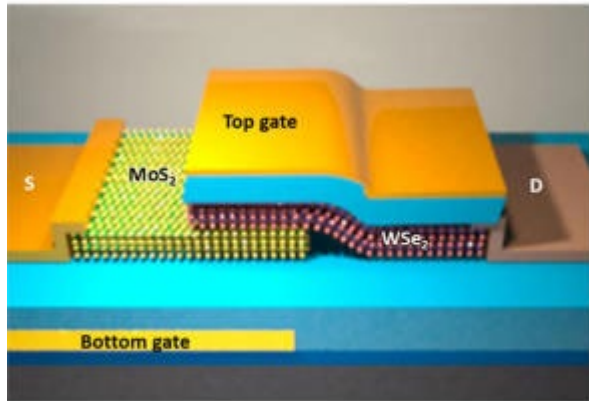
Esaki Diode



- As bias is applied, electrodes flow from the filled emitter states in the conduction band on the left to empty state in the valence band on the right.
- Initially, the current increases with the increasing bias.
- When the conduction band of the emitter is eventually raised above the valence band of the collectors, electrons can no longer tunnel into a valence-band state while conserving both total energy and transverse momentum, and the current is reduced to a minimum.

A. Seabaugh, Encyclopedia of Applied Physics, 335, 1998

Esaki diodes based on TMD heterostructures

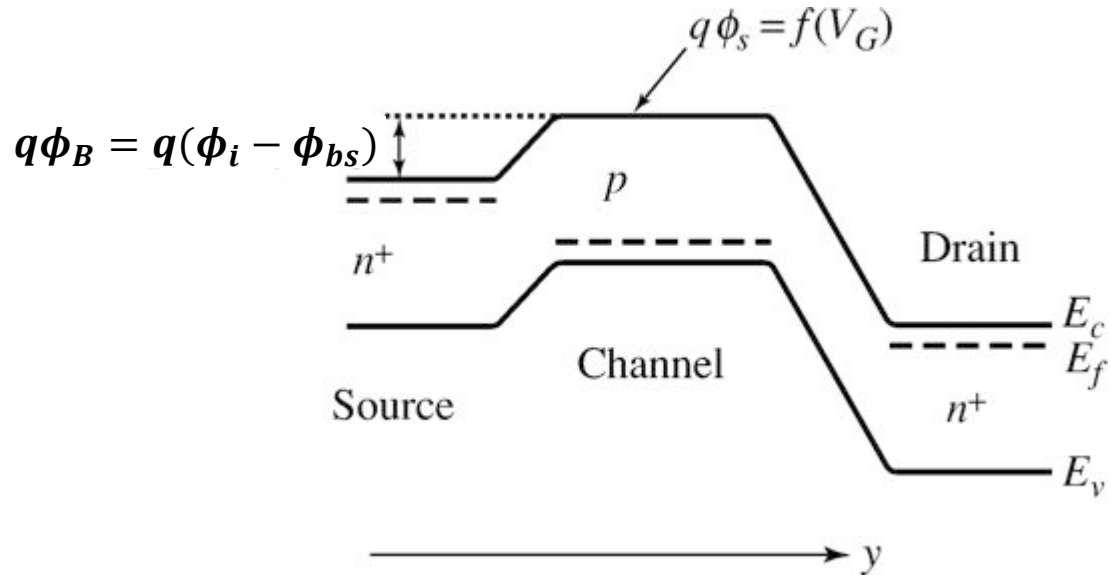


- Interlayer band-to-band tunneling was demonstrated in vertical $\text{MoS}_2/\text{WSe}_2$ van der Waals (vdW) heterostructures using a dual-gate device architecture.
- The device can be gate modulated to behave as an Esaki diode with negative differential resistance.

Tania Roy, Ali Javey, et.al. ACS Nano, 9, 2071, 2015

Subthreshold conduction of MOSFET

When the gate voltage is slightly lower than threshold voltage $V_G < V_T$, the small drain current that flows is called the subthreshold current.



The subthreshold drain current is

$$I_D = I_{D0} \exp\left(-\frac{q\phi_{bs}}{KT}\right)$$

The subthreshold slope is defined as:

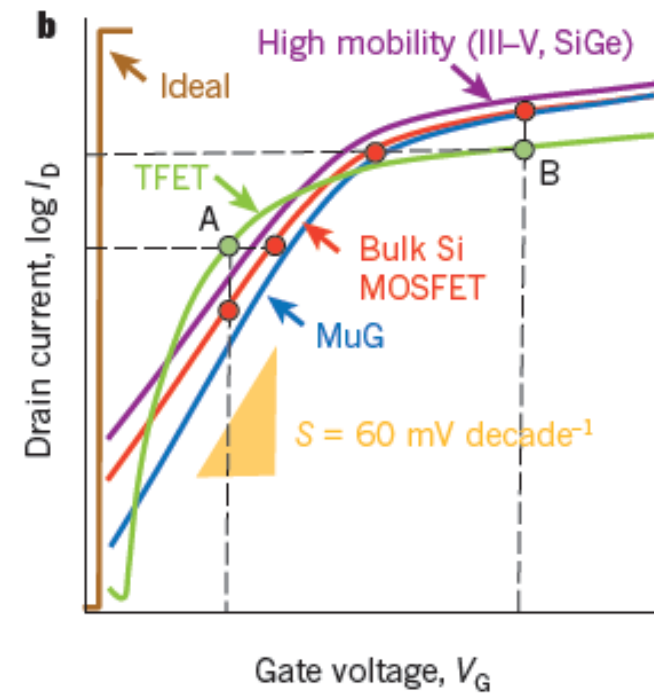
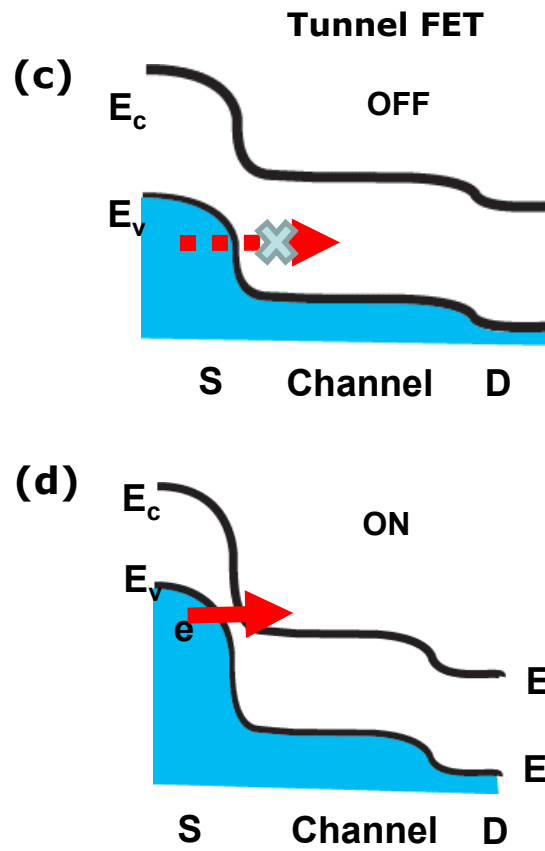
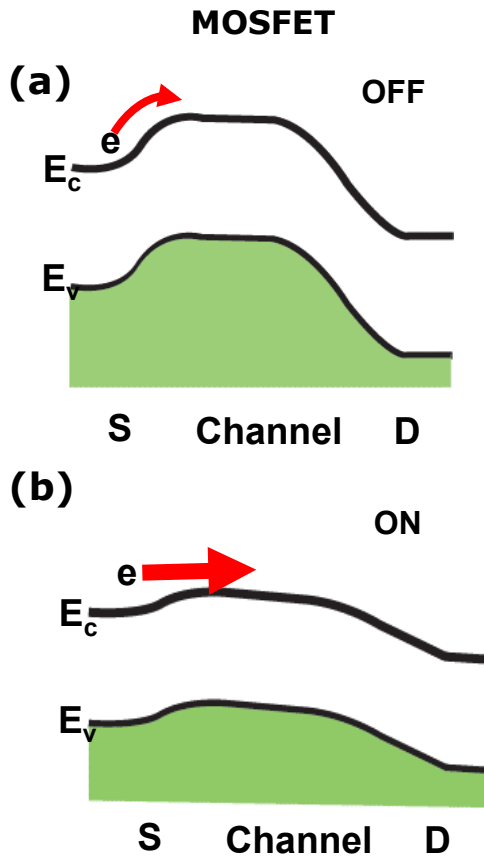
$$S \equiv \frac{dV_G}{d\log(I_D)} = \frac{kT}{q} \ln(10) (1 + C_s/C_{ox})$$

At 300K,

$$S = \frac{60mV}{decade} * (1 + C_s/C_{ox})$$

The minimum S is 60mV/dec at 300K.

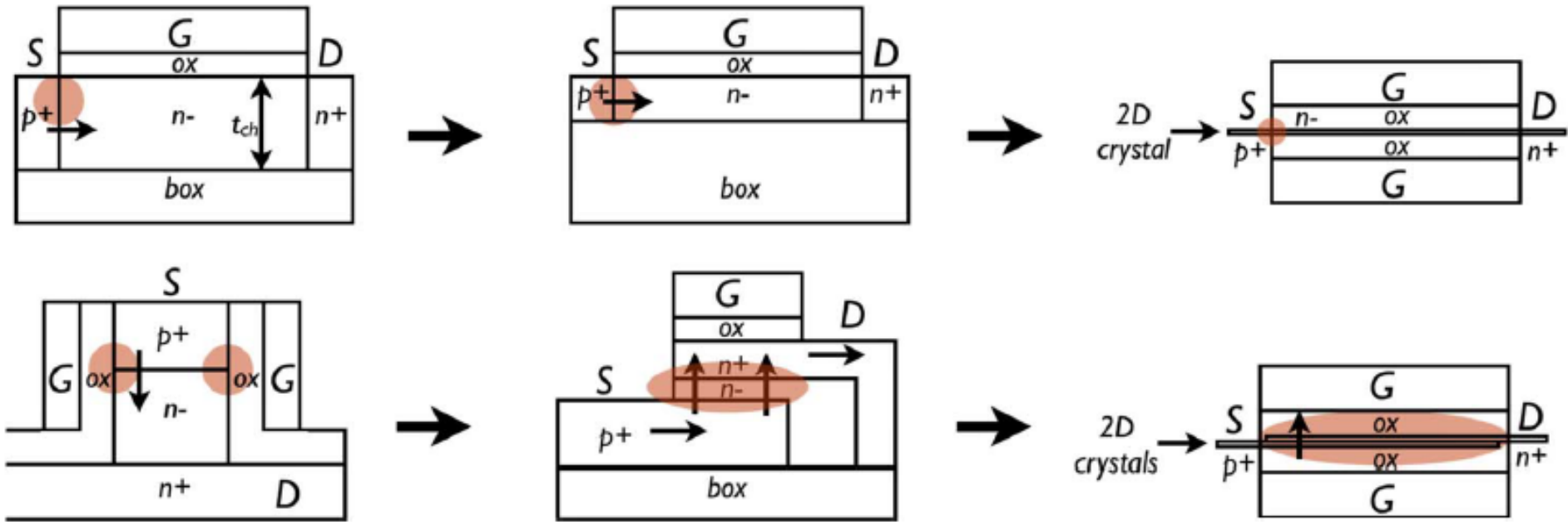
TFET operating principles



- Field-effect transistors (FETs) require at least 60 mV of gate voltage to increase the current by one order of magnitude at room temperature.
- Tunnel field-effect transistor (TFET) can overcome this limit by using band-to-band tunneling, rather than thermal injection, to inject charge carriers into the device channel.

A. Ionescu, et al., Nature, Vol. 479, 329, 2011

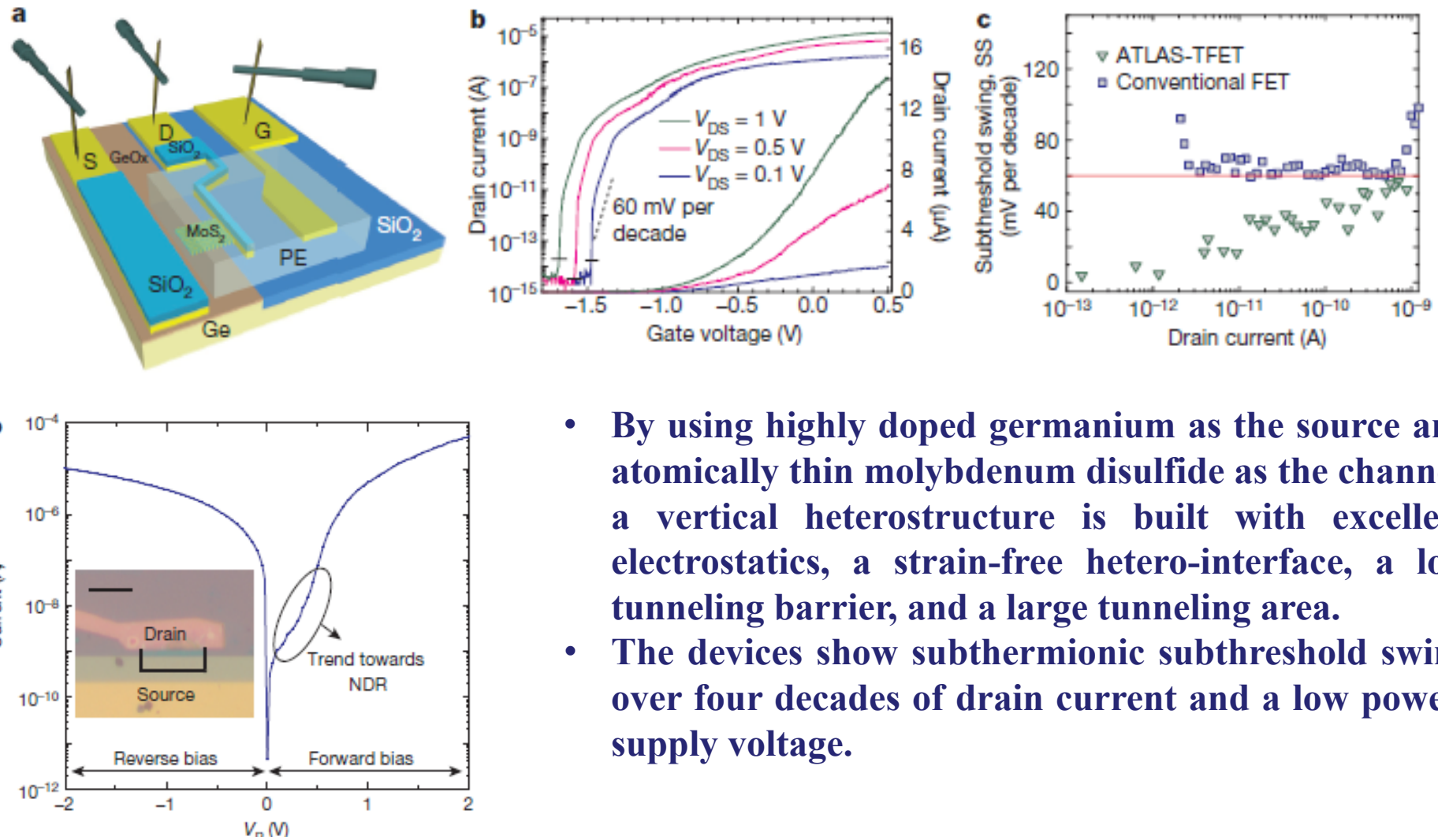
Various topologies of TFETs



- To increase the tunneling current per unit width, it is necessary to increase the net area of tunneling current flow. The vertical geometries allow this change.
- For this geometry, two layers of 2-D crystals, one doped p-type and the other n-type, promise efficient vertical scaling and electrostatic control.

Debdeep Jena, Proceedings of the IEEE, 101, 1585, 2013

Ge/MoS₂ TFETs



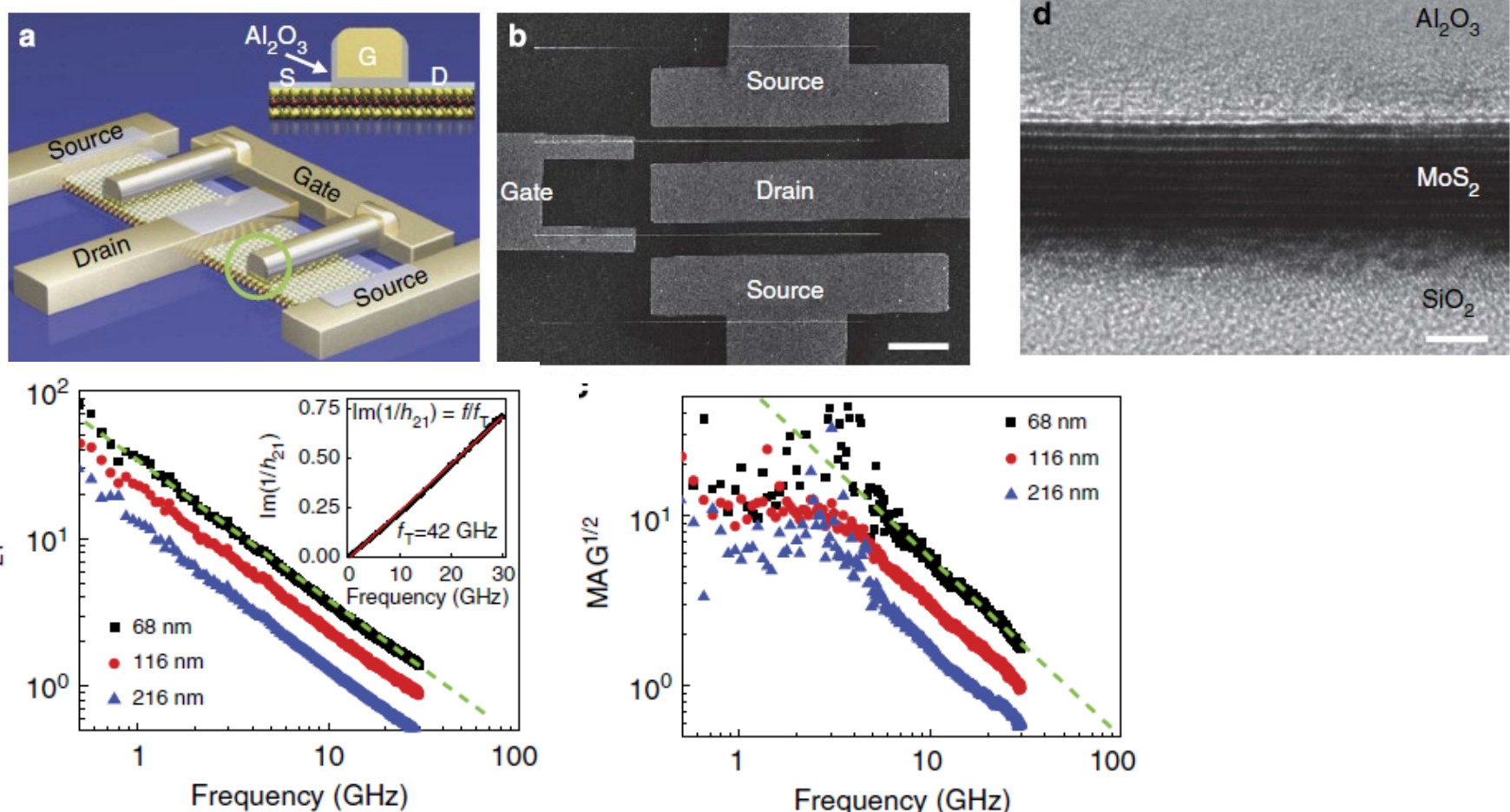
- By using highly doped germanium as the source and atomically thin molybdenum disulfide as the channel, a vertical heterostructure is built with excellent electrostatics, a strain-free hetero-interface, a low tunneling barrier, and a large tunneling area.
- The devices show subthermionic subthreshold swing over four decades of drain current and a low power-supply voltage.

Deblina Sarkar, Kaustav Banerjee, at.al., Nature, 526, 91, 2015

Outline

- **Introduction of TMDs**
- **Synthesis of TMDs**
- **Electronic properties and electronic devices**
 - **Electronic properties**
 - **Electronic devices**
 - **Logic devices**
 - **Tunneling field effect transistor (TFET)**
 - **RF devices**
 - **Memory devices**
 - **Integrated circuits**
- **Optical properties and photonic devices**

RF device based on multilayer MoS₂



- MoS₂-based RF transistor shows an intrinsic gain over 30, an intrinsic cut-off frequency f_T up to 42 GHz and a maximum oscillation frequency f_{MAX} up to 50 GHz.

Rui Cheng, Xiangfeng Duan, et.al., Nature Communications, 5, 5143, 2014

RF device figure-of-merit

- Intrinsic cut-off frequency

$$f_T = \frac{g_m}{2\pi C_{gs}}$$

- Intrinsic maximum oscillation frequency can be written as:

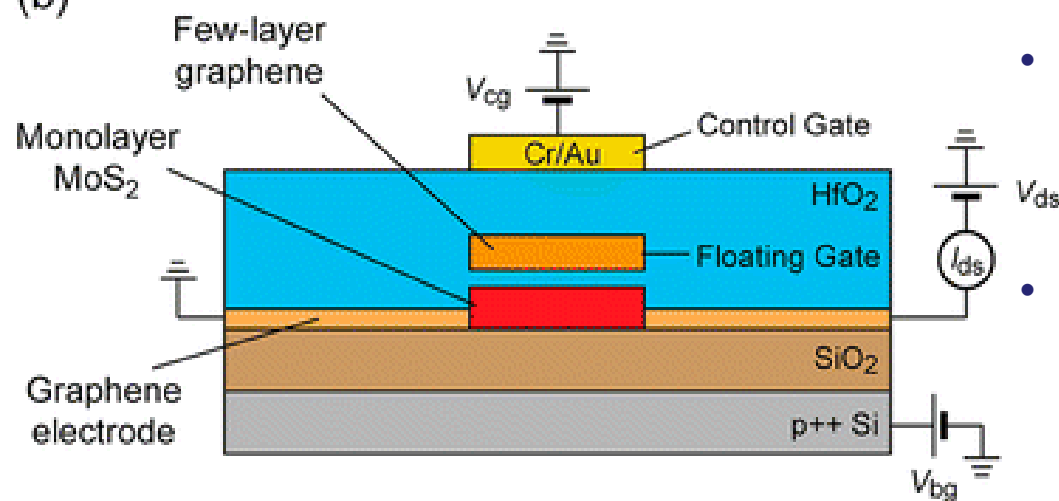
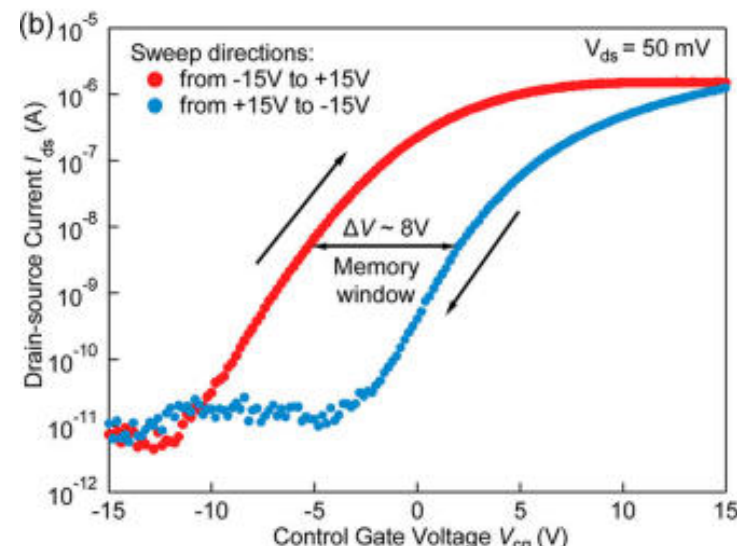
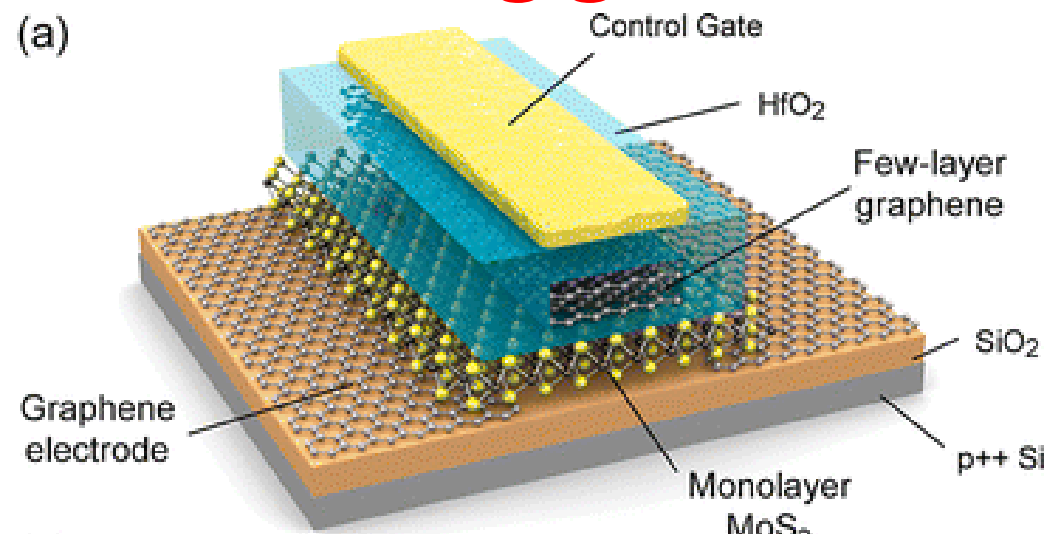
$$f_{max} = \frac{g_m}{4\pi C_{gs}\sqrt{g_{ds}R_i}}$$

- MoS₂ has lower mobility than graphene, which leads lower cut-off frequency in MoS₂ than in graphene.
- However, graphene has zero bandgap, which MoS₂ has sizable bandgap, which means the output conductance g_{ds} is smaller in MoS₂, i.e. the maximum oscillation frequency is higher in MoS₂ than in graphene.

Outline

- **Introduction of TMDs**
- **Synthesis of TMDs**
- **Electronic properties and electronic devices**
 - **Electronic properties**
 - **Electronic devices**
 - **Logic devices**
 - **Tunneling field effect transistor (TFET)**
 - **RF devices**
 - **Memory devices**
 - **Integrated circuits**
- **Optical properties and photonic devices**

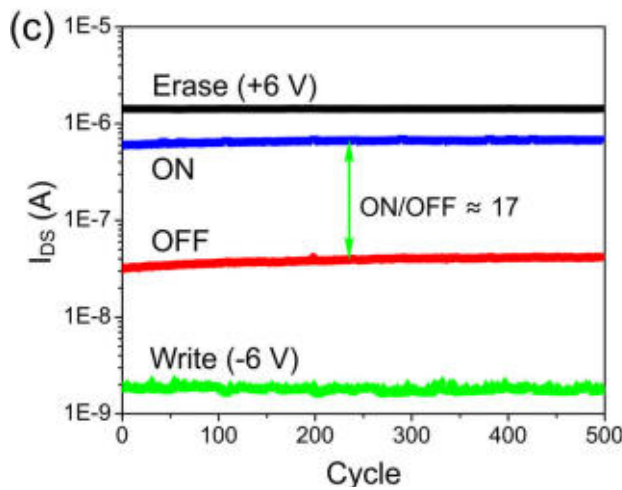
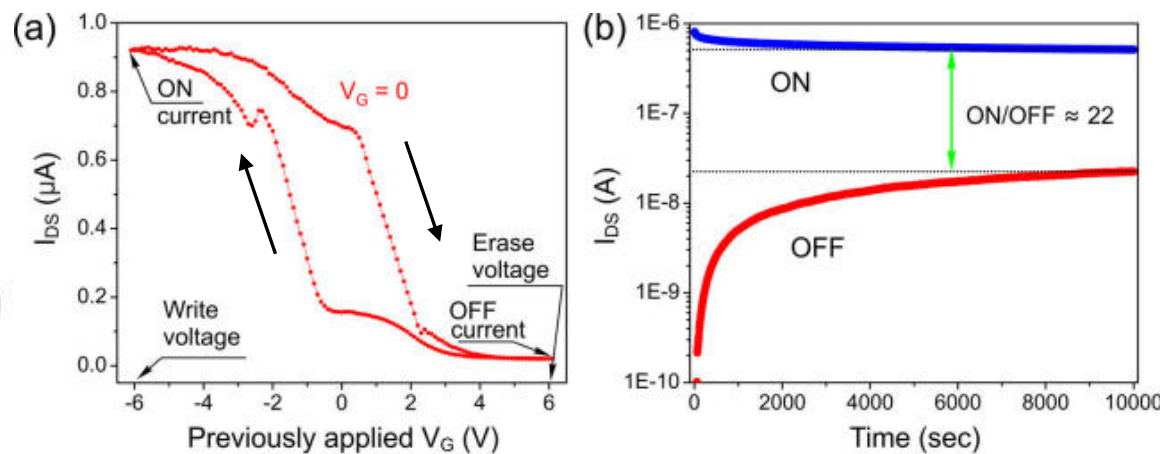
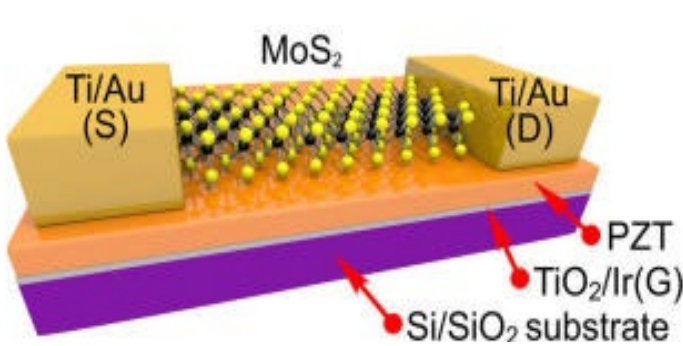
Floating gate memory based on MoS_2



- A nonvolatile memory cell was built using multi-layer graphene as floating gate or charge trapping layer and MoS_2 as a channel.
- Because of its band gap and 2D nature, monolayer MoS_2 is highly sensitive to the presence of charges in the charge trapping layer, resulting in a factor of 10^4 difference between memory program and erase states.

Simone Bertolazzi, Andras Kis, et.al., ACS Nano, 7, 3246, 2013

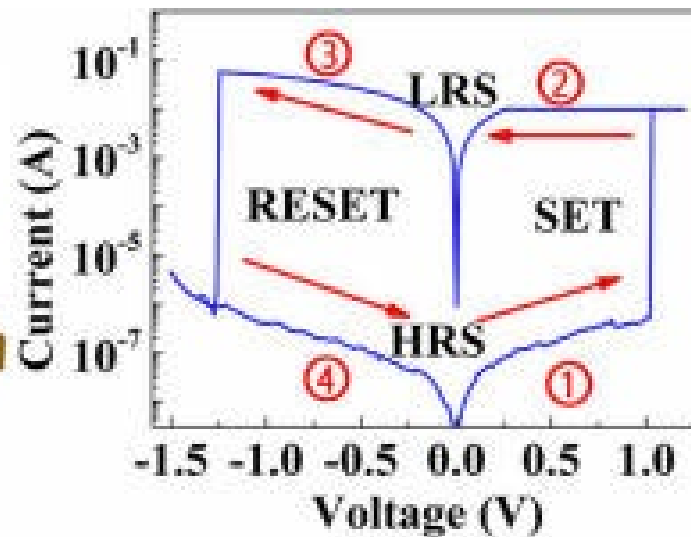
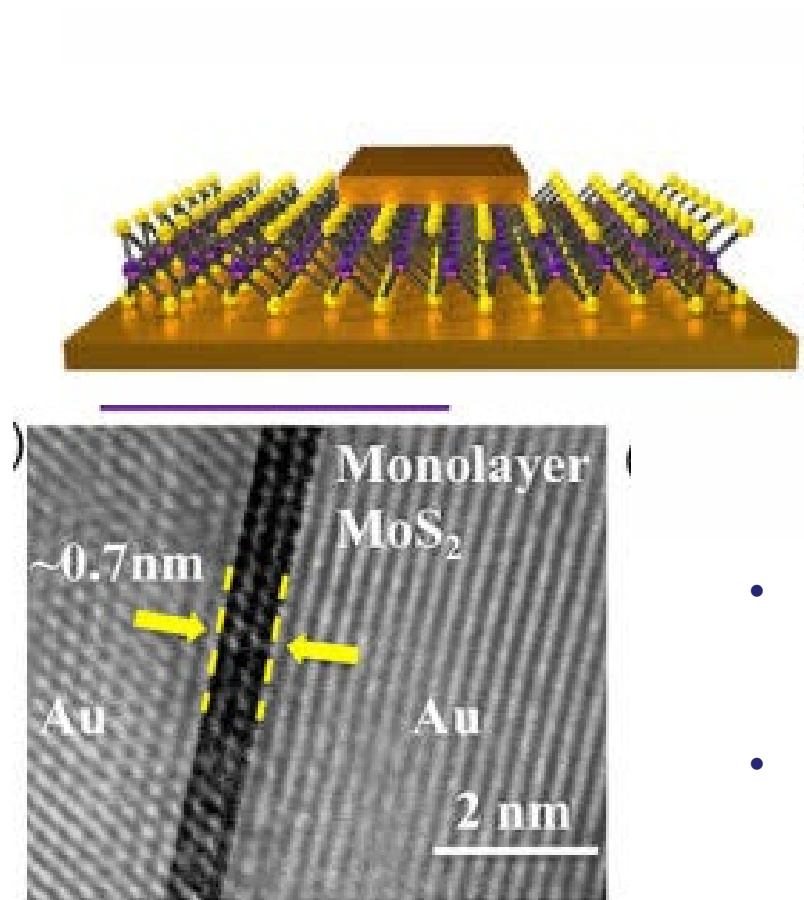
Ferroelectric memory based on MoS₂



- Ferroelectric memory device based on monolayer or few-layer MoS₂ on a lead zirconium titanate (PZT) substrate. The device exhibit a large hysteresis of electronic transport and sizable memory window.

Alexey Lipatov, Alexander Sinitskii, et.al., ACS Nano, 9, 8089, 2015

Resistive memory based on TMDs



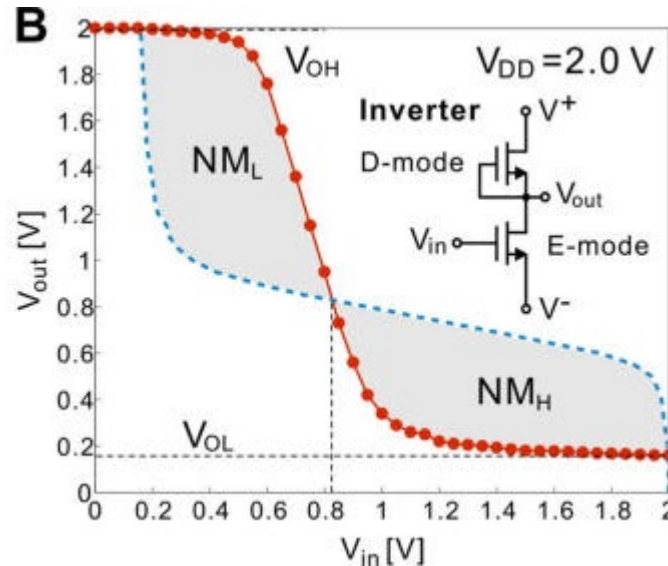
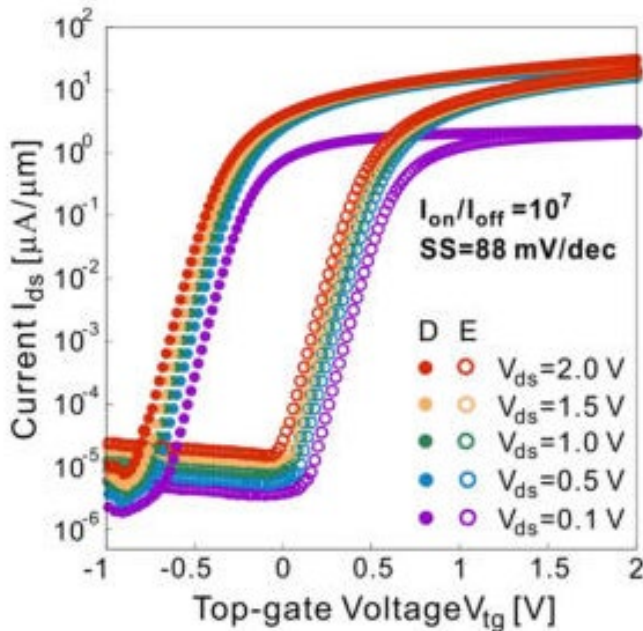
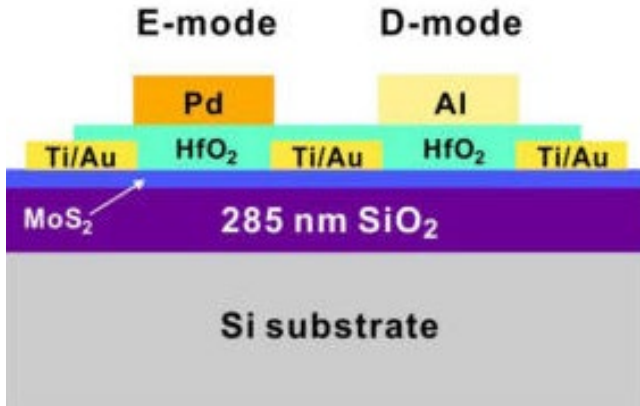
- Resistive memory cells were demonstrated based on single-layer TMD sheets sandwiched between metal electrodes.
- Proposed model: in the SET process, the electrons are transported through a filamentary-like 1D conductive link, and in the RESET process, the conductive path is broken, resulting in a Schottky barrier at the device interface

Ruijing Ge, Deji Akinwande, Nano Letters, 18, 434, 2018

Outline

- **Introduction of TMDs**
- **Synthesis of TMDs**
- **Electronic properties and electronic devices**
 - **Electronic properties**
 - **Electronic devices**
 - **Logic devices**
 - **Tunneling field effect transistor (TFET)**
 - **RF devices**
 - **Memory devices**
 - **Integrated circuits**
- **Optical properties and photonic devices**

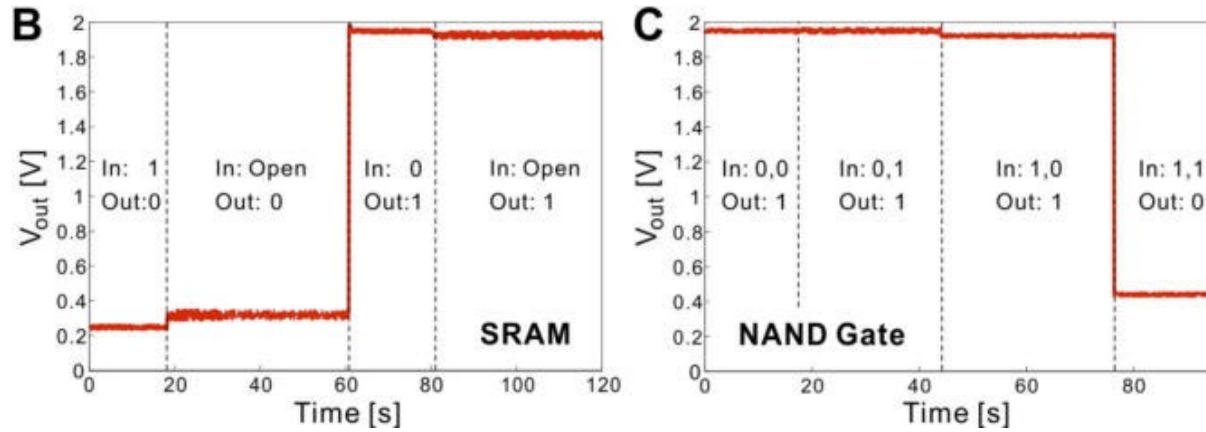
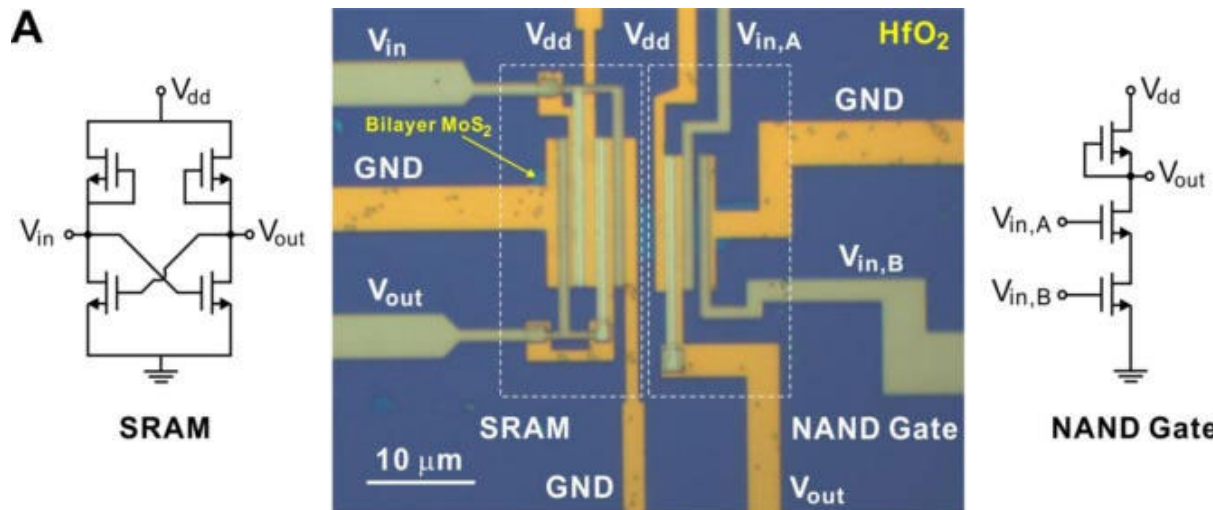
MoS₂ inverter



- Both enhancement-mode and depletion-mode transistors were fabricated using gate metals with different work functions.
- An inverter was built using enhancement and depletion mode transistors based on MoS₂.

Han Wang, Tomas Palacios, et.al. Nano Letter, 12, 4674, 2012

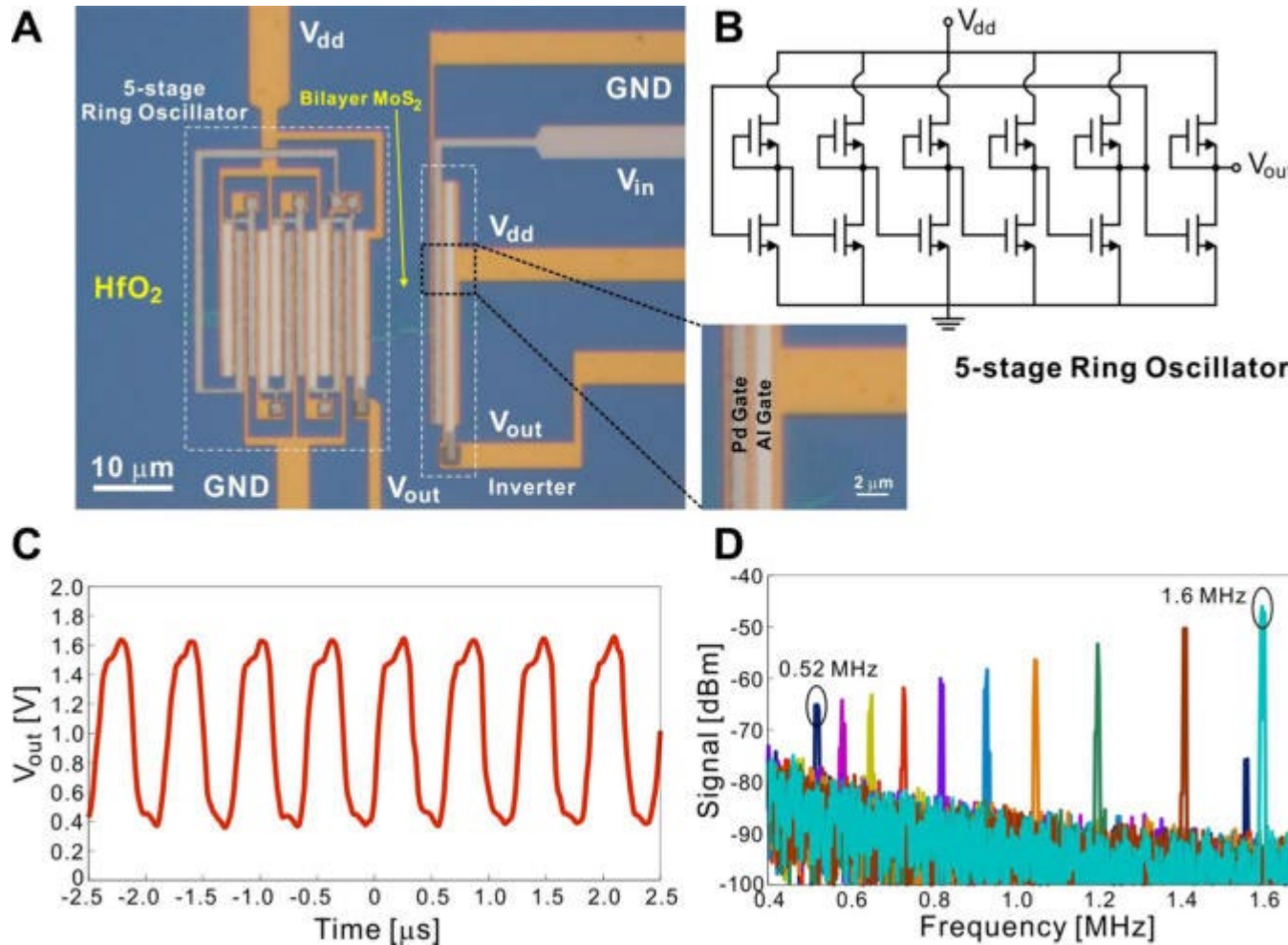
NAND gate and SRAM based on MoS₂



NAND gate and a static random access memory were also built on MoS₂

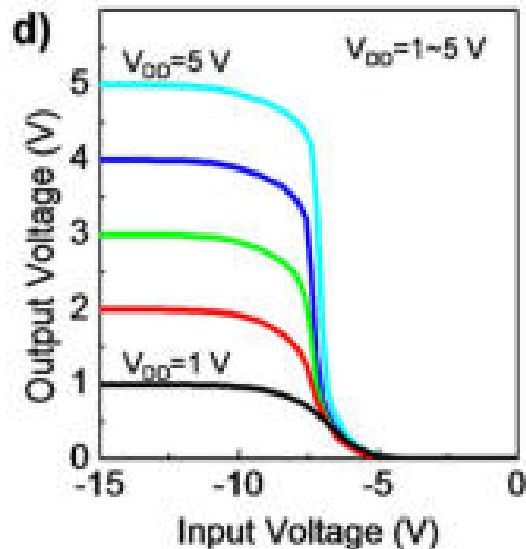
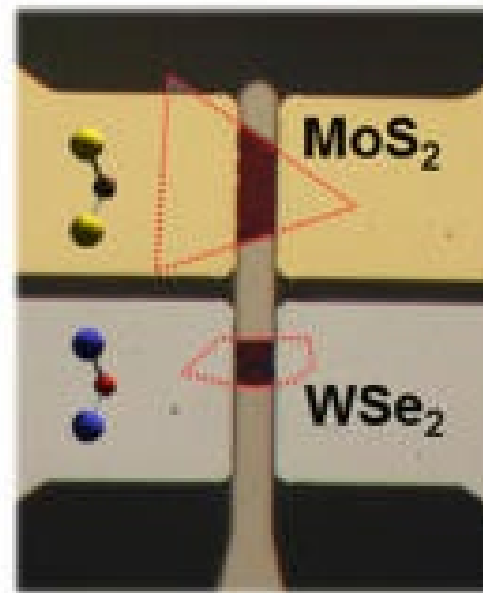
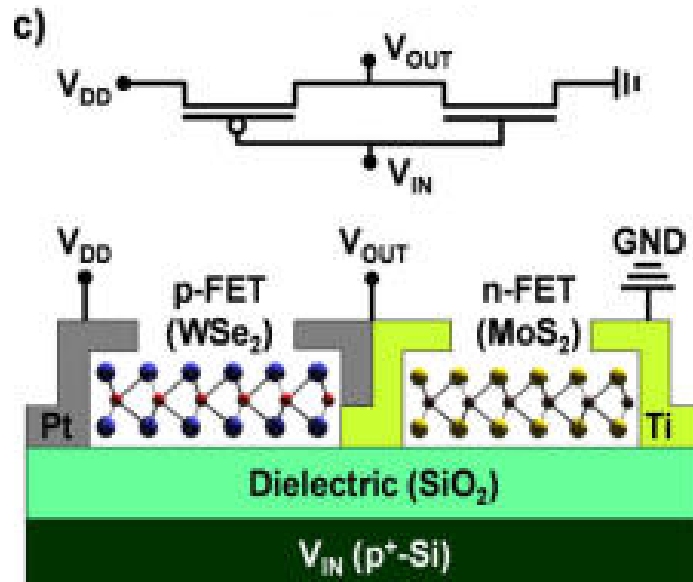
Han Wang, Tomas Palacios, et.al. Nano Letter, 12, 4674, 2012

Ring oscillator based on MoS₂



Han Wang, Tomas Palacios, et.al. Nano Letter, 12, 4674, 2012

Inverter based on n-MoS₂ and p-WSe₂



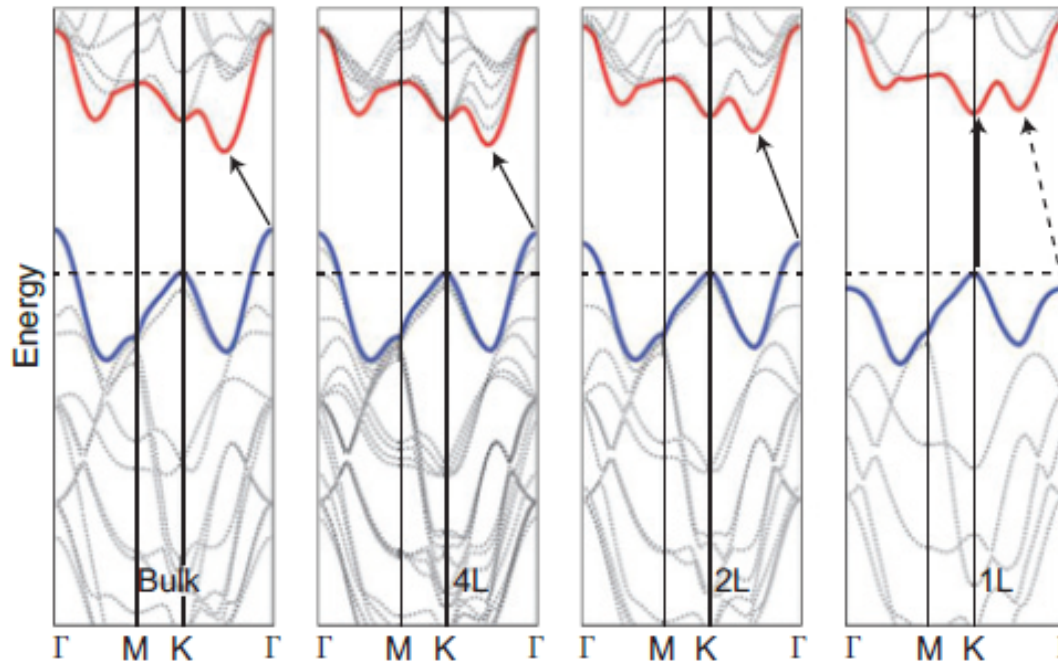
- Hetero-CMOS inverters based on p -WSe₂ transistor and n-MoS₂ transistor were demonstrated on glass substrate.
- A maximum voltage gain of ~ 27 was achieved.

Pyo Jin Jeon, Seongil Im, Applied Materials & Interfaces, 7, 22333, 2015

Outline

- Introduction of TMDs
- Synthesis of TMDs
- Electronic properties and electronic devices
- Optical properties and photonic devices
 - Optical properties
 - • Exciton and trion
 - Valley and spin
 - Photonic devices

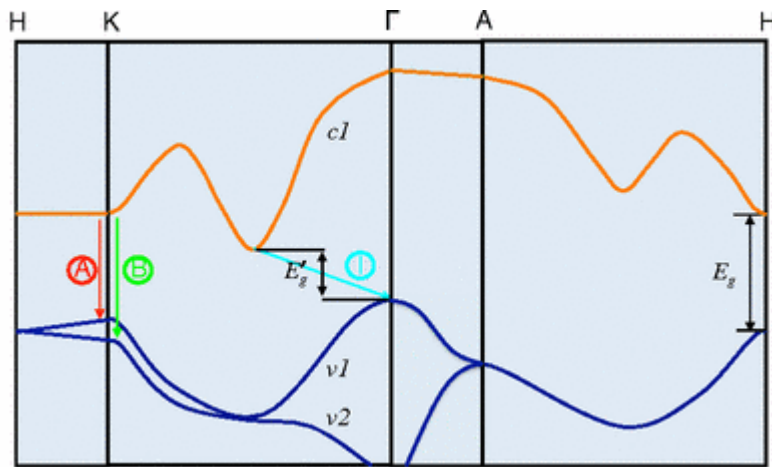
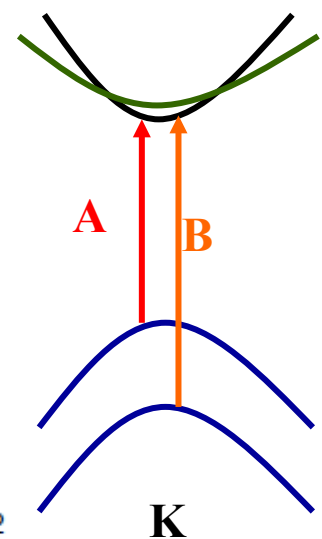
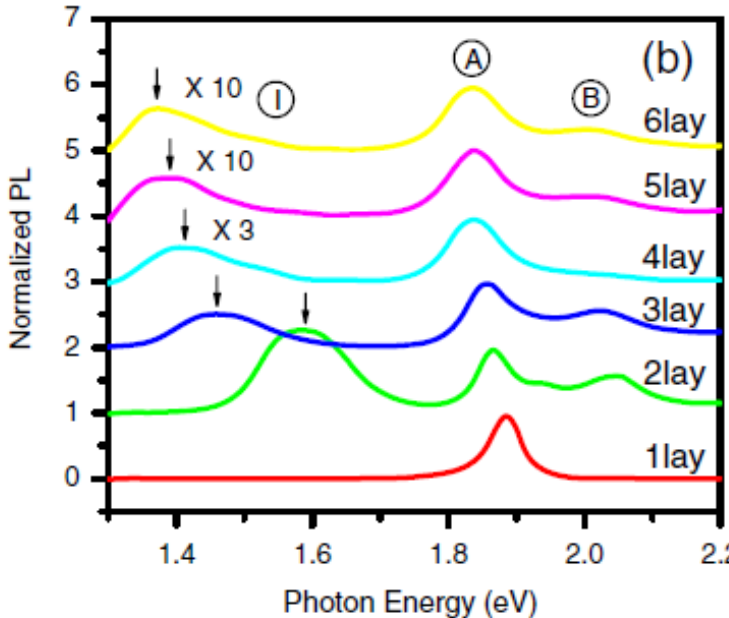
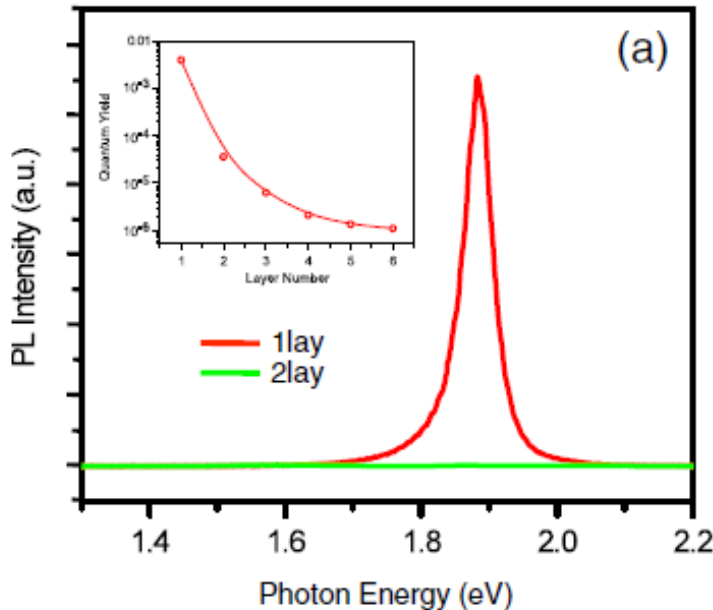
Indirect to direct band transition



- Bulk MoS₂ has a band gap of approximately 1.3 eV, with the valence band maximum at the Γ point and the conduction band minimum halfway along the Γ -K direction in the Brillouin zone. In the monolayer limit, a direct band gap of 1.85 eV at K point is obtained.

A. Splendiani, F. Wang, Nano Lett. 10, 4, 1271, 2010

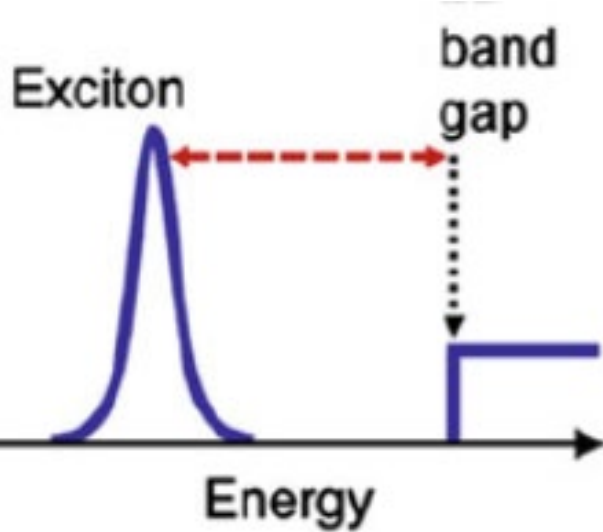
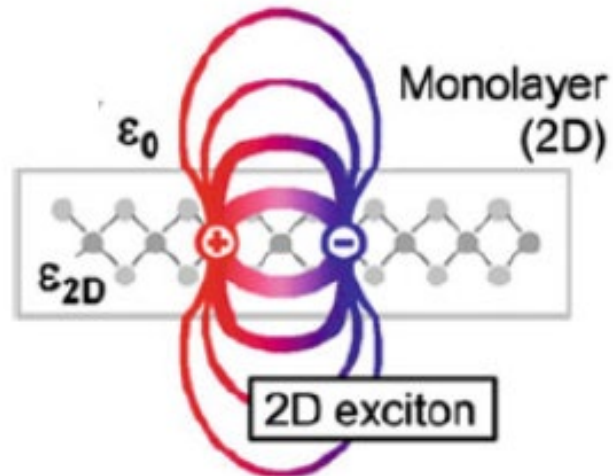
Photoluminescence of MoS₂



- The indirect–direct semiconductor transition is manifested as enhanced PL in monolayers.
- The PL spectrum of monolayer samples consists of a single narrow peak A centered at 1.90 eV.
- With increasing layer numbers, peak I shifts to lower energy, approaching the indirect-gap energy of 1.29 eV.

K. Mak, T. Heinz, PRL 105, 136805, 2010

Excitons in TMDs

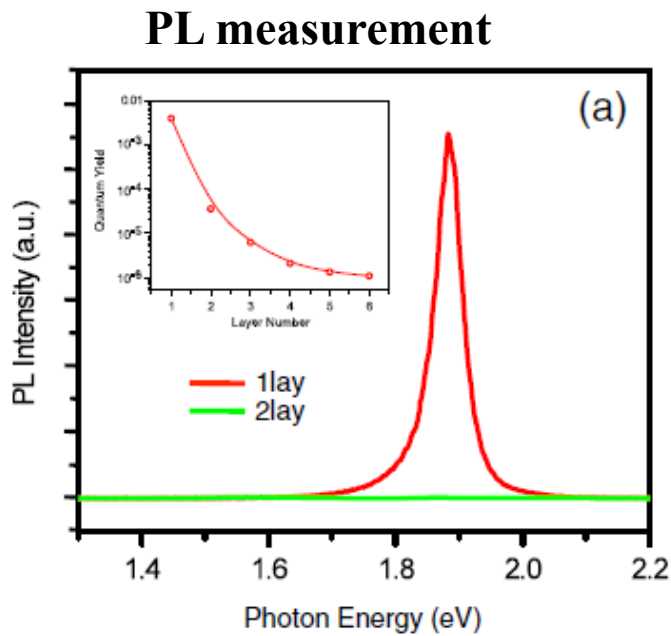


- Excitons are quasi-particles that form when electrons and holes in a semiconductor are bound into pairs by the Coulomb force.
- Excitons are strongly bound in 2D materials due to the enhanced electron–hole interaction in 2D systems and the reduced dielectric screening.
- As a result, the optical absorption spectra of TMDs exhibit pronounced peaks, rather than steps that would be expected for single-particle transitions in 2D systems.
- This is in contrast to 3D semiconductors, in which exciton binding energies are smaller than the thermal energy at room temperature (e.g. 4 meV in GaAs), and excitonic features are only observable at low temperatures.

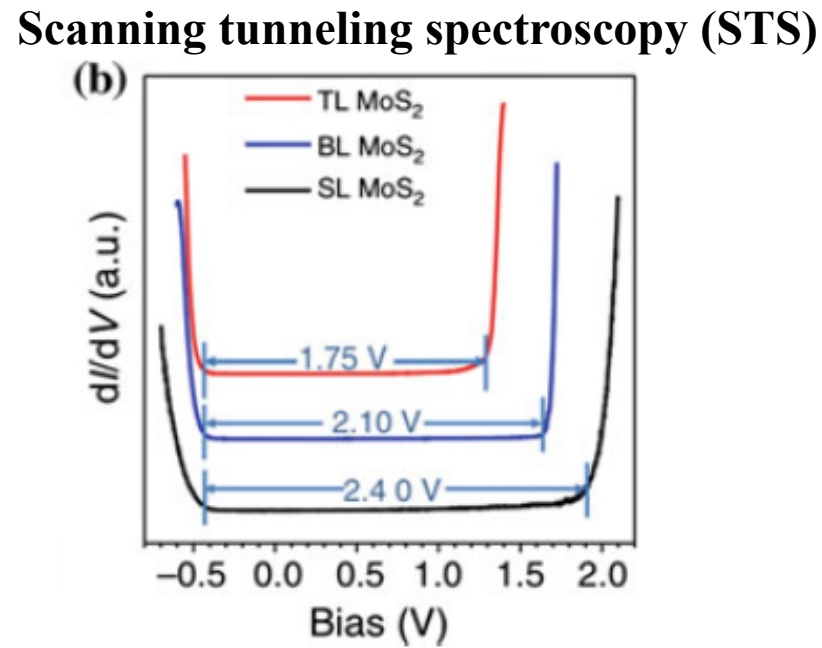
A.V. Kolobov, J. Tominaga, Two-Dimensional Transition-Metal Dichalcogenides, Springer, 2016

Optical band gap and electrical band gap

- Optical band gap is the energy of photons that are emitted (or absorbed).
- Electrical (single-particle) band gap is the energy difference between the top of the valence band and the bottom of the conduction band.



Optical band gap: ~1.85 eV



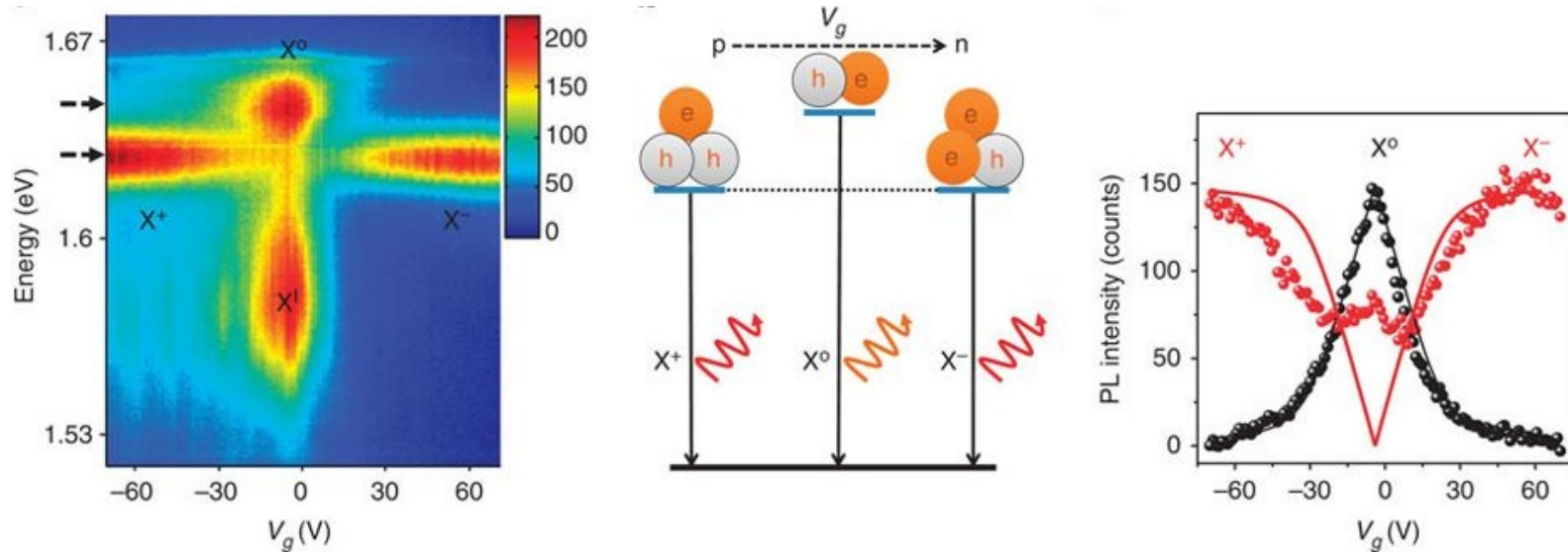
Electrical band gap: 2.4~2.5 eV

- In traditional 3D semiconductors such as silicon, there is barely any difference between the two, due to the small exciton binding energies in these materials. In mono- and few-layer TMDs, on the other hand, the difference is significant.

Y. Huang, Nature Communications, 6, 6298 (2015)

Trions in TMDs

- Trions are quasi-particles that are composed of two electrons and a hole (X^-) or two holes and an electron (X^+).
- Trions are negatively or positively charged excitons.



- Electrostatic tunability of charging effects in positively charged (X^+), neutral (X^0) and negatively charged (X^-) excitons were observed in field-effect transistors via photoluminescence.
- The trion charging energy is large (30 meV). The charging energies for X^+ and X^- to be nearly identical implying the same effective mass for electrons and holes

J. Ross, X. Xu, et.al., Nature Communications, 4, 1474, 2013

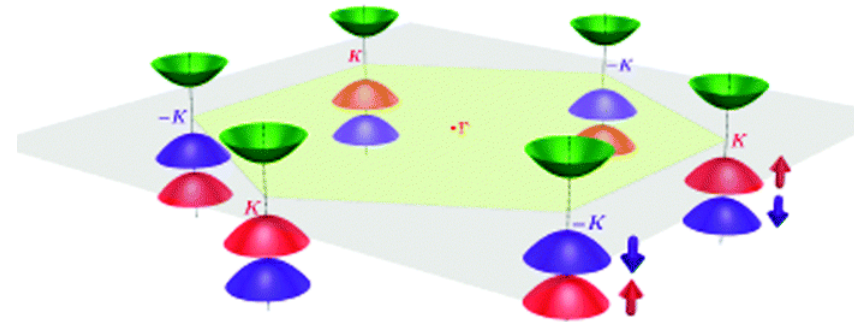
Outline

- Introduction of TMDs
- Synthesis of TMDs
- Electronic properties and electronic devices
- Optical properties and photonic devices
 - Optical properties
 - Exciton and trion
 - Valley and spin
 - Photonic devices

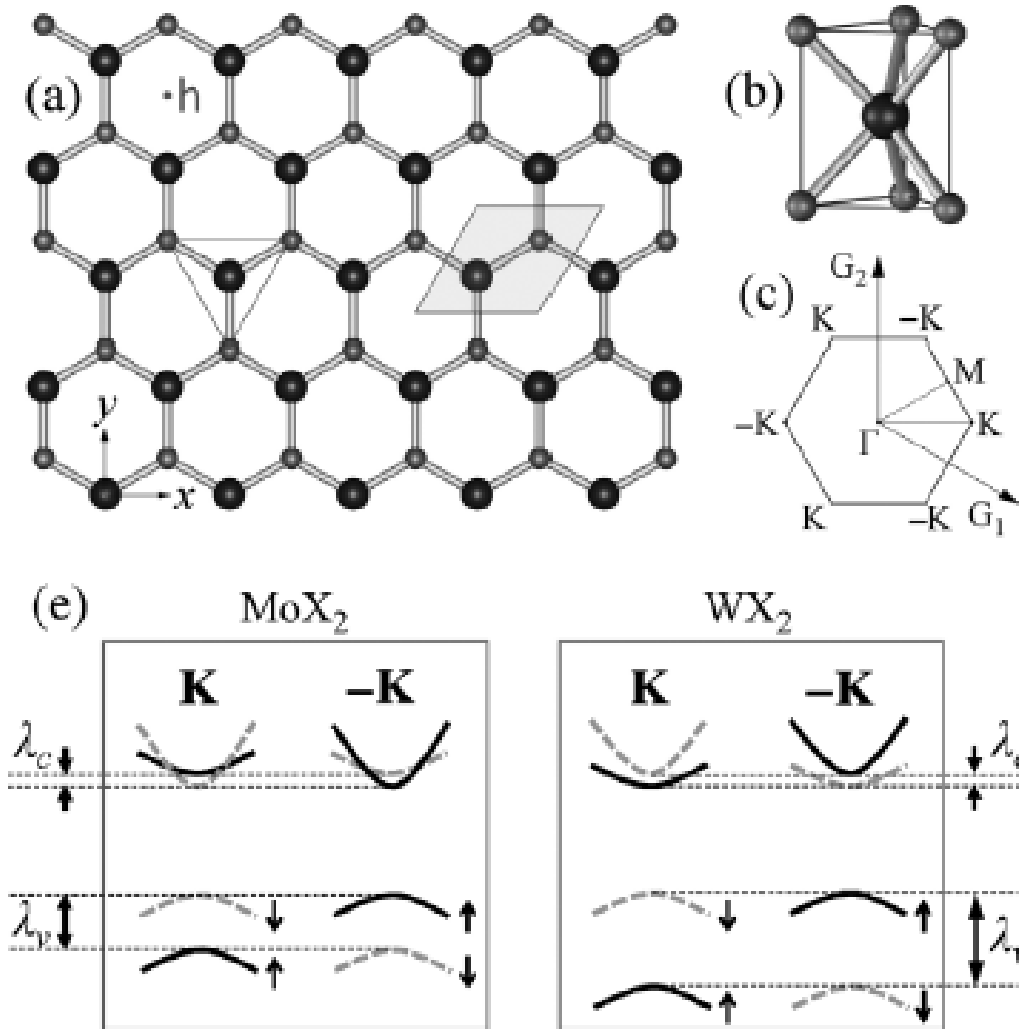


Valley and valleytronics

- A local minimum in the conduction band or local maximum in the valence band is referred to as a valley.
- In addition to charge and spin, an electron is also endowed with a valley degree of freedom, which specifies the valley that the electron occupies.
- The possibility of using the valley degree of freedom to store and carry information (similar to spin in spintronics) leads to conceptual electronic applications known as valleytronics



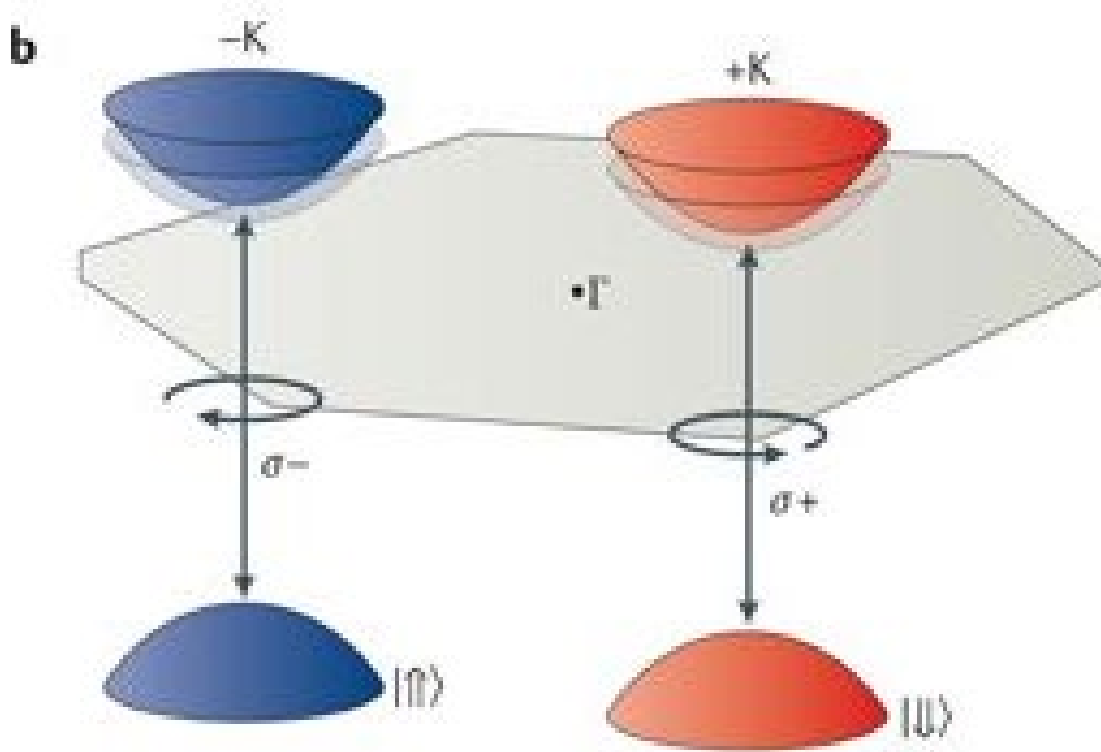
Spin-orbital coupling



- TMDs have a strong spin-orbit-coupling (SOC) originating from the M-d orbitals.
- SOC lifts spin degeneracy in both valence and conduction band.
- The time-reversal symmetry dictates the spin splitting to have opposite signs at the $+K$ and $-K$ valleys, giving rise to an effective coupling between spin and valley.

Ph. Avouris, T. Heinz, T. Low, 2D Materials Properties and Devices, Cambridge University Press, 2017

Control valley polarization by light

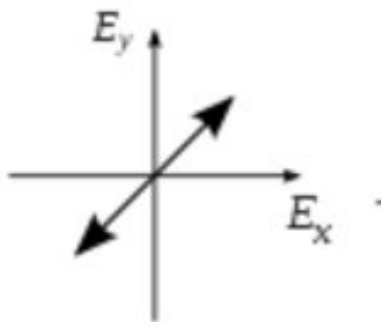


- The broken inversion symmetry of TMD systems gives rise to a valley dependent optical selection rule, in which right circularly polarized light couples to interband transitions in the $+K$ valley, and left circularly polarized light couples to interband transitions in the $-K$ valley.

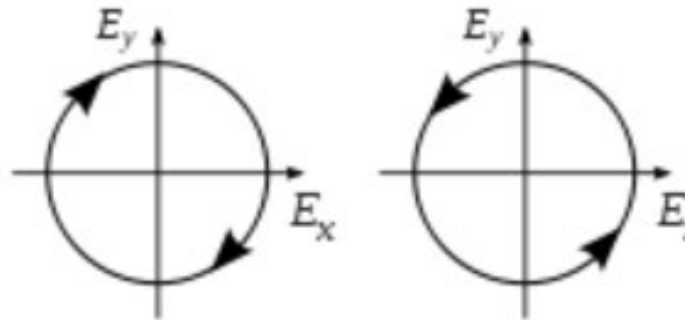
J. Schaibley, Nature Reviews Materials, 1, 16055 (2016)

Circular polarized light

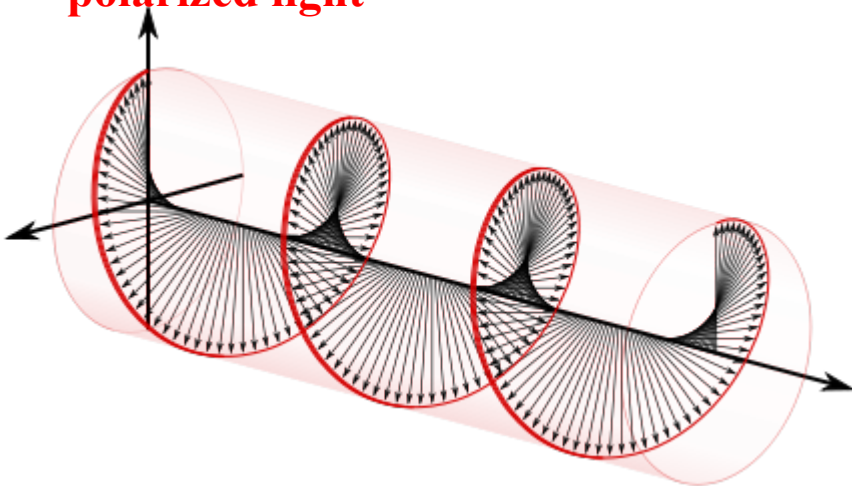
Linear polarized light



Circular polarized light

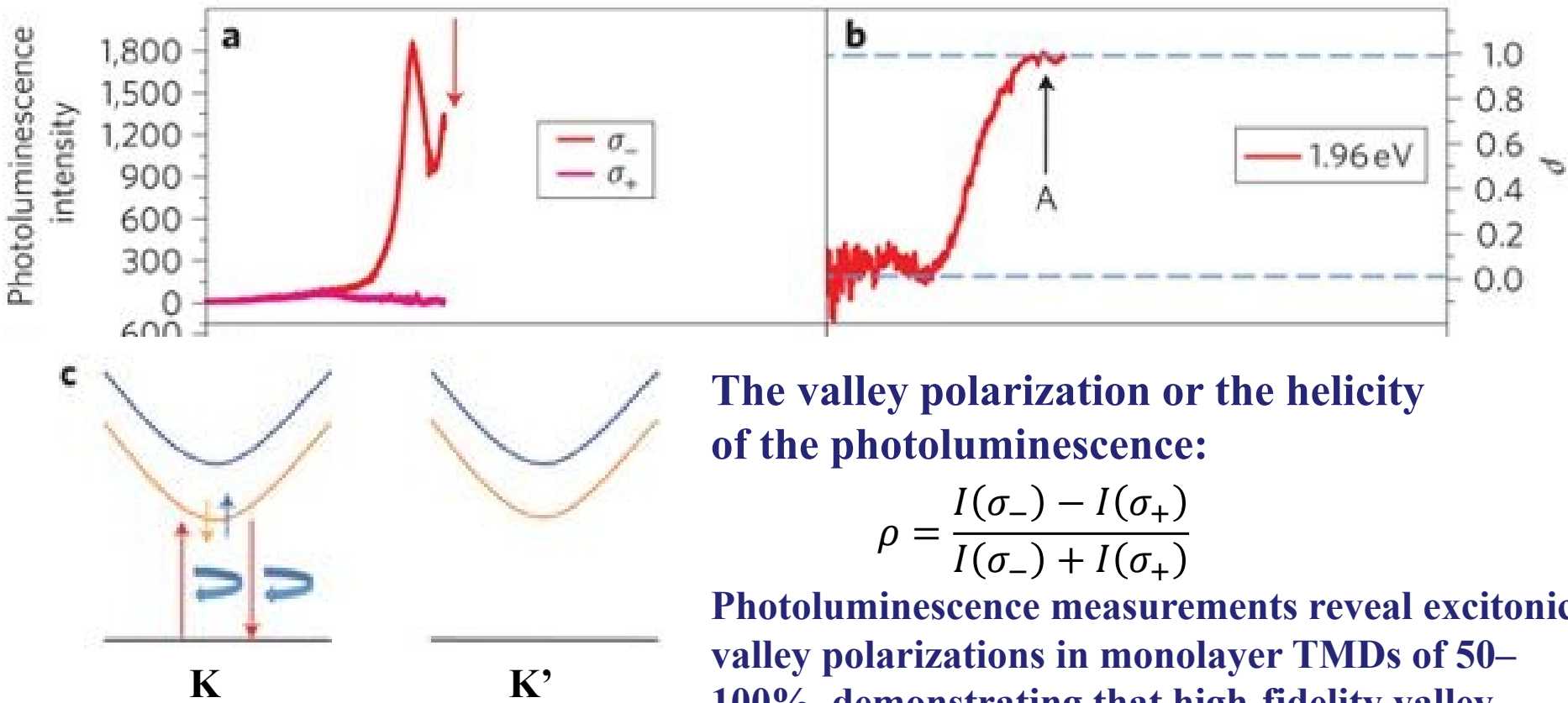


$\sigma+$ Right-handed/clockwise circularly polarized light



- Linear polarization: electric field of light is confined to a single plane along the direction of propagation.
- Circular polarization: electric field of the light has a constant magnitude but its direction rotates at a constant rate in a plane perpendicular to direction of propagation
- Circular polarized can be viewed as the superposition of two linearly polarized waves with 90° phase shift.

Control of valley polarization in monolayer MoS₂ by optical helicity



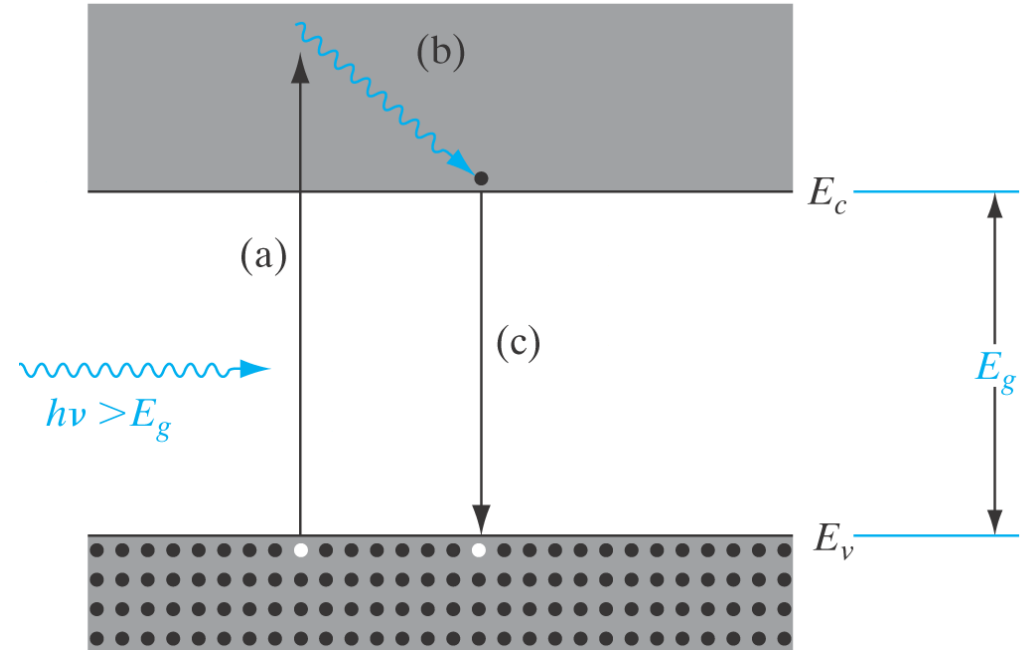
Kin Fai Mak, Tony F. Heinz, Nature Nanotechnology, 7, 494, 2012

Outline

- Introduction of TMDs
 - Synthesis of TMDs
 - Electronic properties and electronic devices
 - Optical properties and photonic devices
 - Optical properties
 - Photonic devices
-  • Photodetectors
 - Solar cells
 - Light emitting diodes (LEDs)
 - Lasers

Review: Photoconductivity

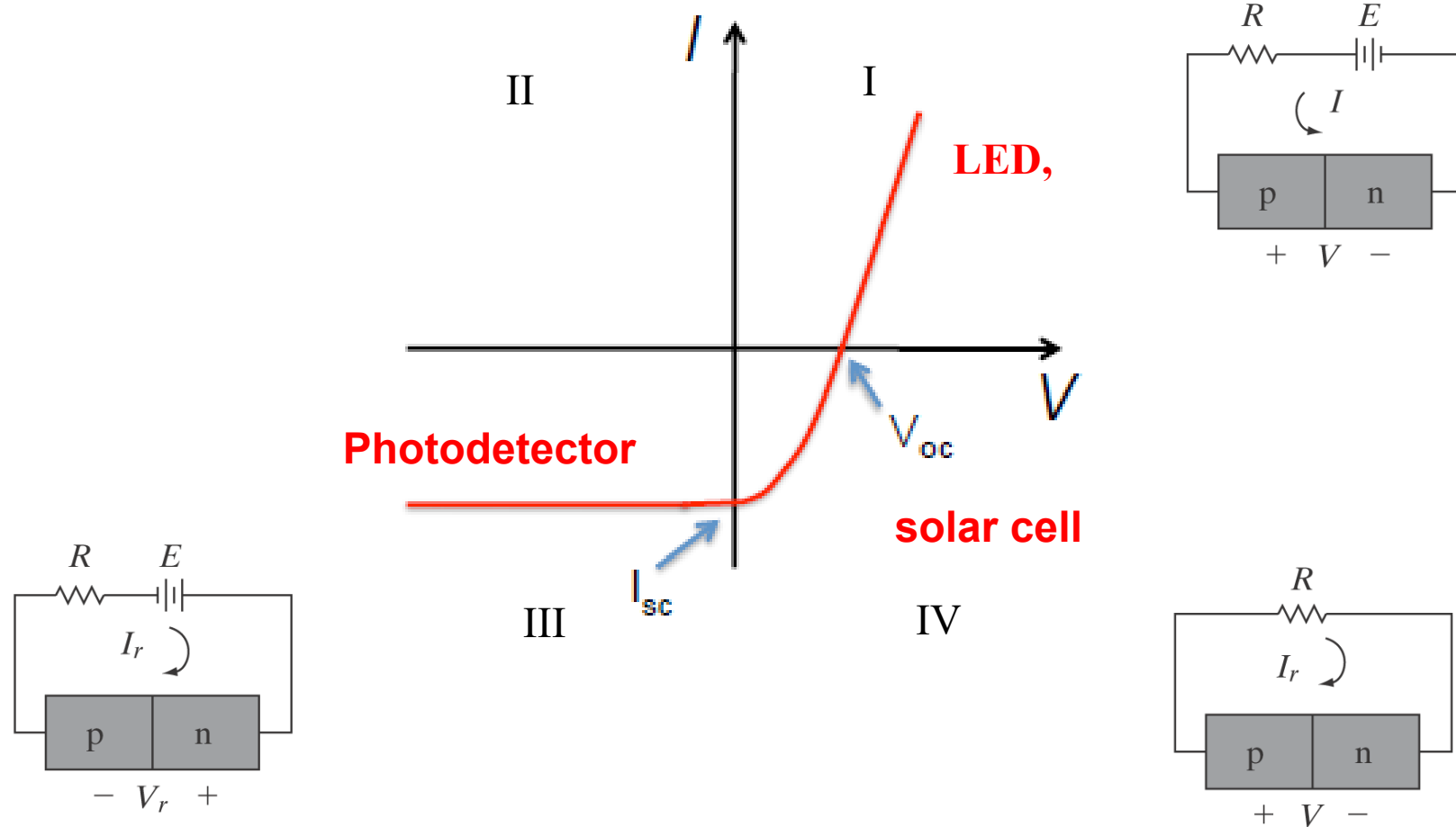
- If $h\nu \geq E_g$,
photon can be
absorbed, and EHP is
generated.
- Photoconductivity is
the conductivity
change due to the
light:



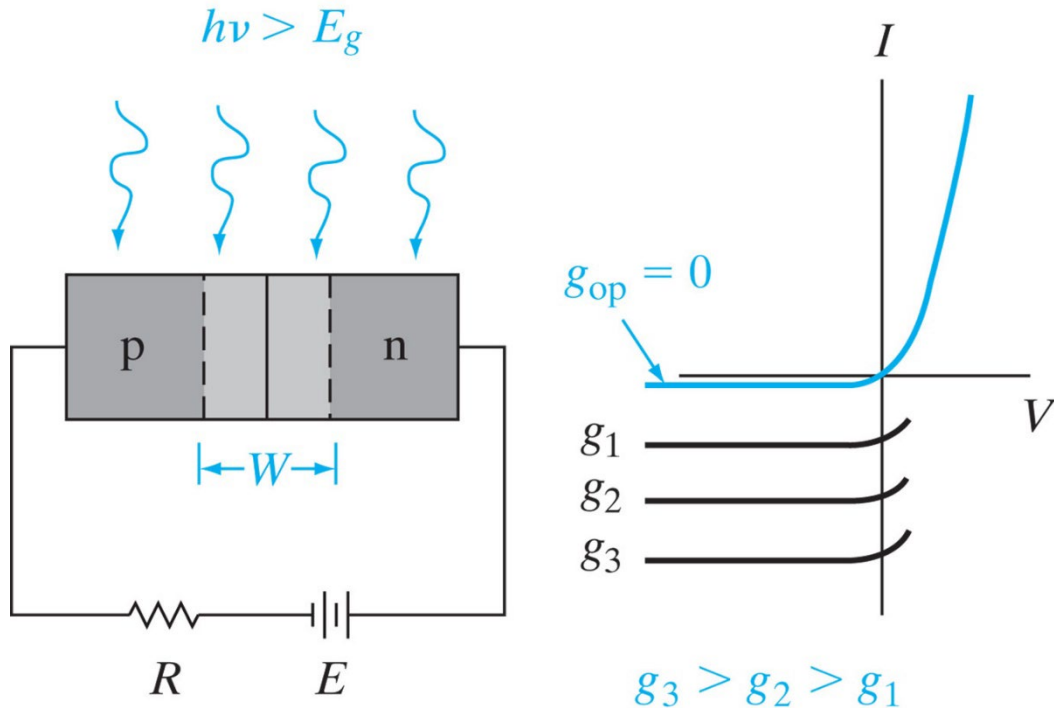
$$\Delta\sigma = \sigma - \sigma_0 = q(\delta n \mu_n + \delta p \mu_p)$$

With light Without light

Optoelectronic devices based on pn junction



Review: photodetectors base on pn junction



- Convert light to electric signal.
- Operate in reverse bias, 3rd quadrant.
- The current is Independent of voltage and proportional to the optical generation rate.

- The total reverse current with illumination

$$I = I_{th} (e^{qV/kT} - 1) - I_{op}$$

Figure-of-Merit for photodetectors

- Internal quantum efficiency: $\frac{\text{number of carriers collected}}{\text{number of absorbed photons}}$

$$\eta_{in} = \frac{J_{op}/q}{P_{obs}/h\nu}$$

- External quantum efficiency: $\frac{\text{number of carriers collected}}{\text{number of incident photons}}$

$$\eta_{ext} = \frac{J_{op}/q}{P_{in}/h\nu}$$

- Maximum response frequency

$$f_{max} \approx \frac{1}{\text{transit time}} \approx \frac{1}{W/V_{sat}} = \frac{V_{sat}}{W}$$

- Responsivity:

$$R = \frac{I_{op}}{P_{in}} = \frac{q\eta_{ext}}{h\nu}$$

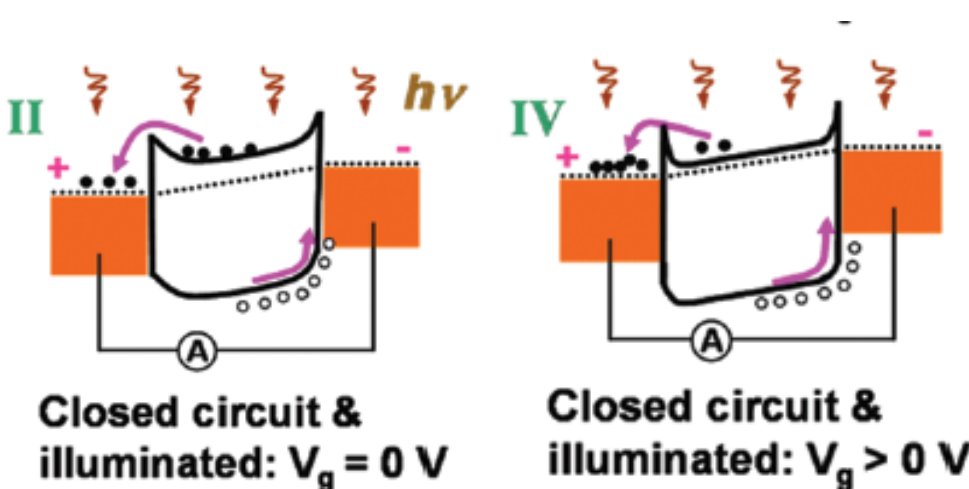
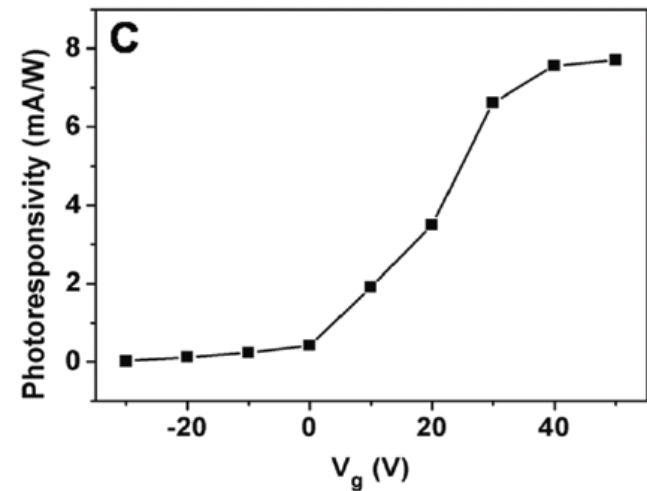
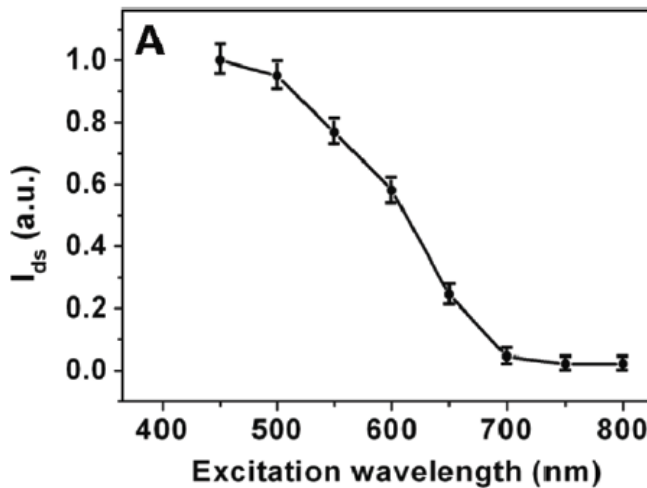
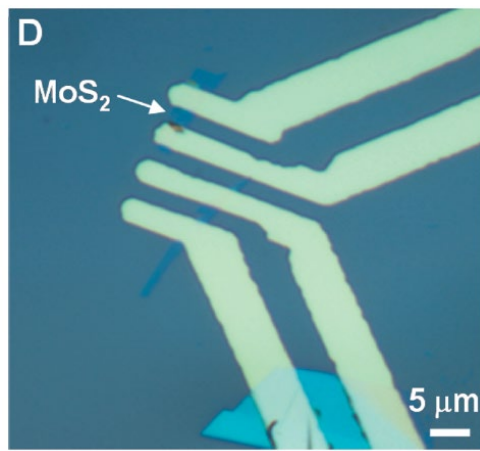
Photodetectors based on TMDs

- Graphene photodetectors are being envisaged for applications in high-speed optical communications and long-wavelength (e.g. terahertz and mid infrared) detection.
- TMDs are advantageous for applications that require high sensitivity and low dark current. TMD photodetectors work mainly in the visible and near infrared spectral regions.

Three groups of TMD-based photodetectors have been investigated:

- Lateral metal–TMD–metal detectors
- Hybrid devices with sensitizing centers
- Van der Waals heterostructure devices

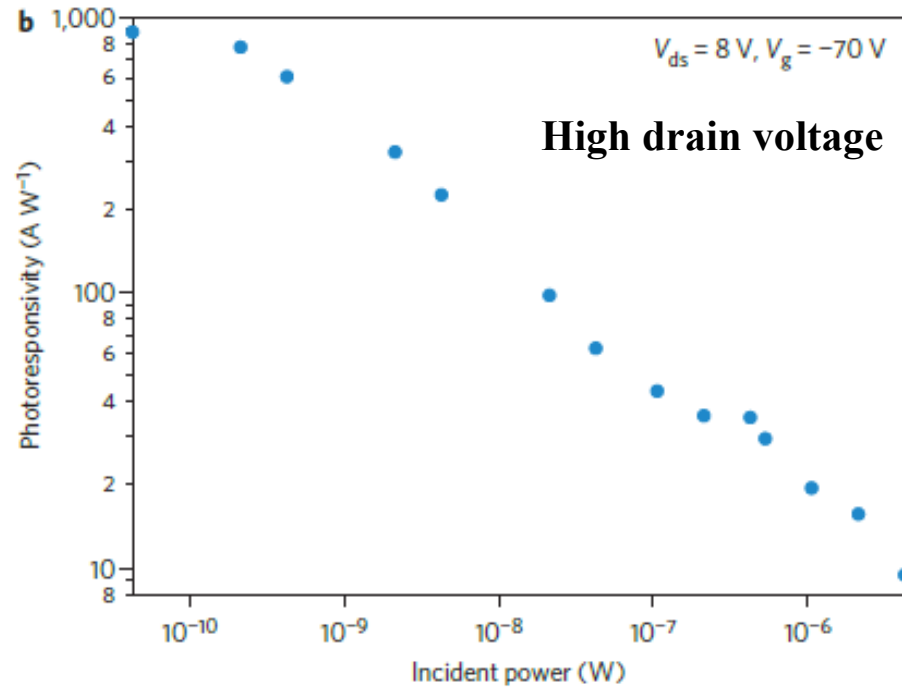
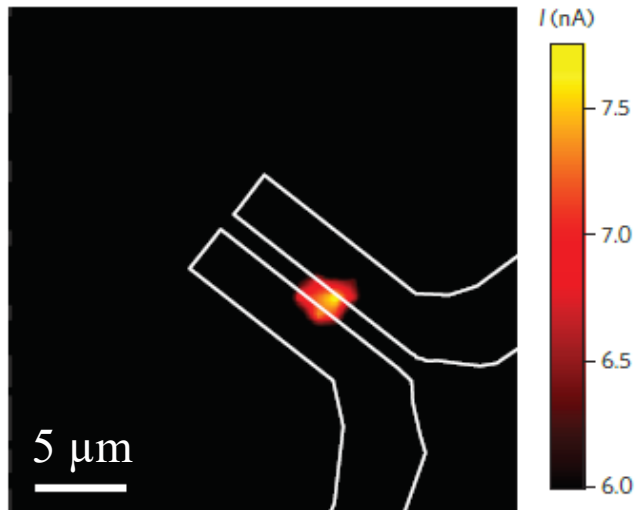
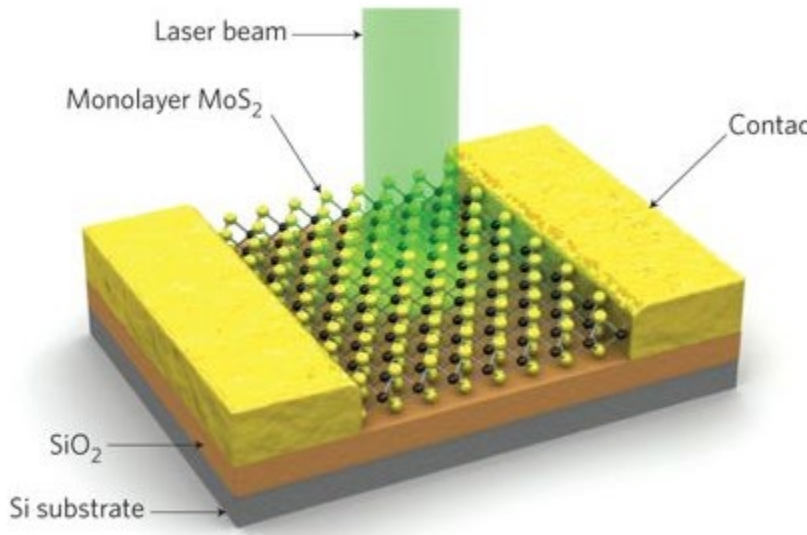
Single-layer MoS₂ photodetector



- Photodetector based on exfoliated single-layer MoS₂ were demonstrated.
- The photoresponsitivity reaches 7.5 mA/W at the gate voltage of ~ 50 V, proving that the back gate plays an important role in tailoring the photocurrent in the n-type single-layer MoS₂ phototransistor.

Z. Yin, ACS Nano, 6, 74, (2012)

TMD–metal photodetectors

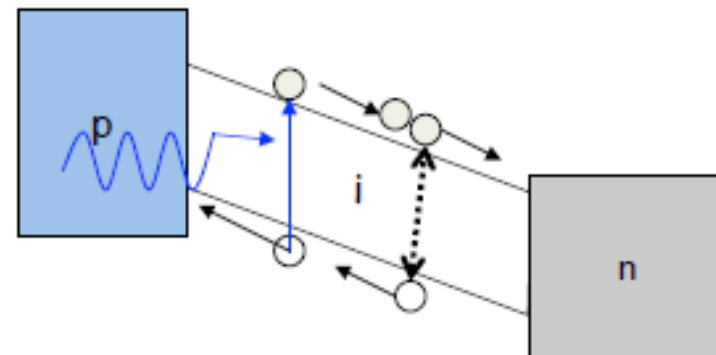
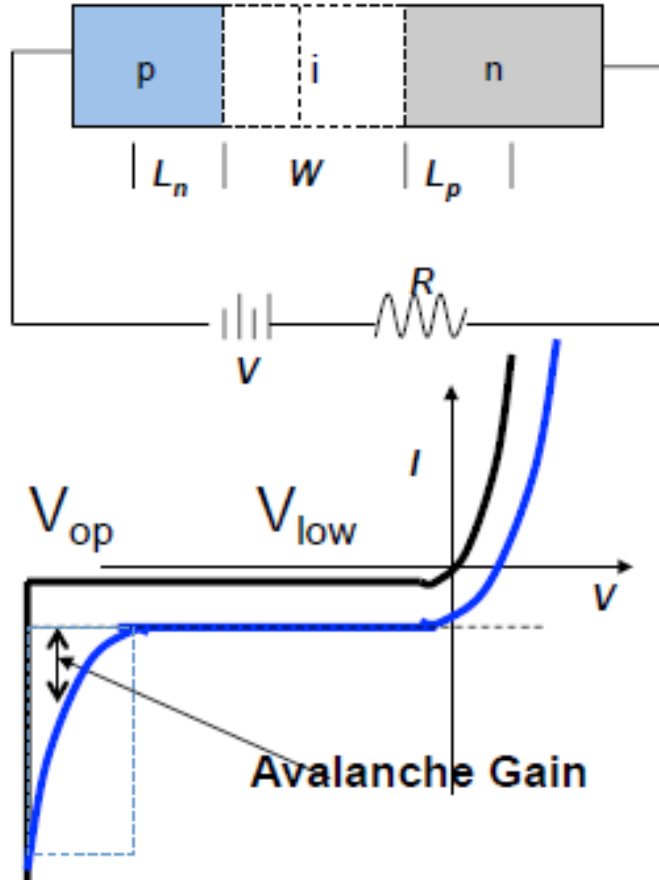


- Monolayer MoS₂ phototransistors was demonstrated. The devices show a maximum external photoresponsivity of 880 AW^{-1} at a wavelength of 561 nm and a photoresponse in the 400–680 nm range.

Oriol Lopez-Sanchez, Andras Kis, et.al., Nature Nanotechnology, 8, 497, 2013

Avalanche Photodiodes

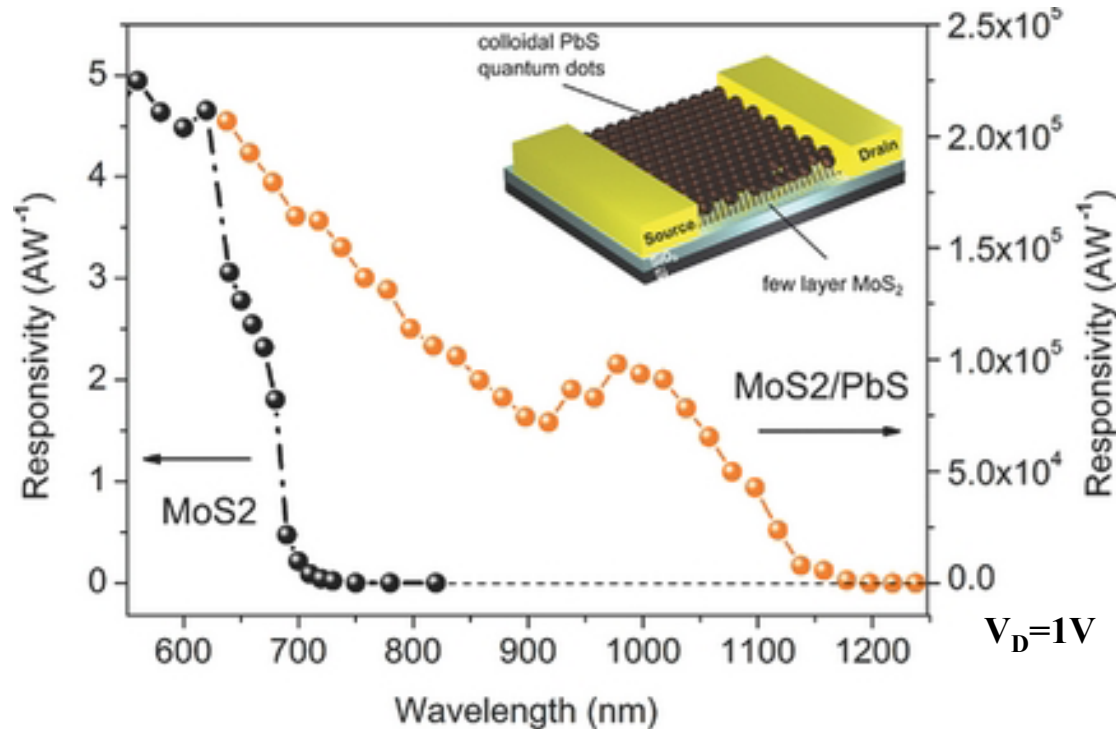
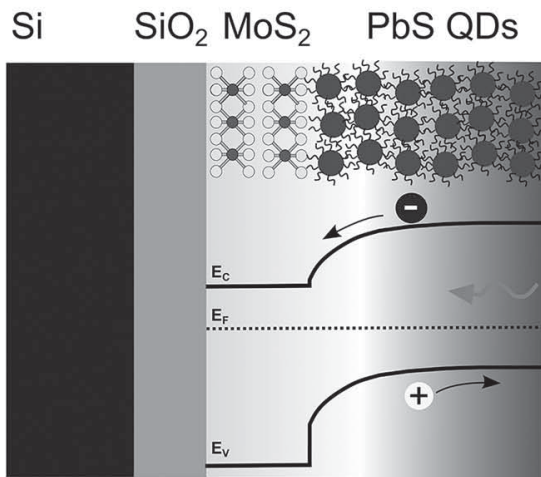
An electron or a hole with high energy in “i” layer can break chemical or ionic bonds in crystal to create an EHP



- An avalanche photodiode (APD) is operated under a reverse-bias voltage that is sufficient to enable avalanche multiplication
- An electron or a hole with high energy in the “i” layer can break chemical or ionic bonds in crystal to create an EHP
- The multiplication results in internal current gain

$$\text{Gain} \equiv \frac{(I_p - I_d)_{V_{op}}}{(I_p - I_d)_{V_{low}}}$$

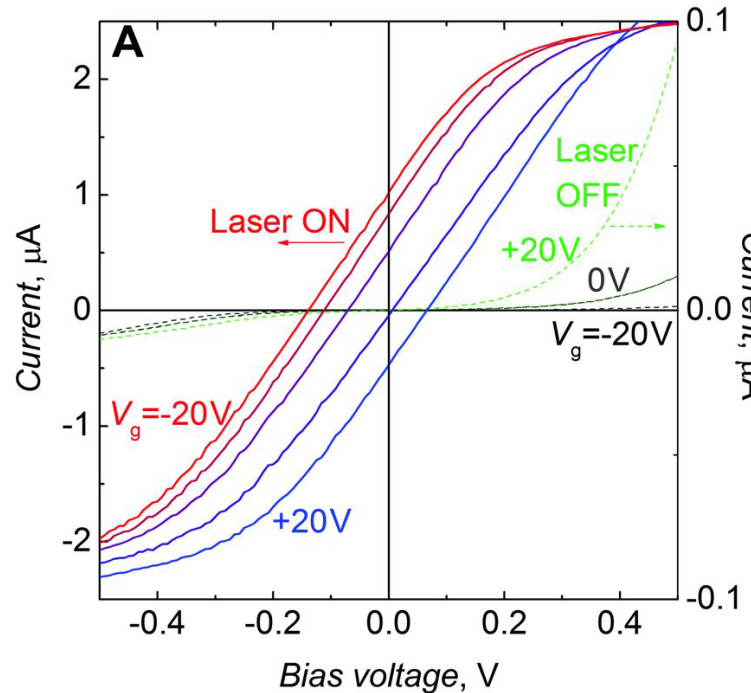
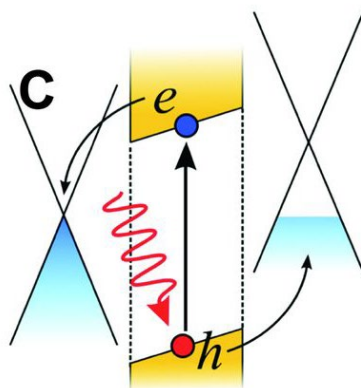
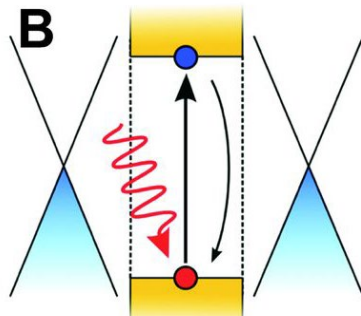
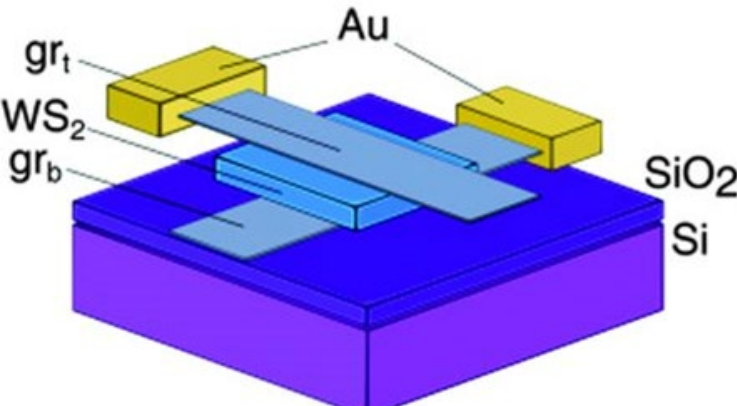
Hybrid devices with sensitizing centers



- Photogain can be accomplished by integration of 2D semiconductors with other materials to produce a hybrid phototransistor.
- Light absorption in the PbS quantum dots leads to charge transfer to MoS_2 .
- The hybrid $\text{PbS}-\text{MoS}_2$ detector showed a responsivity of up to 10^6 A/W , and a low dark current which resulted in a high detectivity.

Dominik Kufer, Gerasimos Konstantatos, et.al., Advanced Materials, 27, 176, 2015

Heterostructure photodetectors

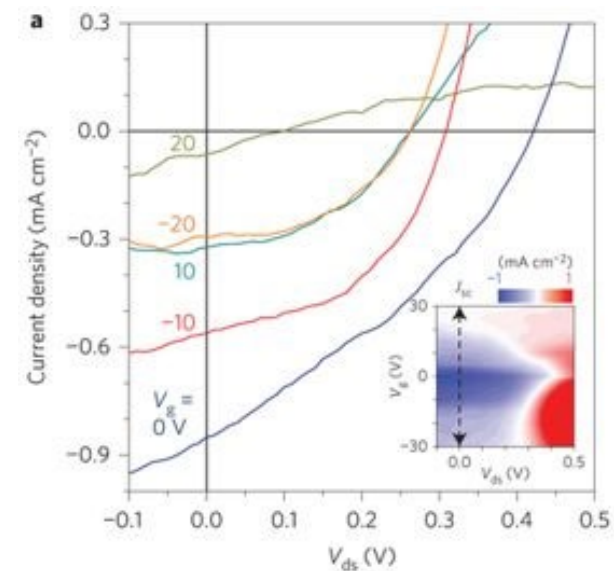
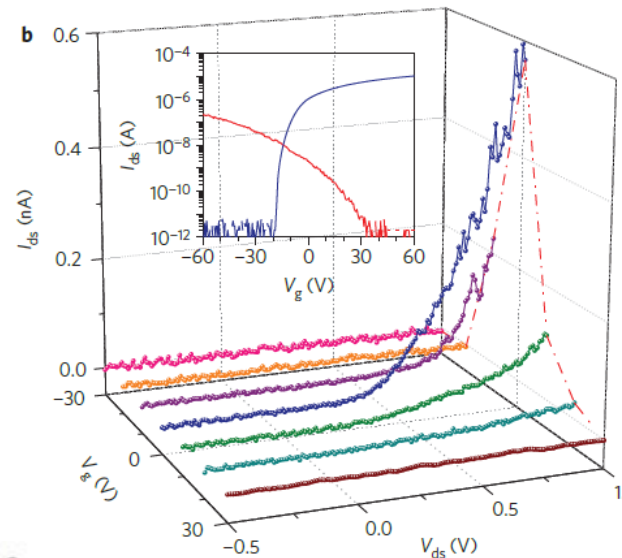
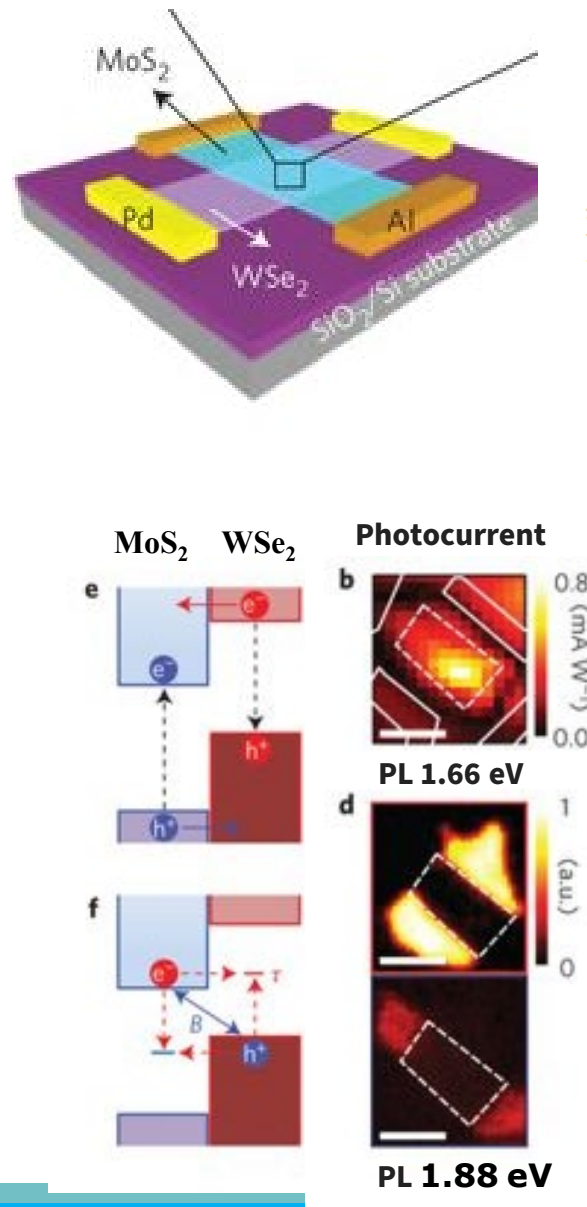


- Heterostructure photodetectors, comprising vertical stacks of graphene–TMD–graphene layers, have been demonstrated.
- In these devices, graphene was employed as a work function-tunable electrode, whereas a TMD semiconductor was utilized as a photoactive material, showing strong light–matter interactions and photon absorption.

Photoresponsivity > 0.1 A/W (i.e., external quantum efficiency > 30%).

L. Britnell, K. S. Novoselov, Science, 340, 1311, 2013

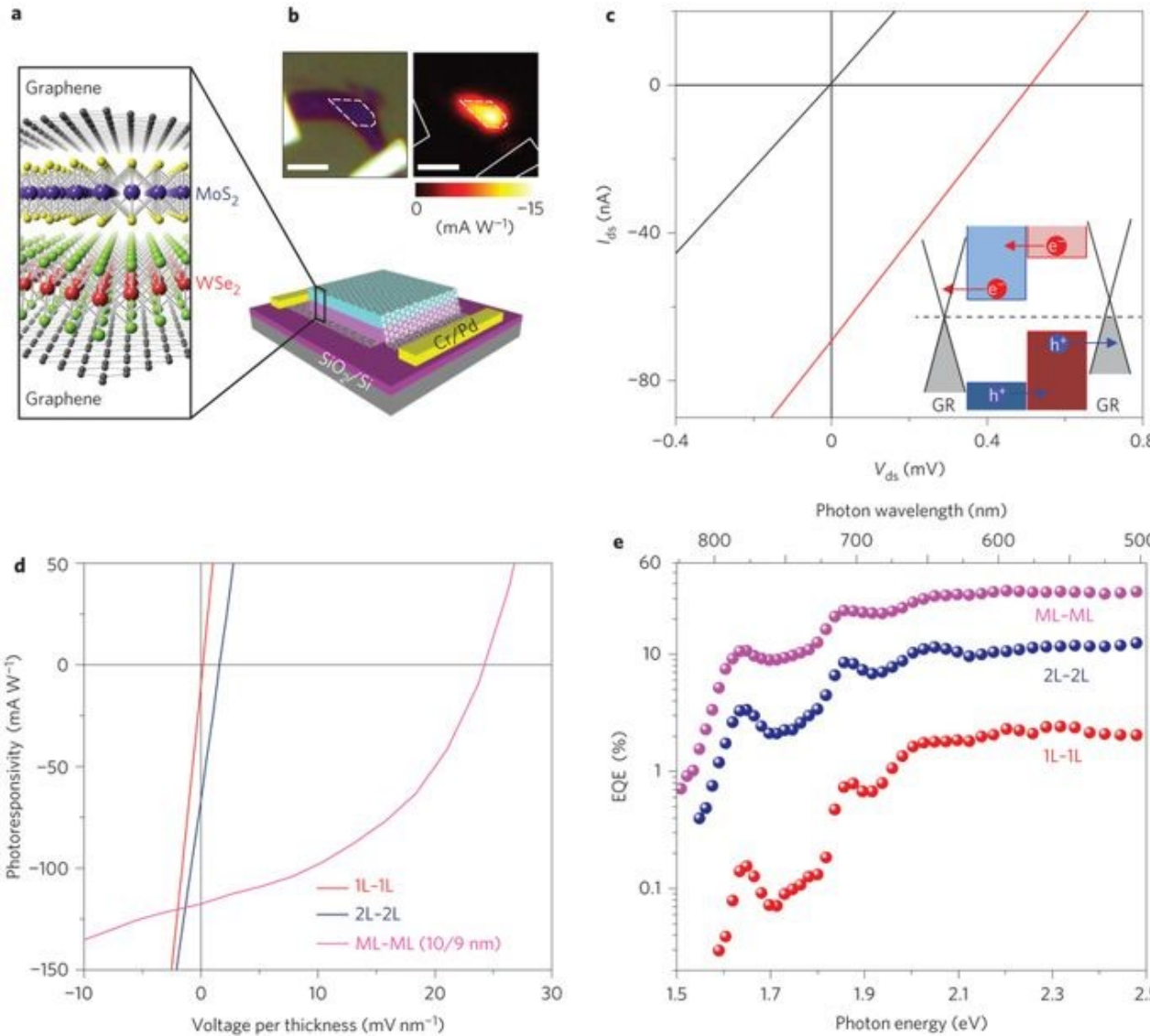
TMD heterostructure photodetector



- Gate-tunable diode-like current rectification and a photovoltaic response across the p–n interface was observed.
- The strongest photoresponse is observed in the $\text{MoS}_2/\text{WSe}_2$ junction area, indicating spontaneous charge separation occurring at the junction.

Chul-Ho Lee, Philip Kim, et.al, Nature Nanotechnology, 9, 676, 2014

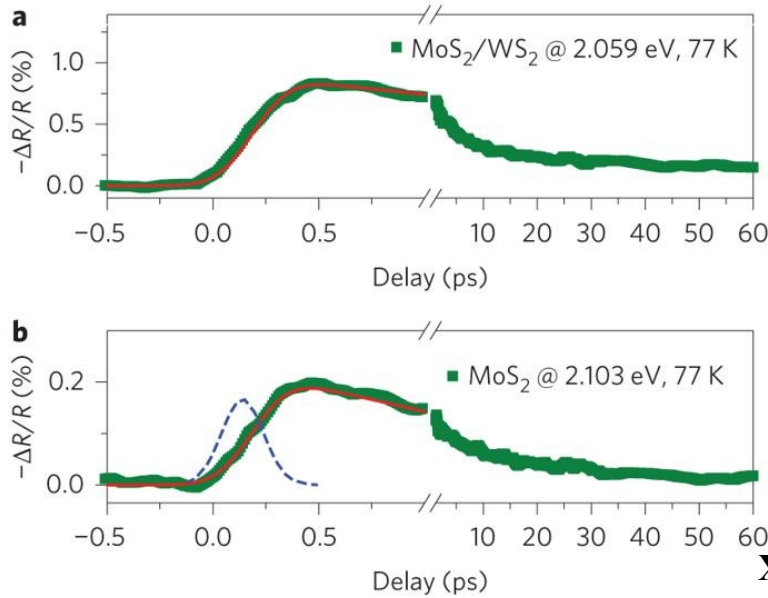
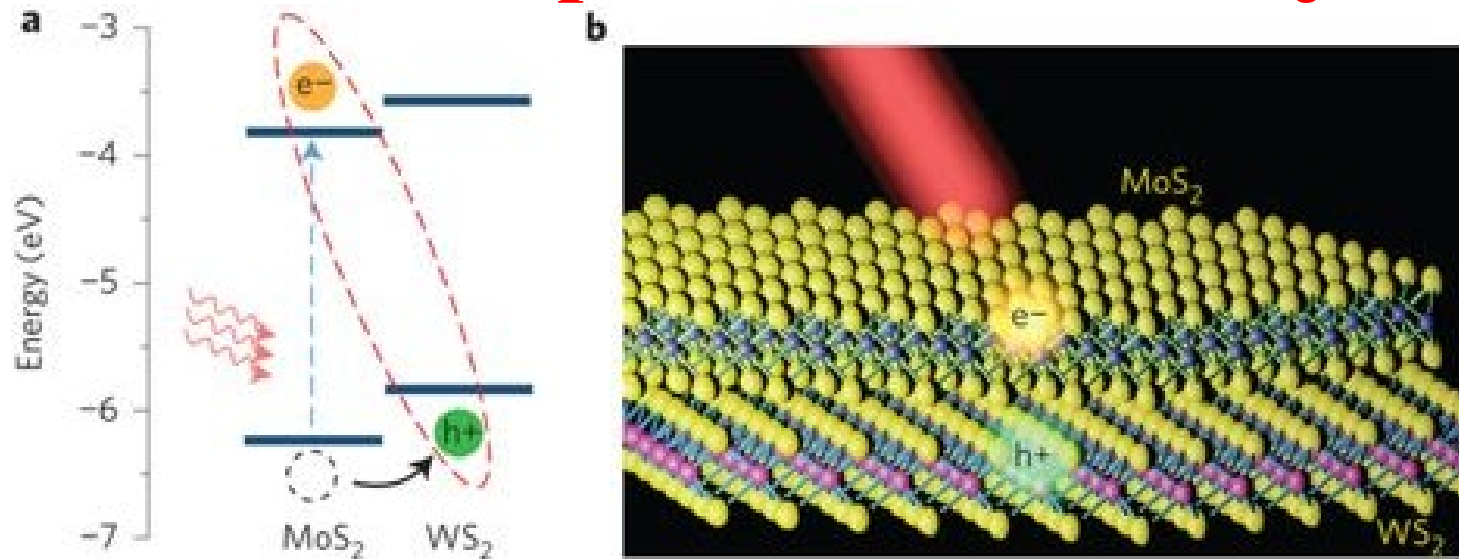
Graphene/TMD heterostructure photodetector



- Sandwiching an atomic TMD p–n junction between graphene layers enhances the collection of the photoexcited carriers.

Chul-Ho Lee, Philip Kim, et.al, Nature Nanotechnology, 9, 676, 2014

Photocarrier separation at heterojunction



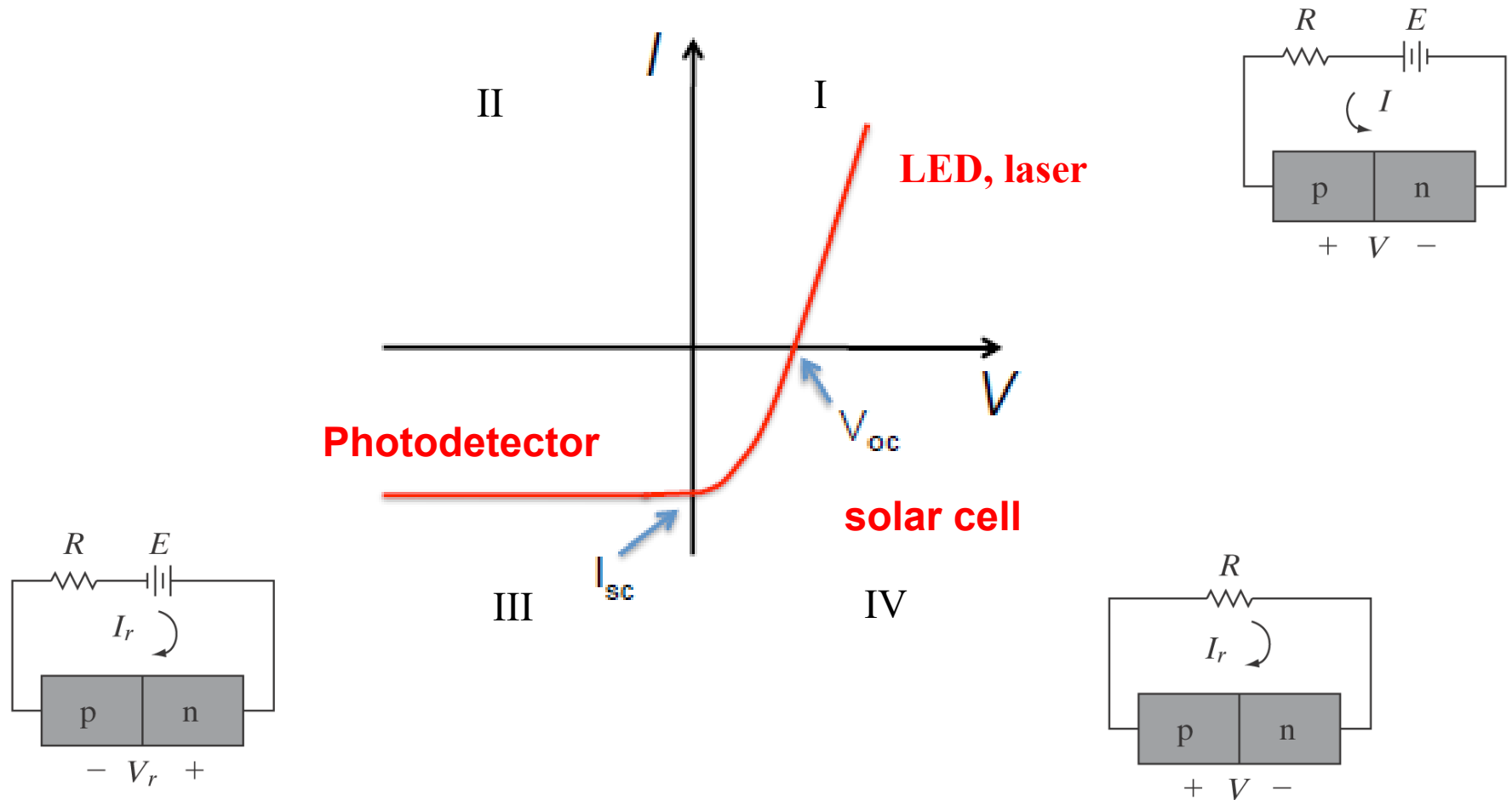
- Stacked TMD heterostructures form type II semiconductor heterojunctions that facilitate efficient electron–hole separation for light detection and harvesting.
- It was observed that hole transfer from the MoS₂ layer to the WS₂ layer takes place within 50 fs after optical excitation.

Xiaoping Hong, Feng Wang, et.al, Nature Nanotechnology, 9, 682, 2014

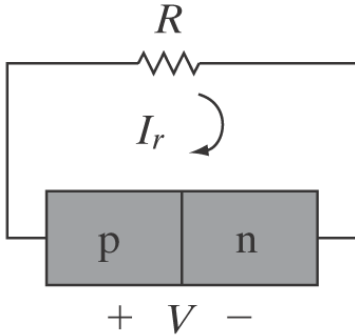
Outline

- Introduction of TMDs
- Synthesis of TMDs
- Electronic properties and electronic devices
- Optical properties and photonic devices
 - Optical properties
 - Photonic devices
 - Photodetectors
 - Solar cells
 - Light emitting diodes (LEDs)
 - Lasers

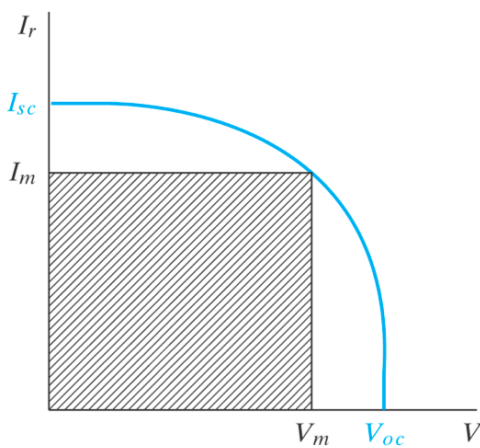
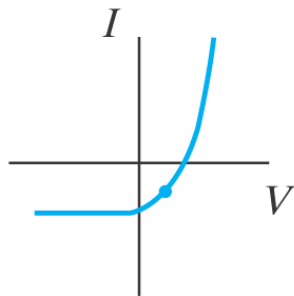
Optoelectronic devices based on pn junction



Review: solar cell



4th quadrant



- Maximum power delivered to a load by the solar cell occurs when VI_r is maximum:

$$P_m = I_m V_m$$

- Fill factor:

$$FF = \frac{I_m V_m}{I_{sc} V_{oc}}$$

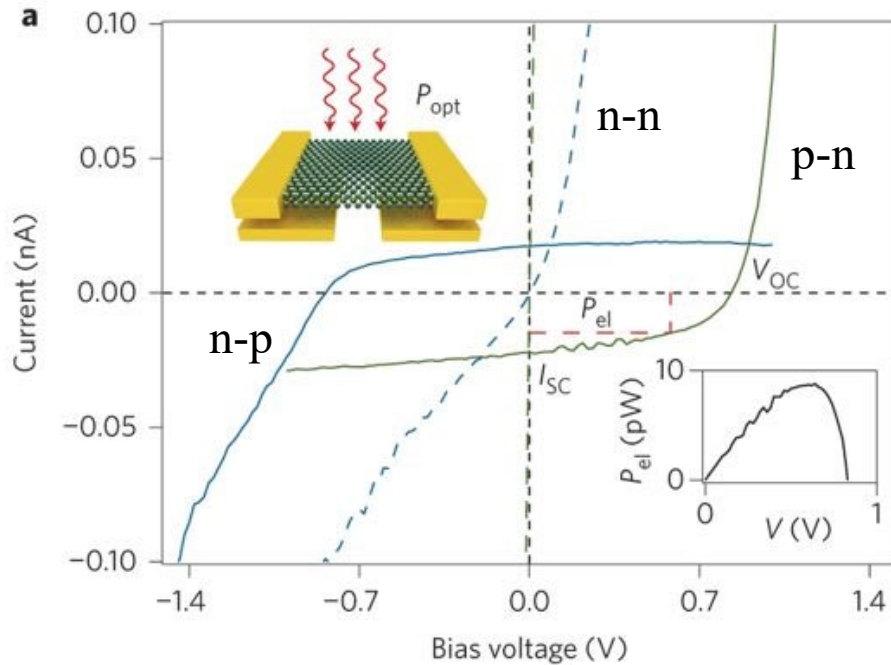
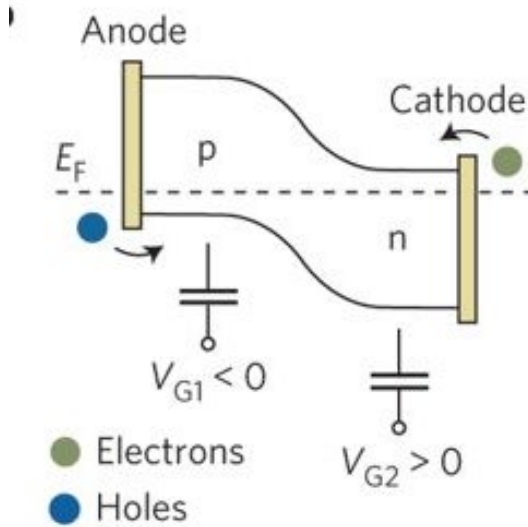
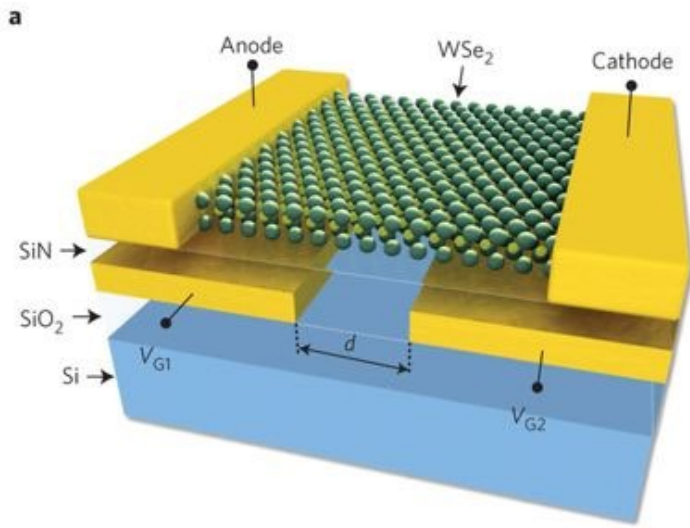
- Efficiency:

$$\eta = \frac{P_m}{P_{in}} = \frac{I_{sc} V_{oc} FF}{P_{in}}$$

Solar cells based on TMDs

- Solar cells (photovoltaic cells) allow the conversion of sun energy into electricity.
- Abundance of source materials, chemical stability, environmental sustainability, and low cost of production are essential requirements for solar cells.
- Typical structures of solar cells based on 2D TMDs:
 - Lateral p–n and Schottky Junctions
 - 2D van der Waals Heterostructures

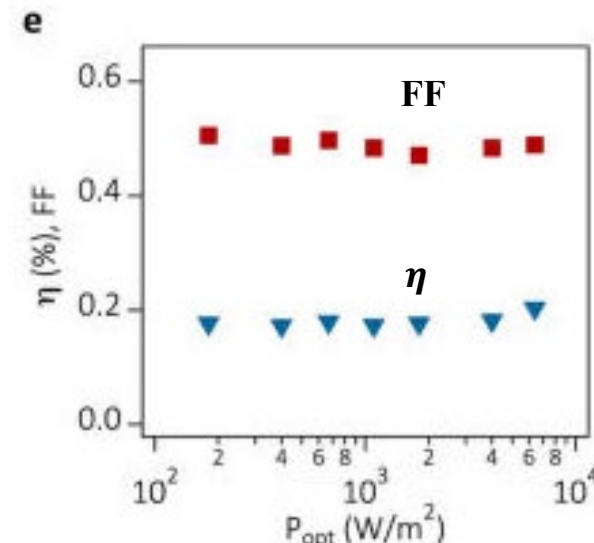
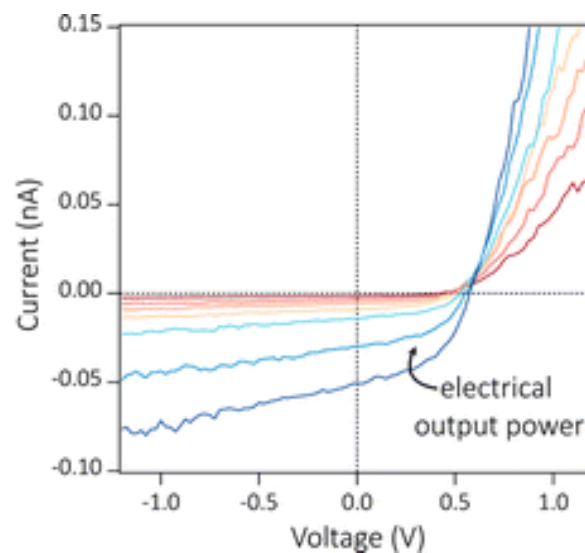
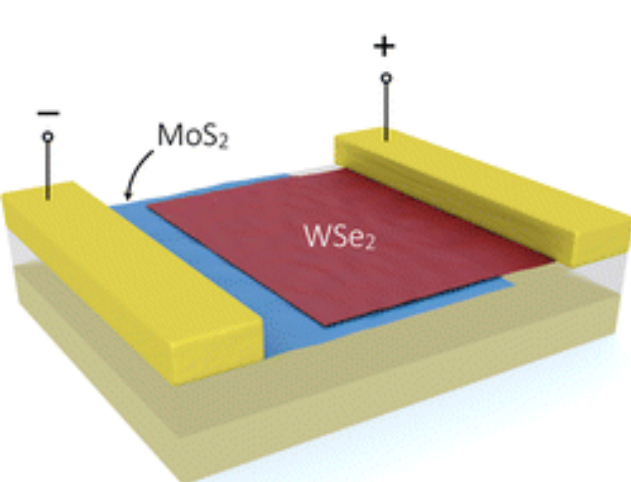
Lateral p–n solar cell



- The authors fabricated a p–n junction diode based on an electrostatically doped WSe₂ monolayer.
- This device can serve as a photovoltaic solar cell, a photodiode and a light-emitting diode, This device has light–power conversion and electroluminescence efficiencies of ~0.5% and ~0.1%, respectively.

Andreas Pospischil, Thomas Mueller, et.al., Nature Nanotechnology, Vol. 9, 257, 2014

TMD heterostructure solar cells



- A type-II van der Waals heterojunction was made of molybdenum disulfide and tungsten diselenide monolayers. The junction is electrically tunable, and under appropriate gate bias an atomically thin diode is realized.
- Upon optical illumination, charge transfer occurs across the planar interface and the device exhibits a photovoltaic effect.

Marco M. Furchi, Thomas Mueller, et.al., Nano Letters, 14, pp 4785, 2014

Outline

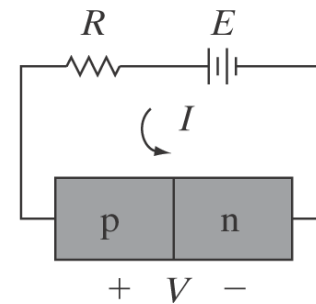
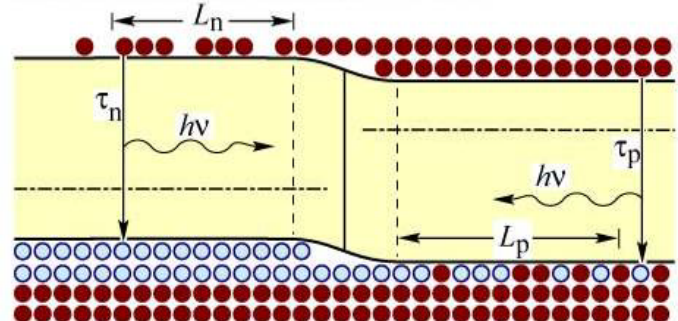
- Introduction of TMDs
- Synthesis of TMDs
- Electronic properties and electronic devices
- Optical properties and photonic devices
 - Optical properties
 - Photonic devices
 - Photodetectors
 - Solar cells
 - Light emitting diodes (LEDs)
 - Lasers



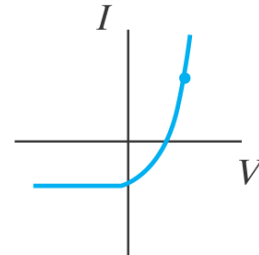
Review: Light-emitting diode

- Forward bias pn junction
- Minority & majority carriers recombine and emit light
- Operate in 1st quadrant
- Emitted light energy

$$h\nu_{out} = E_g$$

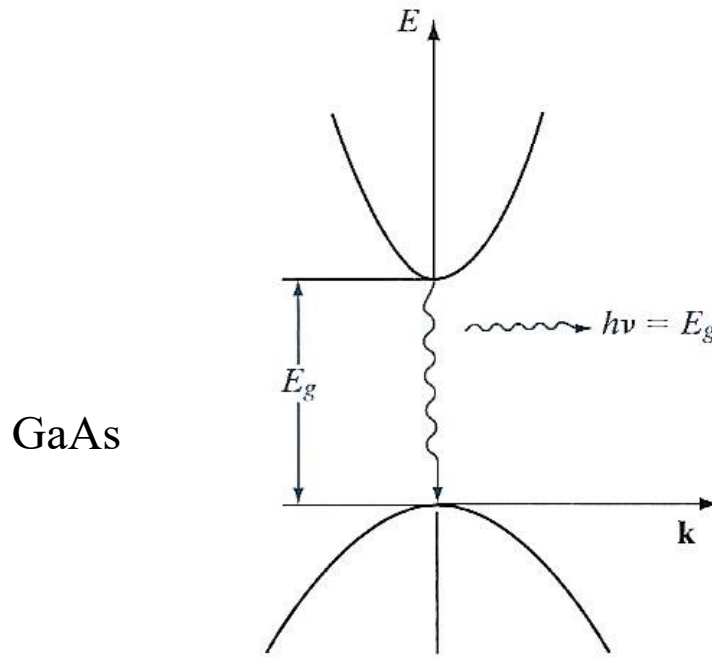


1st quadrant

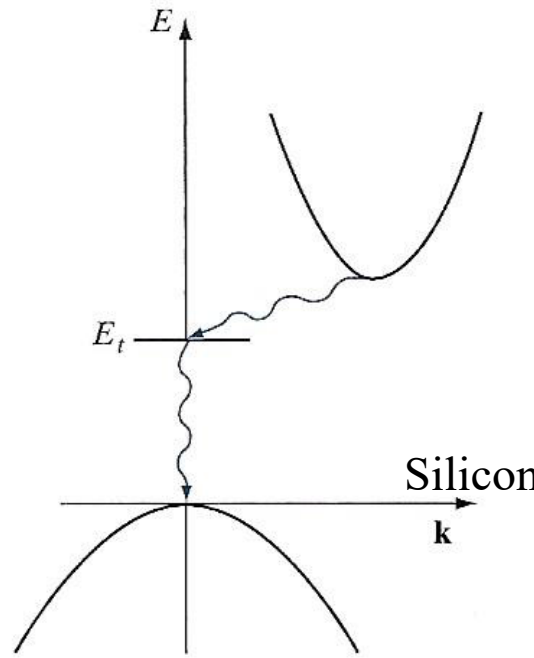


Review: Direct and indirect band gap

Direct band gap

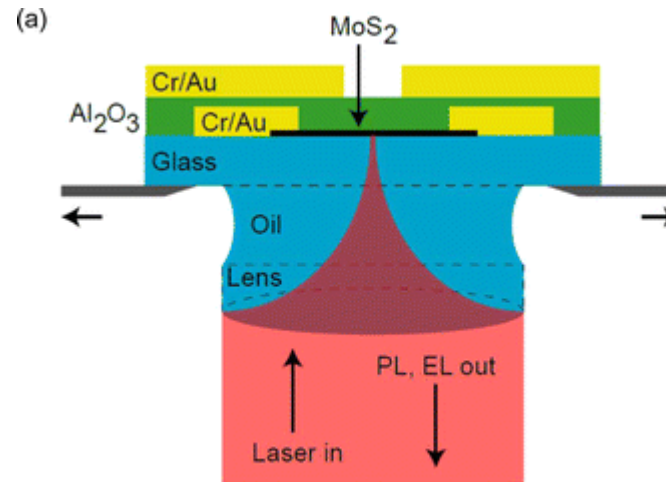
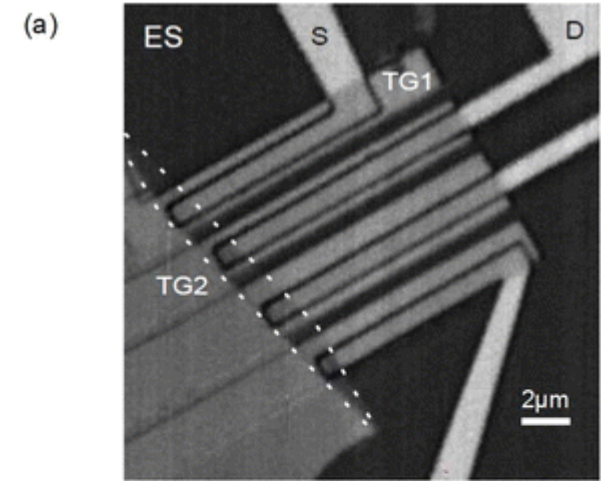
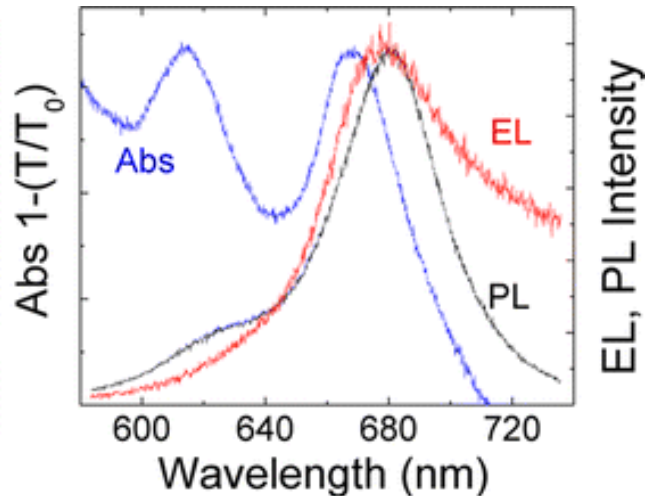
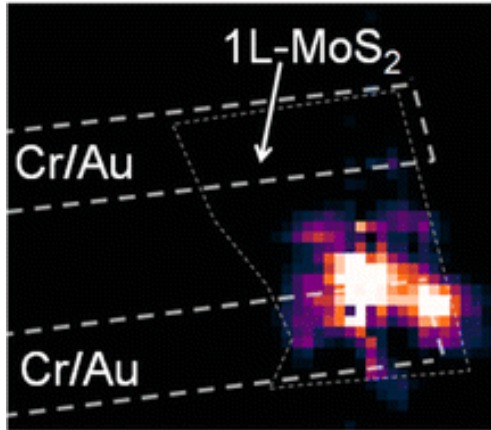


Indirect band gap



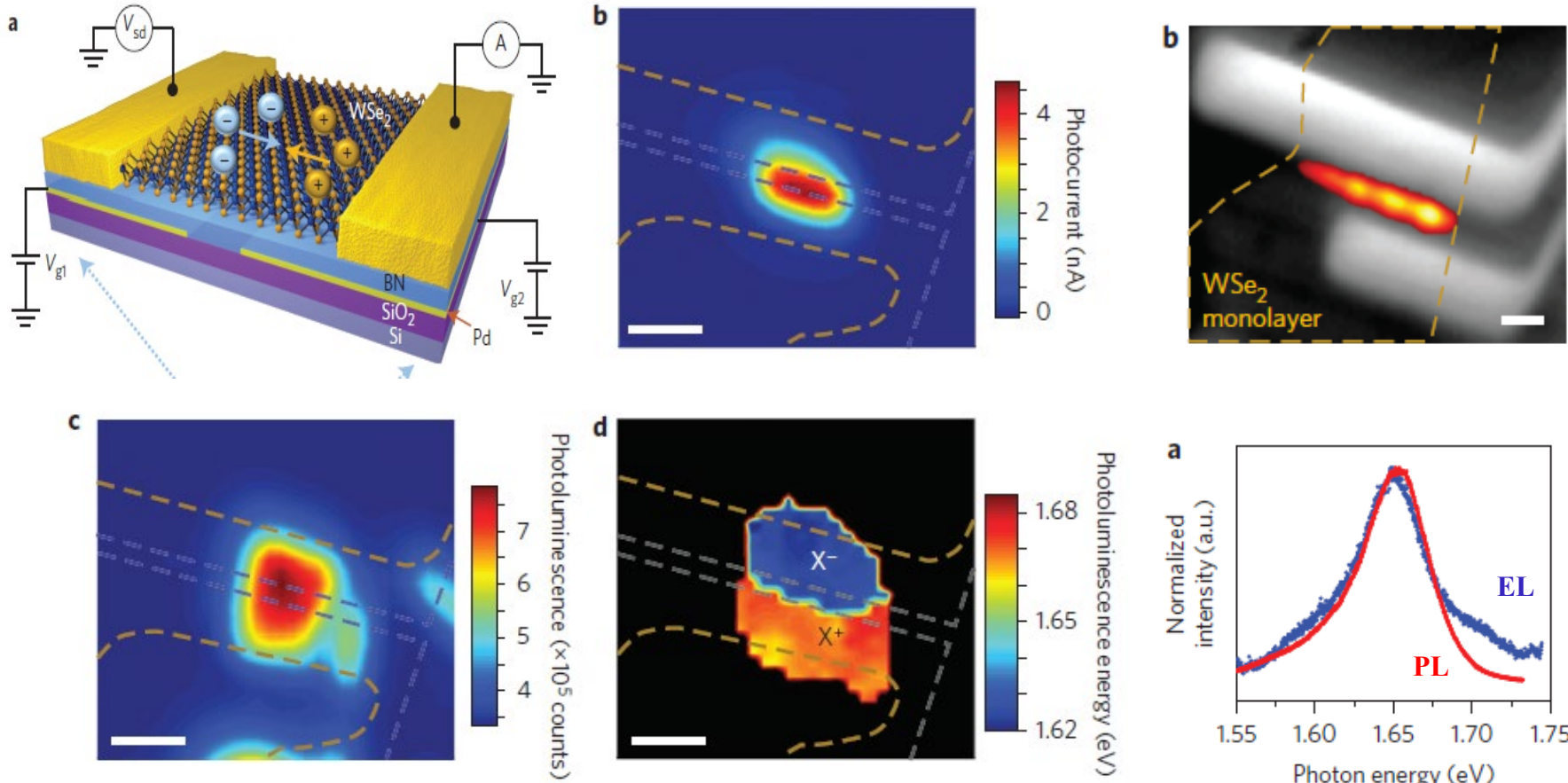
- **Direct band gap:** minimum in the conduction band and maximum of valence band occurs at the same k value. **Indirect band gap:** minimum in the conduction band and maximum of valence band occurs at the different k value
- For light emission, the material need to be direct band gap.

Hot-Carrier Electroluminescence



R. Sundaram, Nano Lett. 14(16), 2013

LED based on WSe₂ pn junction



- Electroluminescence from lateral p–n junctions in monolayer WSe₂ was induced electrostatically using multiple metal gates beneath.
- This structure yields bright electroluminescence with 1,000 times smaller injection current and 10 times smaller linewidth than in MoS₂.

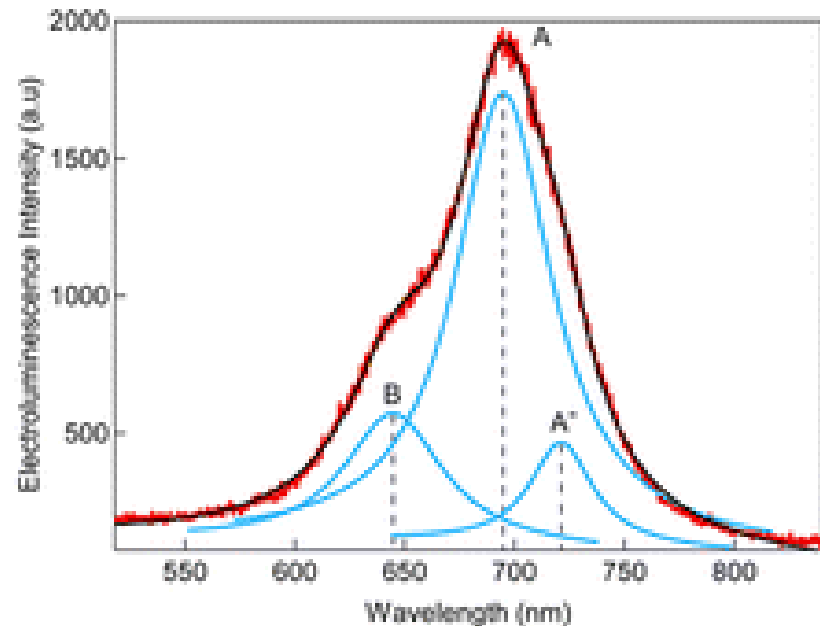
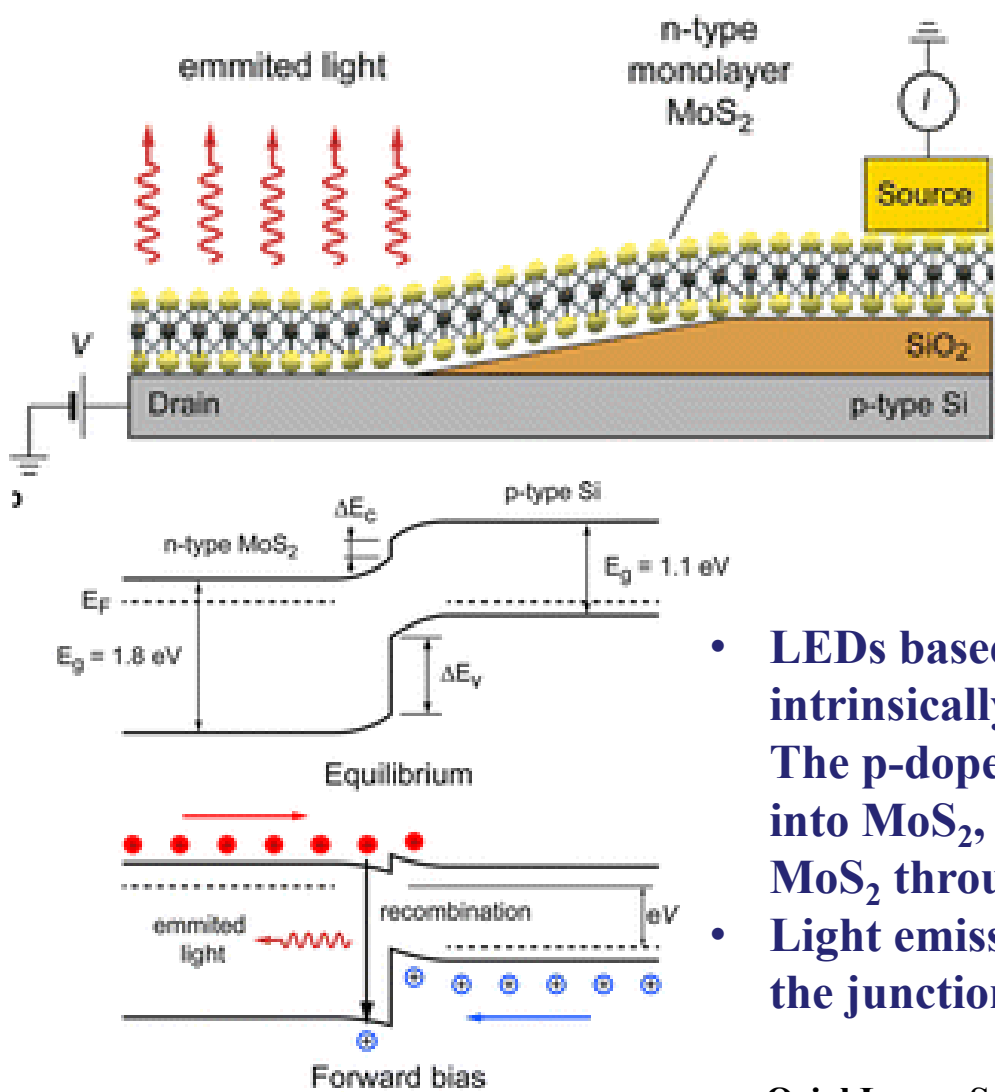
Jason S. Ross, Xiaodong Xu, at.al., Nature Nanotechnology, 9, 268, 2014

Vertical heterostructures for optoelectronic devices

The vertical heterostructure design allows the performance to be improved in several respects:

- reduced contact resistance due to the larger contact area
- higher current densities which allows for brighter emission
- luminescence from the whole device area
- easier scalability

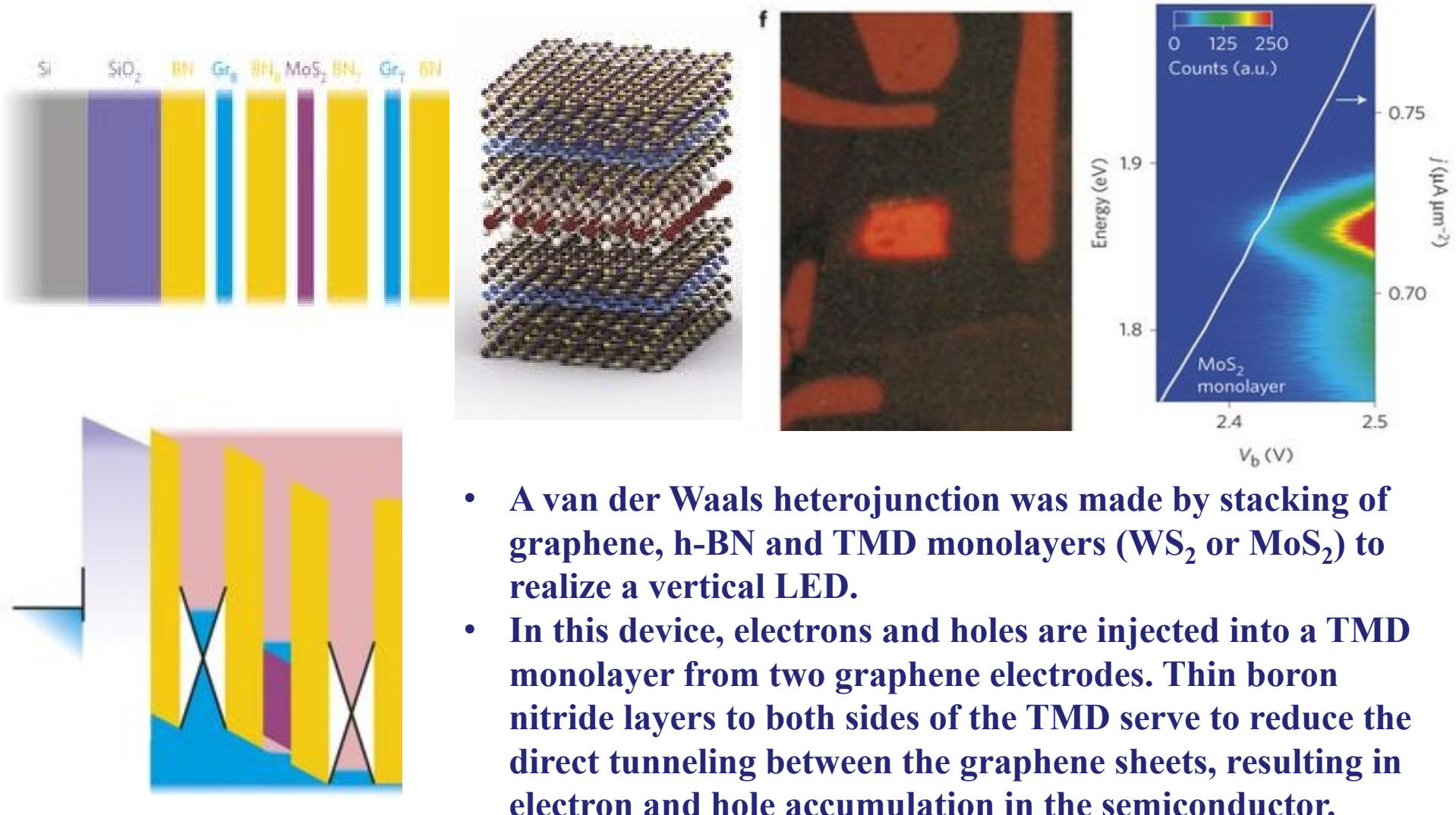
LED based on 2D/3D heterostructure



- LEDs based on a MoS₂ monolayer, which is intrinsically n-doped, and a p-doped silicon wafer. The p-doped silicon served as a hole injection layer into MoS₂, whereas electrons were injected into MoS₂ through a standard metal contact.
- Light emission occurred across the entire face of the junction.

Oriol Lopez-Sanchez, Andras Kis, et.al., ACS Nano, 8, 3042, 2014

LED based on 2D heterostructure



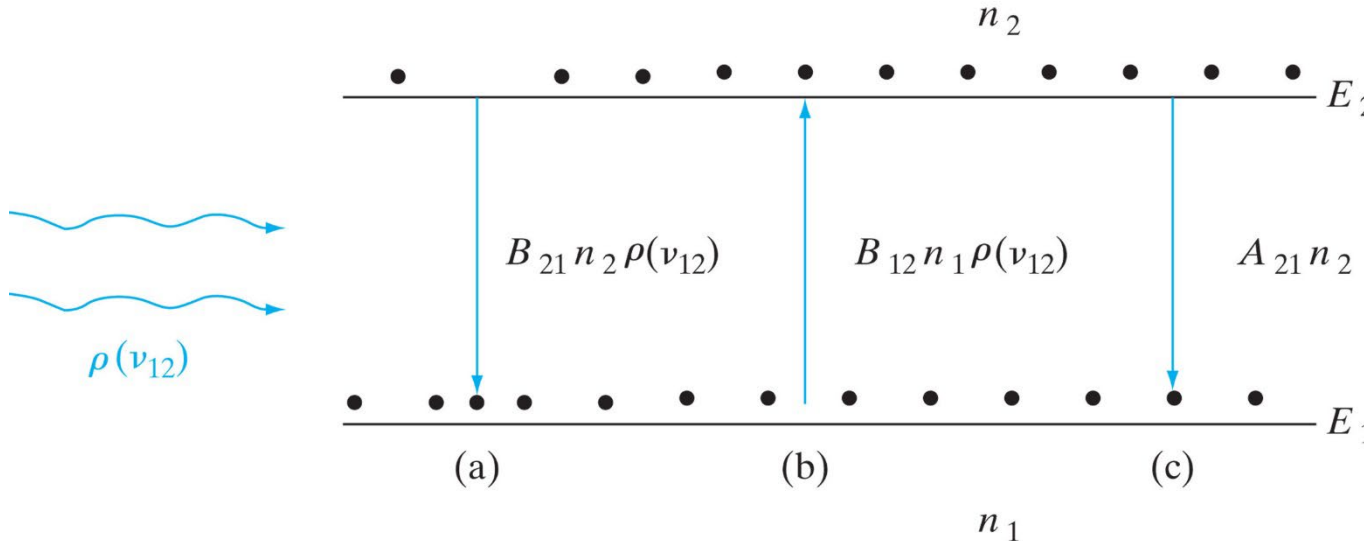
F. Withers, K. S. Novoselov, et.al., Nature Materials, 14, 301, 2015

Outline

- Introduction of TMDs
- Synthesis of TMDs
- Electronic properties and electronic devices
- Optical properties and photonic devices
 - Optical properties
 - Photonic devices
 - Photodetectors
 - Solar cells
 - Light emitting diodes (LEDs)
 - Lasers



Steady state condition



Copyright ©2015 Pearson Education, All Rights Reserved

In steady state, the emission rates must balance the absorption rate:

$$\frac{dn_2}{dt} \Big|_{abs} + \frac{dn_2}{dt} \Big|_{spont} + \frac{dn_2}{dt} \Big|_{stim} = 0 \quad \text{or}$$

$$B_{12} n_1 \rho(\nu_{12}) = A_{12} n_2 + B_{21} n_2 \rho(\nu_{12})$$

↓ ↓ ↓
Absorption spontaneous stimulated
emission emission emission

Condition for lasing

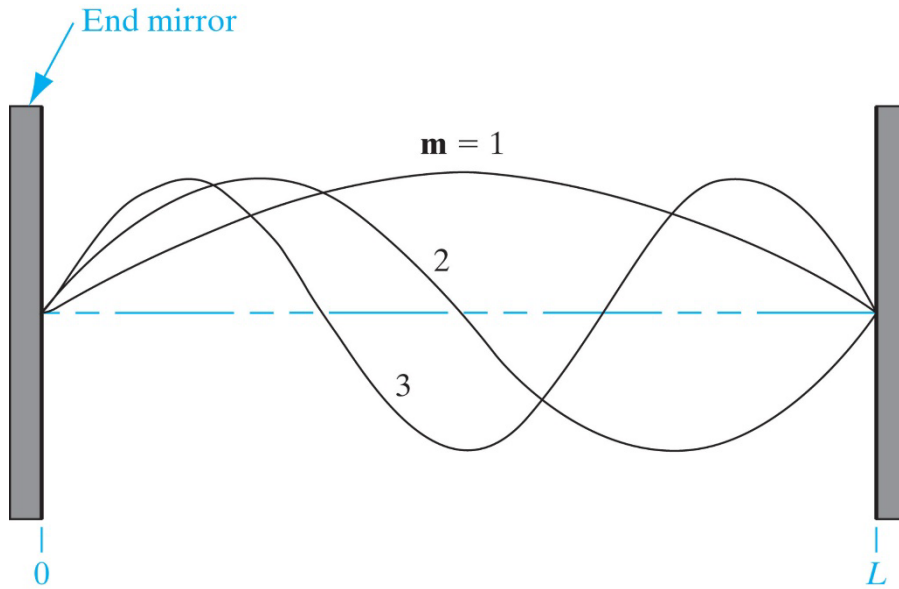
1.
$$\frac{\text{Stimulated emission rate}}{\text{Spontaneous emission rate}} = \frac{B_{21}n_2\rho(\nu_{12})}{A_{12}n_2} = \frac{B_{21}}{A_{12}}\rho(\nu_{12})$$

A large photon field energy density enhances the stimulated emission rate → use optical resonant cavity

2.
$$\frac{\text{Stimulated emission rate}}{\text{absorption rate}} = \frac{B_{21}n_2\rho(\nu_{12})}{B_{12}n_1\rho(\nu_{12})} = \frac{B_{21}}{B_{12}}\frac{n_2}{n_1}$$

For stimulated emission to exceed absorption, $n_2 > n_1$, → need population inversion (negative temperature)

Resonance cavity



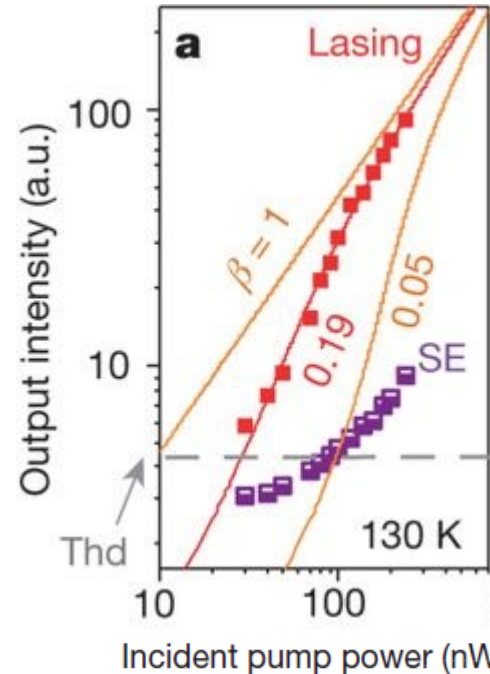
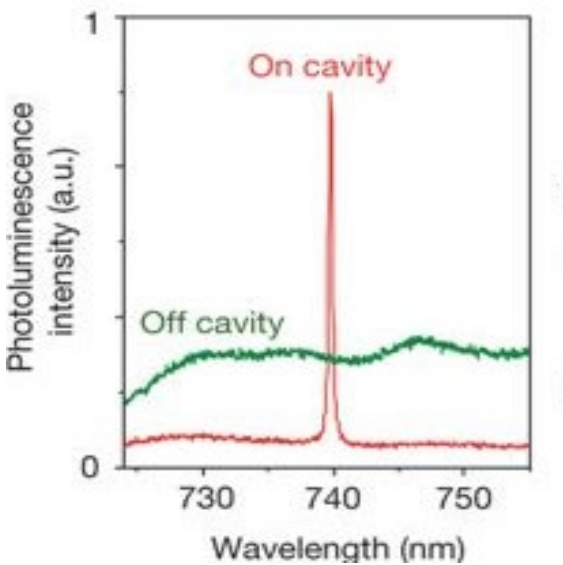
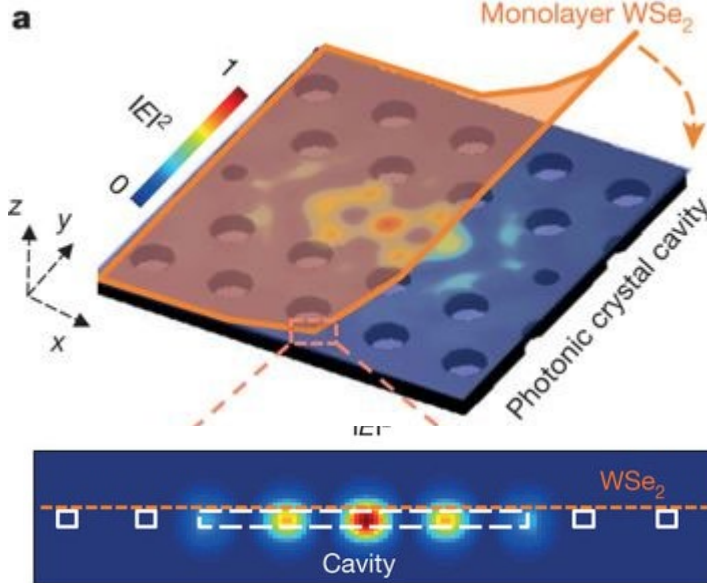
The length of the cavity for stimulated emission must be: $L = \frac{m\lambda}{2} = \frac{m\lambda_0}{2n}$

λ : Photon wavelength within the laser material

λ_0 : output light wavelength in the atmosphere

n: index of refraction of the laser material

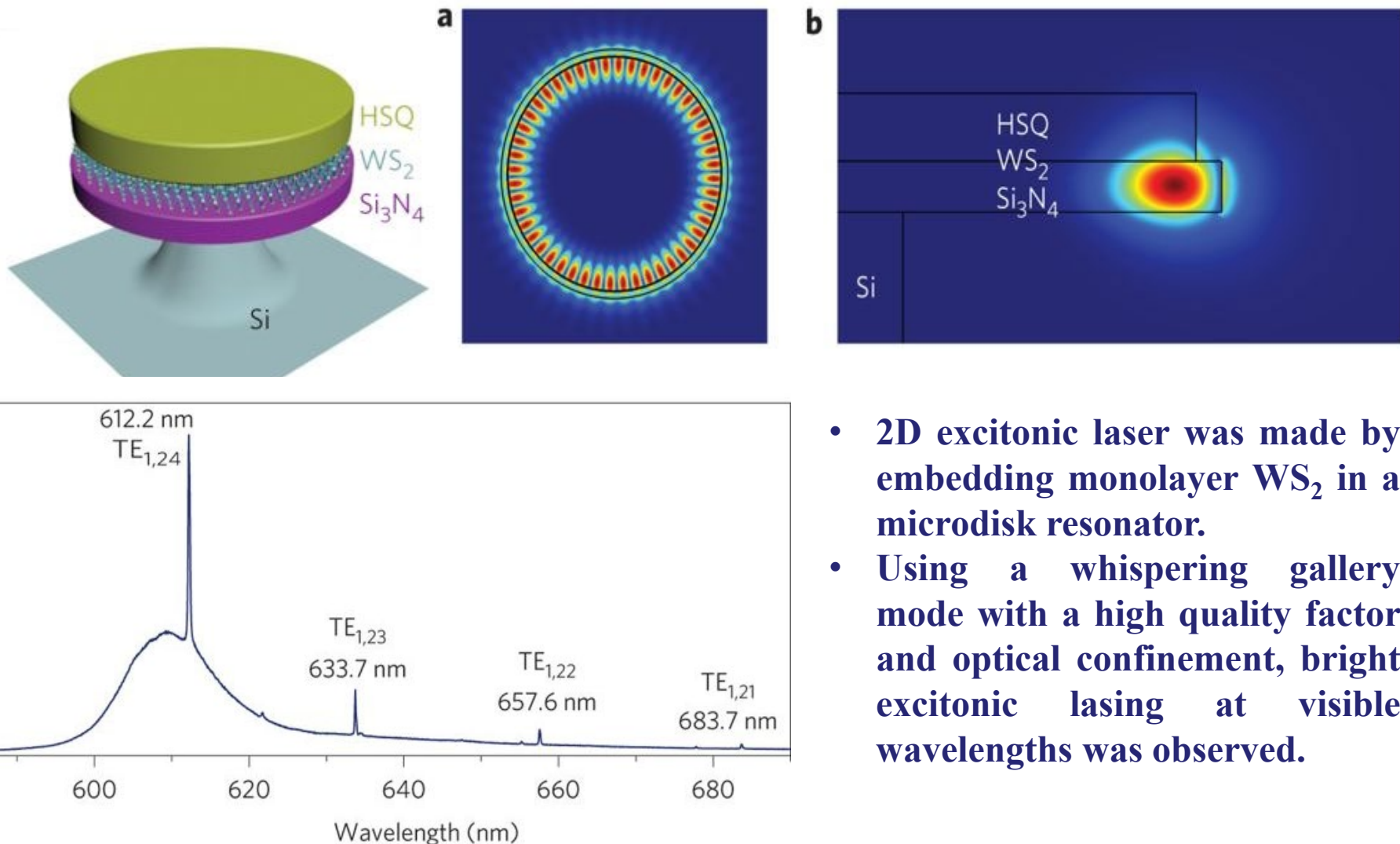
Laser based on TMD



- Coupling a TMD light emitter to an optical cavity can significantly enhance the spontaneous emission rate due to the Purcell effect.
- Using cavities with a high-quality factor, sufficient optical gain can be provided in a TMD by optical pumping to compensate for the cavity losses and to achieve lasing.

Sanfeng Wu, Xiaodong Xu, et.al., Nature, 520, 69, 2015

Lasers based on 2D TMD and microdisks

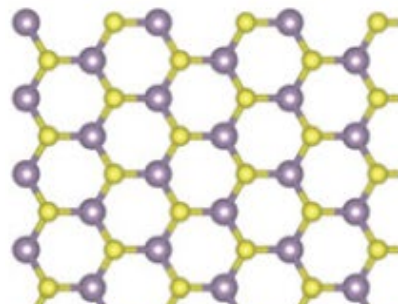


Yu Ye, Xiang Zhang, et.al., Nature Photonics, 9, 733, 2015

Summary (1)

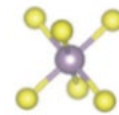
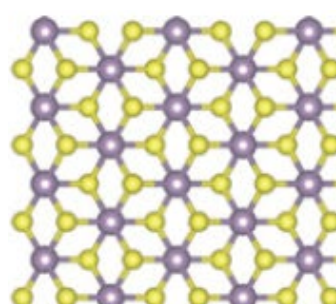
Crystal structure

1H



Semiconducting phase

1T



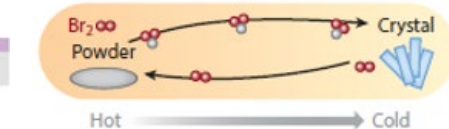
Metallic phase

TMD synthesis

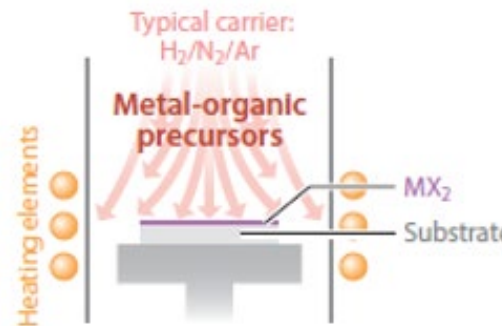
Metal transformation



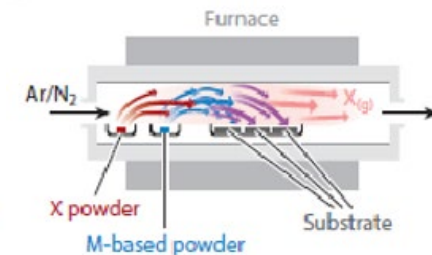
Chemical Vapor transport (CVT)



Metal organic chemical vapor deposition (MOCVD)

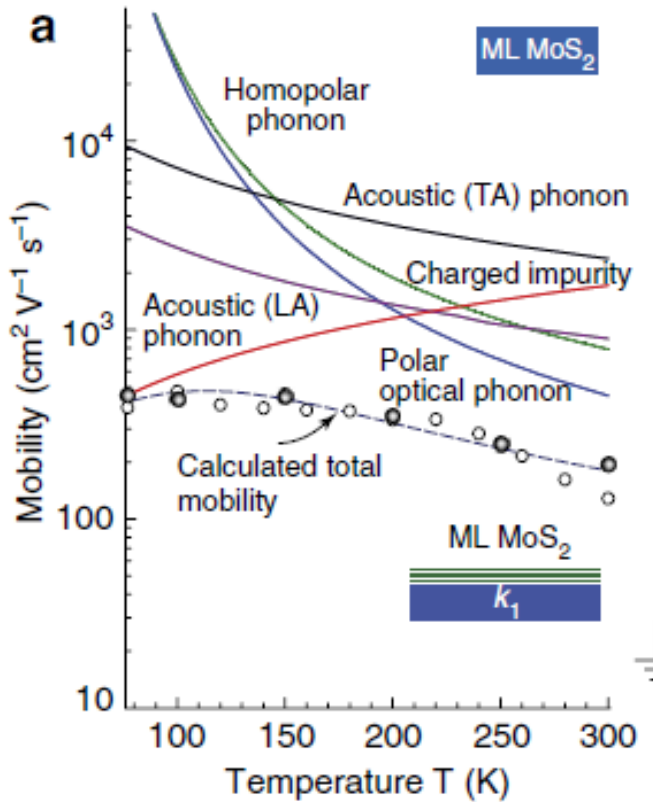


Chemical vapor deposition (CVD)



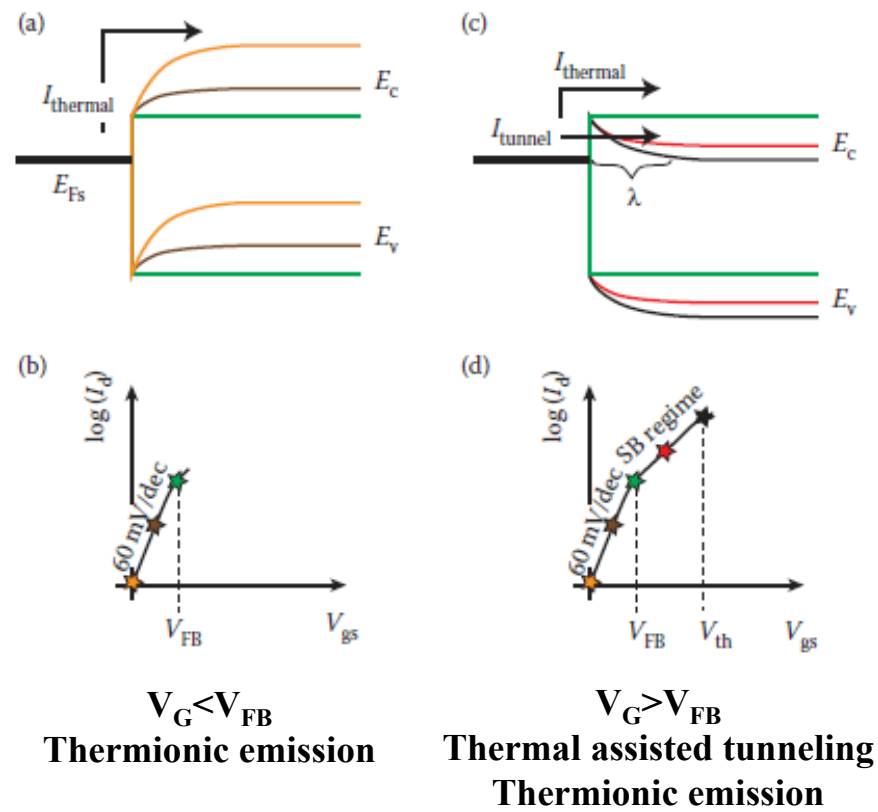
Summary (2)

Carrier Mobility



Dominant scattering mechanisms for mobility are charge impurity and polar optical phonon scattering.

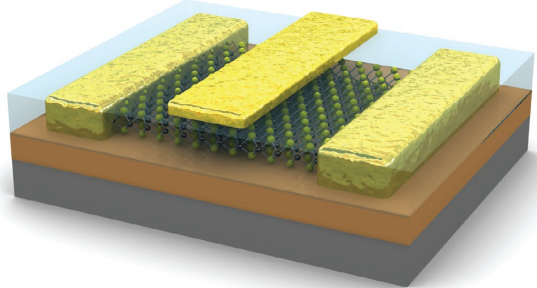
Metal/TMD Contact



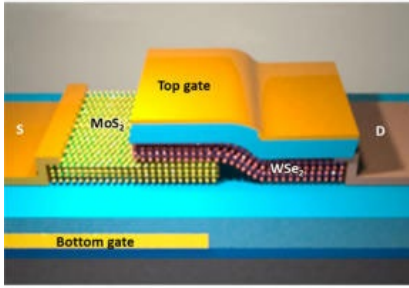
Summary (3)

Electronic and photonic devices based on TMDs

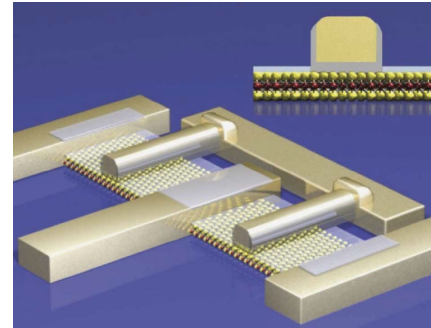
Logic transistors



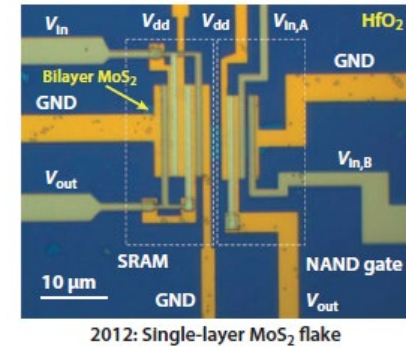
Esaki diode and TFETs



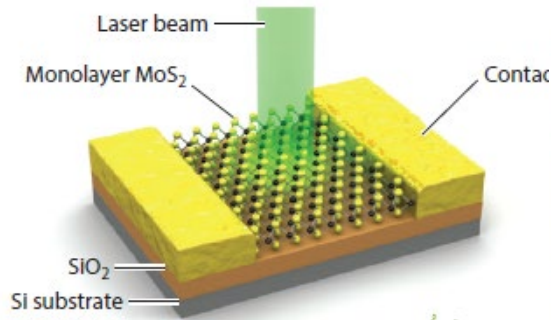
RF devices



SRAM and logic gates



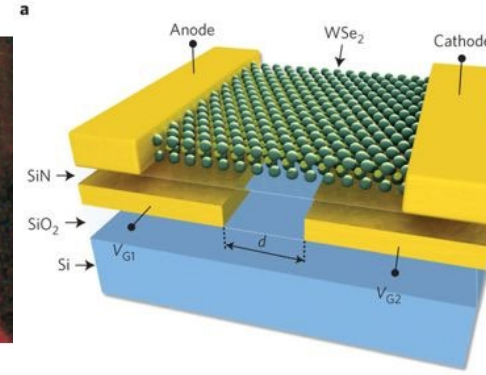
photodetectors



LEDs



Solar Cells



Lasers

